UNIVERSITÀ DEGLI STUDI DI CATANIA

FACOLTÀ DI MEDICINA E CHIRURGIA
DOTTORATO IN BIOLOGIA, GENETICA UMANA E BIOINFORMATICA: BASI CELLULARI E MOLECOLARI DEL FENOTIPO-XXIV CICLO
DIPARTIMENTO DI ANATOMIA, PATOLOGIA DIAGNOSTICA, MEDICINA LEGALE, IGIENE E SANITÀ PUBBLICA
G.F. INGRASSIA
UNITÀ DI BIOMEDICINA MOLECOLARE GENOMICA E DEI SISTEMI COMPLESSI, GENETICA, BIOLOGIA COMPUTAZIONALE

Luisa Statello

Specific Alterations of miRNA Transcriptome and Global Network Structure in Colorectal Cancer After Inhibition of MAPK/ERK Signaling Pathway

Tesi di Dottorato

Coordinatore e Tutor:
Chiar.mo Prof. MICHELE PURRELLO

Anno Accademico 2011 – 2012

TABLE OF CONTENTS

1. ABSTRACT

Colorectal cancer (CRC) is one of the most frequent malignancies affecting the western societies. Currently, the gold standard of CRC treatment is cetuximab, belonging to the class of monoclonal antibodies (mAb), alone or in combination with chemotherapy. Not all patients positively respond to cetuximab therapy: the analysis of KRAS mutational status at tumor site, a highly invasive analysis, is the only universally accepted genetic predictor for patient's response. For reasons not clarified yet, some KRAS wild type patients considered as potential good responders don't benefit from this therapy. Many efforts are being made to overcome these obstacles, primarily focusing on the identification of new biomarkers easily detectable in circulating blood or other body fluids that can be used for diagnosis as well as for predicting the response to certain therapies. miRNAs, small RNA molecules involved in all aspects of cellular metabolism through their important activity as regulators of gene expression, have been identified as new important biomarkers for many diseases and cancers, including CRC. On the other hand, the scientific research is investigating on new molecules providing high specificity for the key players of the main cellular pathway affected in cancer. The main pathway involved in CRC is MAPK/ERK signaling pathway, which members are considered good targets for the design of new specific inhibitors that could importantly help to overcome the problems related to non-responsive patients to EGFR-targeted therapy. This thesis is primarily focused on the relationship between the response to certain drugs and miRNA transcriptome changes in CRC human cellular models, based on their KRAS mutational status, an issue that was unexplored so far. We profiled the expression of 667 miRNAs in 2 human CRC cell lines (Caco-2, KRAS wild type, and HCT-116, KRAS

mutated), and 745 miRNAs in 3 CRC cell lines (Caco-2, HCT-116 and SW-620, another KRAS mutated cell line) after cetuximab treatment and after subministration of three specific inhibitors of MAPK pathway, respectively. Our aim was the identification of typical miRNA transcription profiles associated to cetuximab response, as well as the investigation on the global involvement of miRNAs within MAPK/ERK pathway. The first analysis led us to the identification of substantially unique subsets of differentially expressed miRNAs in the sensitive cell line compared to the resistant one. Global network functional analysis on their targets suggested a role of these miRNAs in cancer related processes and reveals the presence of hubs involved in EGFR internalization. With the second analysis we identified six differentially expressed miRNAs (miR-372, miR-663b, miR-1226*, miR-92a-1*, miR-135b*, and miR-720), that we have demonstrated to be involved in cell proliferation, migration, apoptosis, and to globally affect the regulation circuits centered on MAPK/ERK signaling. We evaluated the expression of the main candidate miRNAs identified in both studies in biopsies from CRC patients that we had previously categorized for the presence/absence of KRAS mutation: two miRNAs from the first study (miR-146b-3p and miR-486-5p) and four from the second (miR-92a-1*, miR-135b*, miR-372, miR-720) resulted significantly highly expressed in biopsies from CRC patients than in normal controls. Moreover, the last four miRNAs are overexpressed in CRC patients with mutated KRAS respect to wild-type genotypes. The identification of miRNAs, which expression is linked to the efficacy of therapy, should help to predict the patients' response to treatment and possibly lead to a better understanding of the molecular mechanisms of drug response. On the other hand, our results contribute to deepen current knowledge on some features MAPK/ERK pathway, pinpointing new oncomiRs in CRC and allowing their translation into clinical practice and CRC therapy. Data shown in this thesis were published in 2010 in Molecular Cancer Therapeutics (Ragusa M,

Majorana A, Statello L, et al. *Specific alterations of microRNA transcriptome and global network structure in colorectal carcinoma after cetuximab treatment*. Mol Cancer Ther. 2010 Dec; 9:3396-409), and in 2012 in the Journal of Molecular Medicine (Ragusa M, Statello L, Maugeri M, et al. *Specific alterations of the microRNA transcriptome and global network structure in colorectal cancer after treatment with MAPK/ERK inhibitors*. J Mol Med (Berl). 2012 Jun 4).

2. INTRODUCTION

Colorectal cancer (CRC) is the fourth most prevalent cancer and the second leading cause of death from cancer in both sexes in western society, at present comprising 11% of all cancers [1]. During 1998-2002, colorectal cancer was the 4th most frequently diagnosed cancer among males (11.3% of all cancers) and the 3rd among females (11.5%) in Italy, while it was the second most relevant among cancer deaths in both sexes (http://www.registri-tumori.it). It is also one of the most preventable and curable cancers if diagnosed in early stages since about 85% of tumors arise from premalignant polyps; it becomes highly lethal, and only partially controlled by therapy when it overgrows the basal membrane, giving rise to metastasis. Invasive CRCs are caused by the abnormal growth of colic mucosa; epidemiologically, colon and rectal cancers can be easily distinguished, since they show different incidence and mortality rates: this suggests that they could have related but not fully overlapping causes, and different biological features. CRC is a heterogeneous syndrome, arising as the cumulative effect of multiple genetic mutations and epigenetic alterations within the cell after prolonged exposures to several different environmental factors and lifestyles, which promote and induce DNA alterations in intestinal mucosa epithelial cells: around 80% of all CRC cases are defined, indeed, sporadic. The main environmental leading causes for sporadic CRC are i) wrong diet (high assumption of saturated fats and low amount of fibers) and related obesity, ii) smoking (long-time smokers are more likely to develop CRC compared to non-smokers), iii) inactive lifestyle, all social features strongly associated to the ‘western way of life’. The remaining 15-20% of CRC cases has a dominant inherited pattern, with several conditions associated to an increased risk of developing CRC; hereditary non-polyposis colorectal cancer

(HNPCC) and Familial adenomatous polyposis (FAP) account for 5% of all CRC with a genetic bases [2]. The stage of a cancer is one of the most important factors in determining prognosis and treatment options: The American Joint Committee on Cancer (AJCC) staging system, also known as TNM system for CRC is the most commonly accepted classification based on the histopathological features of the tumor, and it represents a more detailed CRC grouping respect to the previous staging systems like Duke's and Aster-Coller's (Table 1). Three different parameters (T, N and M), each associated with ascending numeric values, are used in this standardized system: T indicates how far the primary tumor has grown into the wall of the intestine and whether it has grown into nearby areas, N describes the extent of spread to nearby lymph nodes, and M tells whether the cancer has spread to other organs of the body (in case of CRC the most common metastasis sites are liver and lungs).

Table 1. Anatomic stages and prognostic groups for CRC.

Stage	T	N	M	Dukes	MAC
0	Tis	N0	M0	--	--
I	T1	N0	M0	A	A
	T2	N0	M0	A	B1
IIA	T3	N0	M0	B	B2
IIB	T4a	N0	M0	B	B2
IIC	T4b	N0	M0	B	B3
IIIA	T1-T2	N1/N1c	M0	C	C1
	T1	N2a	M0	C	C1
IIIB	T3-T4a	N1/N1c	M0	C	C2
	T2-T3	N2a	M0	C	C1/C2
	T1-T2	N2b	M0	C	C1
IIIC	T4a	N2a	M0	C	C2
	T3-T4a	N2b	M0	C	C2
	T4b	N1-N2	M0	C	C3
IVA	Any T	Any N	M1a	--	--
IVB	Any T	Any N	M1b	--	--

However, CRC is a heterogeneous multifactorial disease, and it is not unlikely that histologically identical tumors may have drastically different prognosis and/or response to treatment. In order to enhance tumors categorization, but also prediction of prognosis and response to treatment, it is important to improve CRC classification by taking in account also the main molecular hallmarks of CRC genomic alterations: chromosomal instability (CIN), microsatellite instability (MSI), and CpG island methylator phenotype (CIMP). CIN, characterized by karyotypic variability resulting from gains and/or losses of whole/portions of chromosomes is commonly found in 50 to 85% of CRCs [3]. MSI, due to inactivation of DNA mismatch repair genes was found in 15% of sporadic CRCs, and is associated to TGFβRII, EGFR, and BAX genes mutations; many other genes, involved in cell proliferation, apoptosis and DNA repair are often affected by MSI [3]. In addition to genomic instability, epigenetic instability appears to be frequent in CRC. The alteration of methylation patterns is crucially involved in the transcriptional silencing of regulators of tumor suppression, cell cycle, DNA repair, and apoptosis: 35-40% of CRC are positive to CIMP [3]. The molecular pathways are determined at an early evolutionary stage and are fully established within precancerous lesions. Based on these molecular features, CRCs can be further classified in 5 molecular subtypes:

1) Type 1 (CIMP-high/MSI-H/BRAF mutation);
2) Type 2 (CIMP-high/MSI-L or MSS/BRAF mutation)
3) Type 3 (CIMP-low/MSS or MSI-L/KRAS mutation)
4) Type 4 (CIMP-neg/MSS)
5) Type 5 or Lynch syndrome (CIMP-neg/MSI-H)

Genetic alterations in CRC

Notwithstanding the molecular differences among sporadic and hereditary cancer forms, all CRCs are considered to evolve through a similar histological progression from adenoma to carcinoma, accompanied by a linear sequence of genetic alterations, as it was proposed by Vogelstein: this process is known as the adenoma to carcinoma sequence [4] (Figure 1). CRC originates from small benign outgrowths due to hyper-proliferation of the intestinal mucosa, called precancerous polyps. Some of them, based on their histological features (villous component, high grade dysplasia), are considered high-risk polyps, 25% of which can turn to malign tumor after accumulation of several genetic mutations.

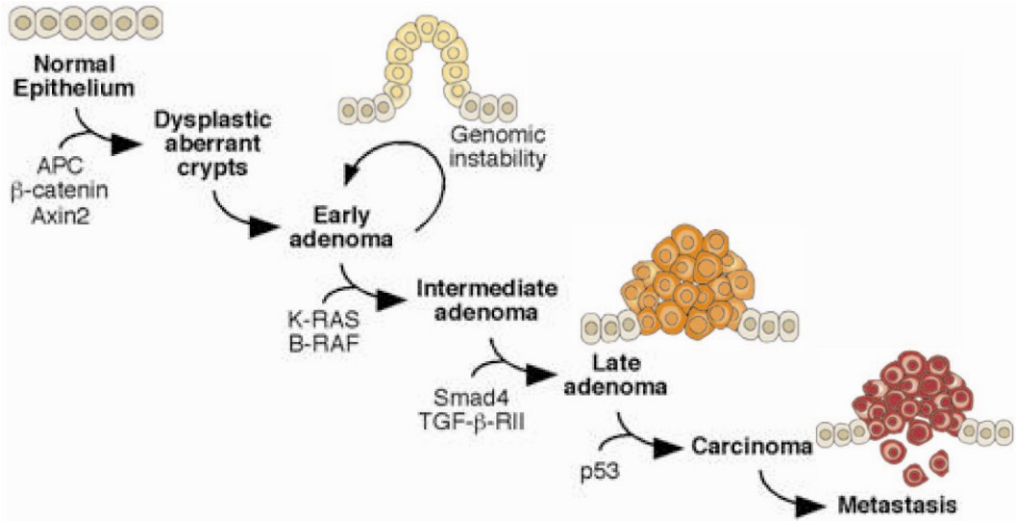

Figure 1. Schematic representation of the adenoma to carcinoma sequence, showing the mutational events associated with histopathological changes.

With the exception of HNPCC, where DNA instability initiates tumorigenesis, the majority of CRCs appear to progress through the selection of a series of mutations

involving several key players in CRC carcinogenesis. The first molecular event associated to adenomatous polyps formation is the inactivating mutation of the APC (*Adenomatous Polyposis Coli*) gene, implicated in the development of FAP and observed in 80% of sporadic CRCs. Its gene product is involved in the regulation of differentiation, adhesion, polarity, migration, development, apoptosis, and chromosomal segregation [5]. APC has a main role in inhibition of Wnt signaling pathway, which is known to play a major role in cancer development through regulation of cell cycle genes: it helps the suppression of Wnt-signaling pathway through β-catenin binding, promoting its targeting for ubiquitin-mediated degradation. In the absence of this regulation, β-catenin escapes degradation and translocates to the nucleus where it initiates the transcription of a wide variety of genes involved in the development and progression of colorectal carcinoma, including cyclin D142 and the oncogene MYC [6]. Larger adenomas and early carcinomas acquire mutations in the small GTPase KRAS, which mutations in exon 2 (codons 12 and 13) and exon 3 (codon 61) occur in 40-50% of CRCs and contribute to the development of colorectal adenomas and hyperplastic polyps, and are considered as predictive markers for CRC [7]. Mutations in each of the three codons compromise the inactivation of KRAS, thus leading to upregulation of RAS function and constitutive activation of its downstream signaling cascades: this in turn increases the invasive properties of mutated cells [8]. KRAS mutation, with promotion of adenomatous growth is followed by biallelic loss of chromosome 18q in up to 70% CRCs, associated to the loss of tumor suppressor genes as DCC (a cell-surface receptor for neuronal protein netrin-1 important in cell adhesion and apoptosis), SMAD2 and SMAD4 (functioning in the TGF-β-signaling pathway), and TP53 mutations in the switch from late adenoma to early carcinoma [4]. Development of CRC in MSI cancers involves different, but analogous, genetic changes to those involved in chromosomal instability. The first steps of tumorigenesis involve Wnt pathway

impairment instead of APC mutations, while BRAF mutations generally occur in place of KRAS ones: the two mutations are mutually exclusive as they are intimately connected in the RAS-RAF-MAPK pathway [9]. MSI cancers are positively selected for mutations affecting microsatellites in several genes, including BAX, which provides a TP53-independent mechanism of progression to carcinoma [10]. The tumor suppressor gene PTEN encodes a dual-specificity phosphatase that negatively regulates the PI3K/AKT-dependent cellular survival pathway, which is responsible of AKT activation, a proto-oncogene involved in several functions such as cell proliferation, cell growth and inhibition of apoptosis [8]. AKT pathway is frequently hyperactivated in CRC, through different genetic mechanisms. Inactivating mutations of PTEN, which is a late event in CRC carcinogenesis correlated to advanced metastatic tumors, occurs in one third of CRCs [8]. The PIK3CA gene encodes for a lipid kinase that regulates, alongside with KRAS, signaling pathways downstream of the EGFR: gain of function mutations of the PIK3CA gene upstream the pathway, occurring in 20% of CRCs, cause AKT signaling even in absence of growth factors; moreover, since this kinase can be activated by RAS signaling, the co-presence of KRAS mutation in CRC can hyperactivate AKT pathway [9].

Prevention and screening tests

For CRC patients showing clear clinical features and a family history consistent with a given familial syndrome, diagnostic tests can be easily performed to identify the germline mutation in patients and other members of the family to check if they have inherited the mutation. In case of sporadic CRC, however, screening and prevention are the main instruments for precocious diagnosis and organization of the best therapeutic strategy. For the identification and subsequent

asportation of adenomatous polyps colonoscopy remains the gold standard for CRC screening, though less than 60% of individuals at risk usually undergo this test, because of its high invasivity. For this reason, and because many early lesions cannot be easily identified by colonoscopy, there is increased interest in the development of other alternative methods for CRC screening. So far, the two main biological specimens in which targets for earlier molecular detection of CRC have been developed are feces and blood. Fecal occult blood testing is a noninvasive method conducted as a first-line screening for CRC, which has reduced CRC mortality by 15–33% [11]. A wide variety of genetic and epigenetic alterations have been suggested as markers to indicate neoplastic growth including KRAS, TP53, APC, and COX-2. Tumor cells circulating in the peripheral blood may be reflective of tumor genetic features and, therefore, useful in predicting metastatic and recurrence potential; at present, around 40 serum proteins have been identified as potential CRC biomarkers [8]. Notwithstanding, mortality rates for CRC are still high, claiming the need of developing new diagnostic testing comprising a wide spectrum of biomarkers, given the high genetic complexity of this tumor, allowing the earlier detection of CRC and the possibility to develop more efficient and personalized therapeutic regimens. Unbiased high-throughput screening, including genome wide association studies (GWAS) and analysis of gene expression signatures, opened new roads to the identification of new markers for CRC, aiming at the identification of discrete and quantitative markers, respectively. Several GWAS identified highly robust SNPs that are significantly associated with CRC risk [4]. It is interesting to note that five of them affect genes connected to the TGF-β-signaling pathway, involved in tumor suppression functions, that play a role in CRC biology: SMAD7, GREM1, BMP2, BMP4 and RHPN2 [12]. This overrepresentation suggests a master role of TGF-β pathway in common inherited predisposition to CRC. Gene expression analysis holds great promise for the understanding of the functional differences between tumor tissue

and normal tissue, having the potential to identify specific tumor tissue signatures compared to the normal counterpart. This kind of analysis can be performed at mRNA level, but it has also been applied to microRNA (miRNA) research, which is at present among the most expanding research areas regarding tumors, and will be deeply discussed later in this thesis. This kind of studies are affected by several limits, one among the others the need of strong statistical validation required for a huge amount of expression data in generally not so big cohorts of patients, leading to a high number of false-positive and false-negative discovery rate. The increased knowledge of gene expression-based technologies and the efforts made to improve the design of such studies giving more statistical strength to the results has allowed reaching good results for breast cancer so far, and encourages the researchers to pursue this road. Anyway, at present, the only validated and reliable marker with sufficient evidence to justify routine clinical assessment is KRAS mutational analysis for selection of patient's EGFR-targeted therapy.

Epidermal growth factor receptor signaling and EGFR-targeted therapy

The epidermal growth factor receptor (EGFR) displays a master role as regulator of cell growth in normal conditions, and alterations of the pathways triggered by this receptor contribute to malignant growth of several tumor types, including CRC [13]. EGFR belongs to ErbB receptors family, which is comprised of transmembrane proteins complexes forming tyrosine kinases receptors activated by different ligands, such as EGF, TGF alpha, Neuregulin family and some others [14]. Ligand binding to the extracellular portion of the receptor induces autophosphorylation of its intracellular tyrosin-kinase domain, which in turn leads to EGFR homodimerization or heterodimerization with other ErbB members and

activation of the molecular signaling cascades within the cell, including the RAS-RAF-MAPK, JAK-STAT and the PIK3-AKT pathways [13]. Through the EGFR-regulated pathways, different extracellular stimuli can drive specific cellular responses such as proliferation, migration, differentiation and apoptosis through selective translocation of various transcription factors to the nucleus, where they can regulate gene expression in a specific direction (Figure 2).

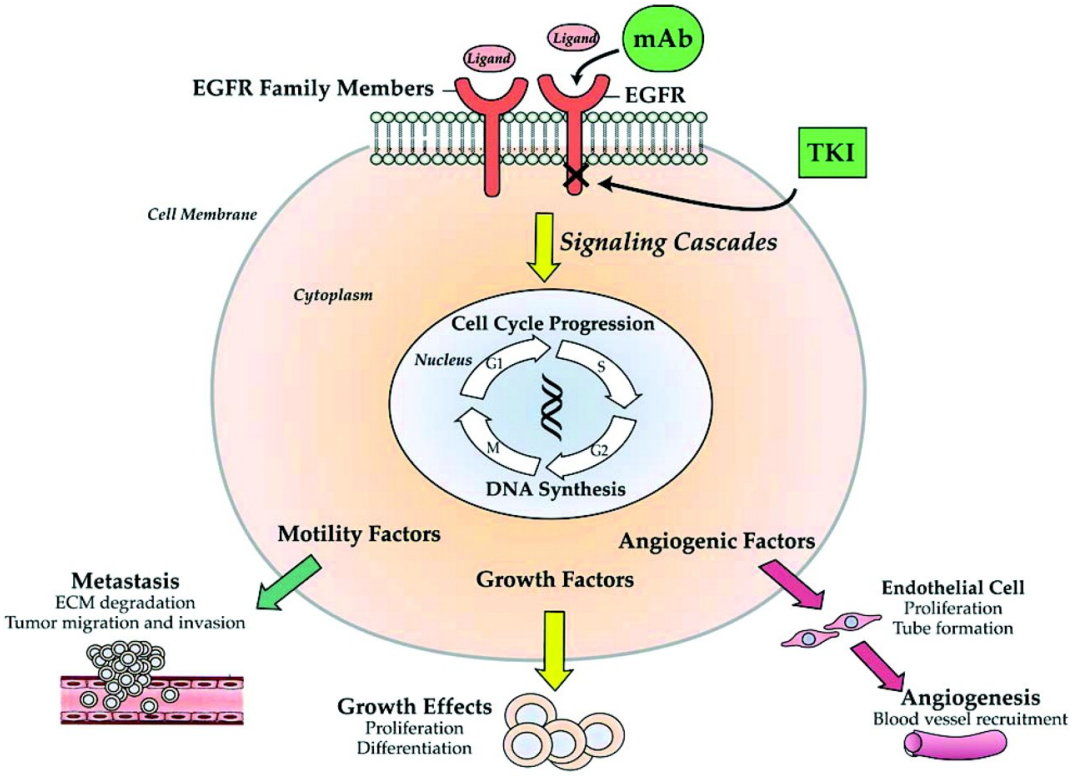

Figure 2. Epidermal growth factor receptor activated cellular pathways, and its main inhibition strategies in oncology (from PM Harari *et al.* Endocr Relat Cancer December 1, 2004; 11: 689-708).

EGFR-mediated cell signaling is frequently and importantly hyperactivated in CRC, mainly due to EGFR overexpression as well as receptor ligands, transforming growth factor-a (TGF-a), heparin-binding EGF-like growth factor (HB-EGF) and amphiregulin [15]. EGFR, overexpressed in 25-77% of CRCs, is associated with a poor prognosis and has been suggested as a potential target for antitumor agents both for its position on the top of several cancer-related pathways and because it's easily reachable by drugs. Two classes of EGFR antagonists, small molecule tyrosine kinase inhibitors (TKIs) and monoclonal antibodies (mAb), have been approved by the Food and Drug administration (FDA) and the European Medicines Evaluation Agency (EMEA) for the treatment of metastatic non-small cell lung cancer (mNSCLC), CRC, squamous-cell carcinoma of the head and neck and pancreatic cancer [16] (Figure 2). Gefitinib and Erlotinib are reversible inhibitors of EGFR tyrosine kinase activity, able to inhibit the receptor autophosphorylation and block downstream signal transduction. The most recent therapeutic approach to colorectal cancer is based on the use of monoclonal antibodies against EGFR, able to compete with its natural ligands within the extracellular space. Since 2004, the introduction of cetuximab (a recombinant, chimeric, IgG1) and panitumumab (a fully humanized IgG2 antibody) in clinical practice, either in combination with chemotherapy or as single agent, has shown to improve the outcome of metastatic CRC patients [16]. Cetuximab is a chimeric human murine derivative IgG1 mAb that binds extra-cellular domain of the EGFR with higher affinity that that of its natural ligands. Binding of cetuximab to EGFR triggers the internalization of the receptor without activation of its tyrosine kinase activity; this results in downregulation of EGFR, which prevents further receptor binding and activation by the natural ligands [17]. The mechanisms through which cetuximab expresses its antitumor activity after downregulating EGFR are numerous and not completely cleared yet. Since cell progression into S-phase is strongly dependent on the interaction of growth factors with their receptors at the

cell membrane, the first evident effect displayed by cetuximab is inhibition of cell cycle progression, leading in some cases to apoptosis [17]. Activity of the EGFR signal transduction pathway is required for stimulation of angiogenesis by malignant cells: in this context, it was demonstrated that cetuximab decreases tumor cell production of angiogenic growth factors such as vascular endothelial growth factor (VEGF), bFGF and interleukin-8 (IL-8). This correlates with a significant decrease in microvessel density and an increase in apoptotic endothelial cells [17]. Through inhibition of both expression and activity of MMPs, a family of zinc-dependent endopeptidases involved in tumor progression and metastatization and known to be strongly expressed in malignant cells, cetuximab inhibits the invasive and metastatic ability of different tumor types. Finally, cetuximab antitumor effect can be driven by triggering antibody-dependent cellular cytotoxicity (ADCC), through activation of cytotoxic host effector cells [18].

Molecular predictors of EGFR-targeted therapy efficacy

In early clinical trials, EGFR expression status on tumor specimens was thought to be a predictive factor for cetuximab efficacy; notwithstanding, further clinical studies failed to identify a strong association between clinical outcome and EGFR status, since high clinical responses have been registered also in patients with undetectable EGFR protein [14]. Currently, the only confirmed molecular marker for cetuximab response in CRC treatment is KRAS mutational status. KRAS encodes a membrane-associated GTPase playing a major role in many signal transduction pathways, which acts as on/off switch molecule for the recruitment and activation of proteins necessary for the propagation of many signals, such as RAF1 and PI3-kinase [19]. KRAS activation is thrilled by ligand binding to

EGFR; activated KRAS is involved in the hydrolysis of GTP to GDP, after which it is turned off. Activating mutations of the KRAS gene occurring mainly at codons 12 and 13 have been detected in about 50% of CRC patients. KRAS mutation lead to a constitutive downstream activation of the RAS/MAPK pathway, which is independent from EGFR receptor: this leads to an increase of cell proliferation signals that cannot be significantly inhibited by cetuximab, since this mAb acts upstream the KRAS protein (Figure 3).

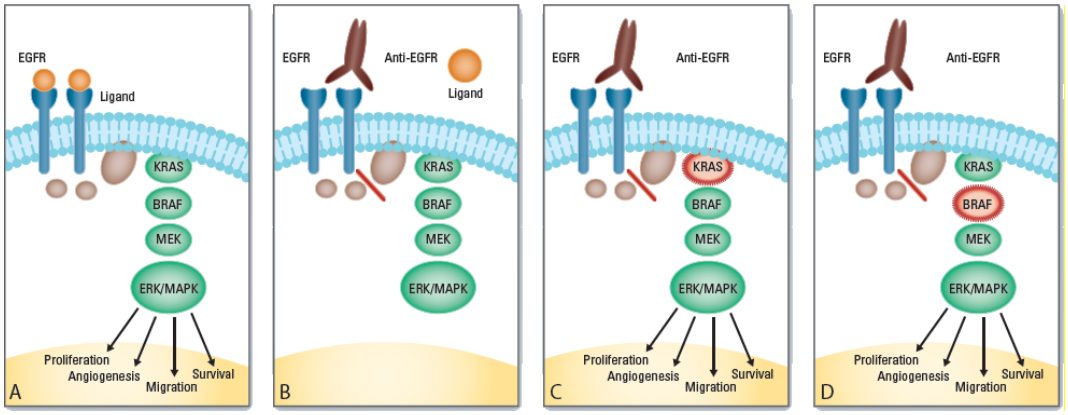

Figure 3. EGFR targeted therapy and effect of KRAS and BRAF mutations in the constitutive activation of MAPK pathway.

The idea that failure of EGFR-targeted therapy could be due to mutations in molecules downstream EGFR has directed to the search of BRAF and PIK3CA activating mutations and on PTEN deregulation. Similar to KRAS mutations, BRAF V600E mutation induces structural changes in RAF protein, which is the first effector identified downstream of RAS, increasing its kinase activity [20]. BRAF mutations are responsible for an additional 12-15% of patients who fail to respond to anti-EGFR treatment. This finding suggests that testing for the BRAF V600E mutation complements KRAS mutation analysis and may be as important

as KRAS testing for treatment decisions, though the relationship between BRAF mutation and cetuximab resistance is not as clear as in KRAS case [16]. Mutations in the PIK3CA gene occur in about 15% of CRCs: while KRAS and BRAF mutations are mutually exclusive, PIK3CA mutations can be found in the same tumor together with either KRAS or BRAF ones: for this reason it is difficult to evaluate the predictive role of these mutations in CRC patients. Patients with mutation in KRAS or BRAF and PIK3CA do not respond to cetuximab while KRAS and BRAF wild type patients mutant for PIK3CA may have different sensitivity, depending on the kind of mutation they harbor [21].

New therapeutic perspectives in RAS/RAF/MEK/ERK pathway targeting

As discussed above, the main alterations leading to the malignant transformation of adenomatous polyps to adenocarcinoma span the regulatory system of cell cycle, which is affected both by external stimuli and alterations of internal cell signaling, such as EGFR overexpression and RAS mutations. Mitogen-activated protein kinases (MAPK) belong to a large evolutionarily conserved family of serine-threonine kinases kinase linking extracellular signals to the machinery that controls fundamental cellular processes such as growth, proliferation, differentiation, migration and apoptosis in response to several extracellular and intracellular stimuli, such as the presence of mitogen agents (e.g. growth factors), LPS, oxidative stress and inflammation [19]. These stimuli are able to trigger MAPK pathway through a signaling cascade starting from specific receptor molecules that lead to the consecutive activation of the kinases RAS/RAF/MEK/ERK, involved in the control of growth signals, cell survival, and invasion in cancer. MAPK/ERK pathway could also influence the activity of

miRNAs through the modulation of transcription factors, which control their expression [22]. Moreover, it was recently demonstrated that through ERK-mediated TRBP phosphorylation, MAPK pathway can positively influence the activity of the miRNA generating complex [23]. This pathway includes several proto-oncogenes and is deregulated in about 30% of all cancers, including CRC [24] (Figure 4).

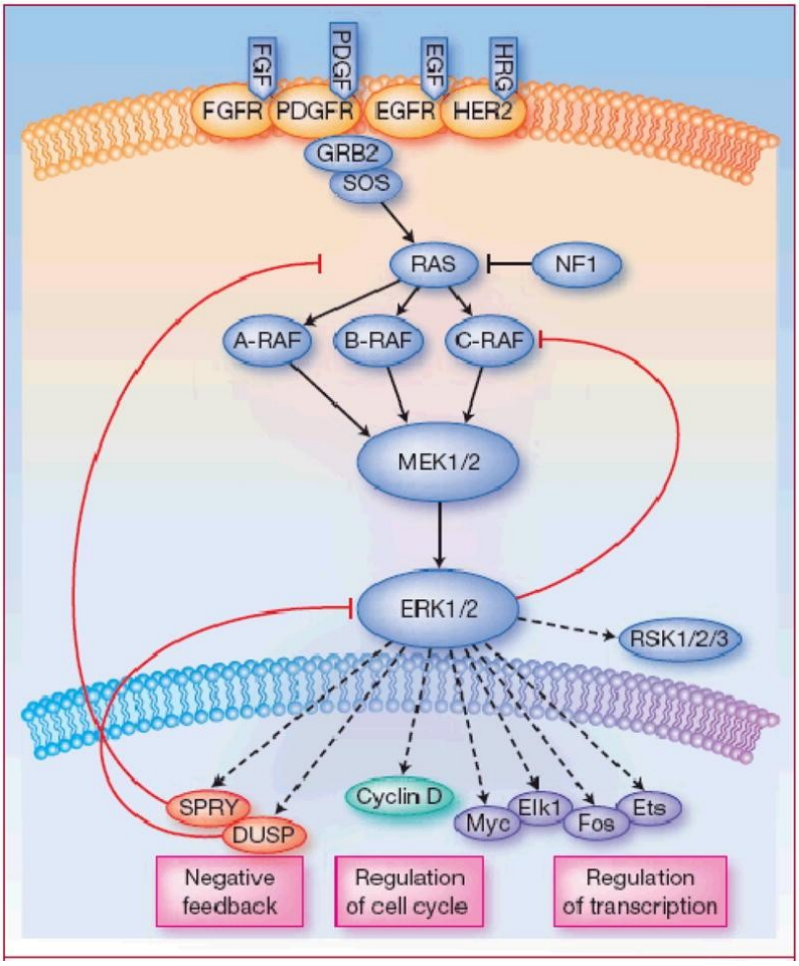

Figure 4. The RAS/RAF/MEK/ERK signaling pathway (from CA Pratilas *et al*. Clin Cancer Res 2010 July 1; 16(13): 3329–3334).

Epidermal growth factor receptor (EGFR) is the main switch of MAPK pathway through activation of RAS protein. Beyond EGFR other receptors, such as TRK A/B, fibroblast growth factor receptor (FGFR) and PDGFR can activate MAPK pathway via the adaptor protein GRB2 [25]. Activated RAS binds to RAF (A-RAF, B-RAF, or RAF-1) which is recruited to the cell membrane. RAF proteins directly activate kinases MEK1 and MEK2 via phosphorylation of multiple serine residues. MEK1/2 in turn activate ERK1/2 through threonine and tyrosine residues phosphorylation. ERK has multiple targets through which it displays diverse cellular functions, including regulation of cell proliferation, survival, mitosis, and migration [26]. Aberrant activation of this pathway is very frequent in CRC as well as other human cancers, and can be driven either by ligand-induced stimulation of membrane associated receptor tyrosine kinases or by ligand-independent mechanisms such as mutational activation of proteins that constitute the pathway, one among the others KRAS and BRAF mutations. Given the well-established role of this pathway in CRC, and the unsolvable question related to mutated KRAS patients treatment, its key components downstream RAS protein represent good putative targets for treatment of colorectal cancer, even though one major problem in this field is that since these pathway displays fundamental functions in many physiological processes, it is not unlikely to find that inhibition of these proteins could lead to unacceptable toxicity [15, 27, 28]. Since the high frequency of RAF gene mutations has been reported, we assisted a significant increase in the design of therapeutic strategies targeting RAF, with varying selectivity profiles. Sorafenib (BAY 43-9006), affecting tumor signaling and the tumor vasculature, is the first oral RAF inhibitor which was approved for the treatment of advanced renal cell carcinoma in 2005 by Food and Drug Administration (FDA), while in 2011 a selective inhibitor against mutant (V600E) BRAF tumors, Vemurafenib, was approved by FDA for the treatment of metastatic melanoma [29, 30]. The option of targeting MEK1 and MEK2 is a promising

therapeutic strategy, since for these kinases no substrates other than ERK1 and ERK2 have been identified, and this suggests the possibility of a selective inhibition of the pathway with minor collateral effects on other cellular processes [31]. Highly selectivity was reported both for PD98059 and U0126, the latter showing increased potency compared to PD98059 [32]. Notwithstanding, their chemical features make them not exploitable as *in vivo* therapeutic agents, even if their application in research gave a high contribution in understanding the molecular mechanisms of MAPK inhibition in human tumors; recent clinical trials have identified Selumetinib (AZD6244) as one the most promising MEK inhibitors capable of eliciting oral anticancer activity for biliary cancers [31]. Doubtless, since ERK is the final effector of MAPK pathway directly responsible of transcription regulation downstream the RAS pathway, its selective inhibition would be the ideal therapeutic approach for treatment of cancer and other diseases. One of the first highly selective ERK inhibitors, FR180204, was identified in 2005, while AEZS-131 represents one of the most promising highly selective orally active ERK 1/2 inhibitors so far [33]: notwithstanding, no valid therapeutic options are currently available for a direct targeting of ERK1/2.

MicroRNAs

MicroRNAs (miRNAs) are short 20–22 nucleotides (nts) RNA molecules that function as negative regulators of gene expression in eukaryotic organisms. These highly conserved RNAs regulating gene expression constitute about 1-5% of predicted genes in animals genomes, and 10-30% of protein-coding genes are probably regulated by miRNAs. Recently, many small non-coding RNAs have been also identified in prokaryotic organisms and viruses. Since they were recognized in 2001, the biological significance of these newly identified small

RNAs was elucidated, because more and more evidences suggest that miRNAs play an essential role in multiple biological processes through negative regulation of gene expression at a post-transcriptional level; they perform their functions by partial pairing with one or more 3'UTR (3' untranslated region) of mRNA targets to promote their degradation or transcriptional repression [34]. The majority of known miRNAs are evolutionarily conserved among species, demonstrating that miRNA mediated gene silencing pathways have essential roles in development, cell differentiation, cell proliferation, cell death, chromosome structure and virus resistance, signaling transduction, disease and cancer [35, 36]. From a functional point of view, it has been demonstrated that most of miRNAs are able to recognize several mRNA targets, on the other hand, one specific mRNA can be regulated by more than one miRNA [37]. Moreover, studies from the last years have demonstrated that there is altered expression of miRNA genes in many human malignancies.

Genomic location of miRNA genes

It was estimated that the human genome contains 1600 miRNA loci, encoding for 2042 mature miRNAs, distributed in all chromosomes except for Y chromosome, according to the latest release of miRBase database, the primary online repository for all microRNA sequences and annotation, where all known and newly identified miRNAs are deposited (http://www.mirbase.org). The identification of miRNA genes is the result of a combination of directional cloning together with computational approaches, based on the examination of genomic sequences to identify phylogenetic conservation of known miRNA genes, taking in account the high level of 5' region conservation in all miRNA sequences. An integrative approach leading to the identification of a significantly higher number of miRNAs than previously expected in humans combined bioinformatics predictions with microarray analysis and sequence-directed cloning, allowing the identification of a

huge amount of non-conserved miRNAs [38]. Around 50% of the known miRNAs are organized in genomic clusters and are transcribed as polycistronic primary transcripts. Generally, miRNAs belonging to the same cluster are structurally and functionally related to each other, demonstrating their origin as a result of duplication events during evolution; on the other hand, some miRNAs lying in close genomic regions can be unrelated to each other. One possible explanation for the existence of clustered miRNAs with related functions or structure is the possibility that they may play a synergic role in regulating the same genes, or different genes involved in the same pathway [37]. Despite it was originally inferred that most of miRNA are located in intergenic regions, more recent analysis have shown that a vast majority of mammalian miRNA genes is located in well-defined transcription units, many of them within introns of coding genes in the sense orientation. Based on these findings, miRNAs can be categorized as follows:

a) intronic miRNAs in coding regions;

b) intronic miRNAs in non-coding regions;

c) exonic miRNAs in coding regions;

d) exonic miRNAs in non-coding regions (Figure 5).

Based on the splicing pattern, some miRNAs have mixed features; moreover, for miRNAs comprised within coding regions, as expected for genes sharing the same promoters, miRNAs usually have similar expression profiles to their host transcript [37].

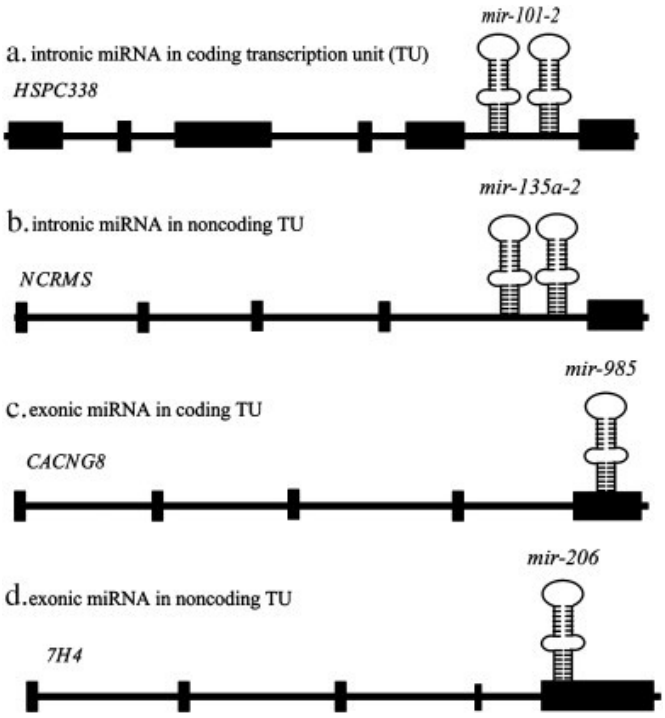

Figure 5. Genomic organization of miRNA genes (from F Wahida *et al*. BBA 2010; 1803(11): 1231–1243).

miRNA biogenesis

miRNA biogenesis is a multistep process where a mature miRNA is generated from a miRNA gene, with several enzymes playing critical roles in the process (Figure 6). As it was already discussed, intronic miRNAs share their regulatory elements and primary transcript with their pre-mRNA host genes, and are undoubtedly transcribed by RNA-polymerase II (pol II). This gives a possible mechanism for coordinated miRNA and protein-coding gene expression [39].

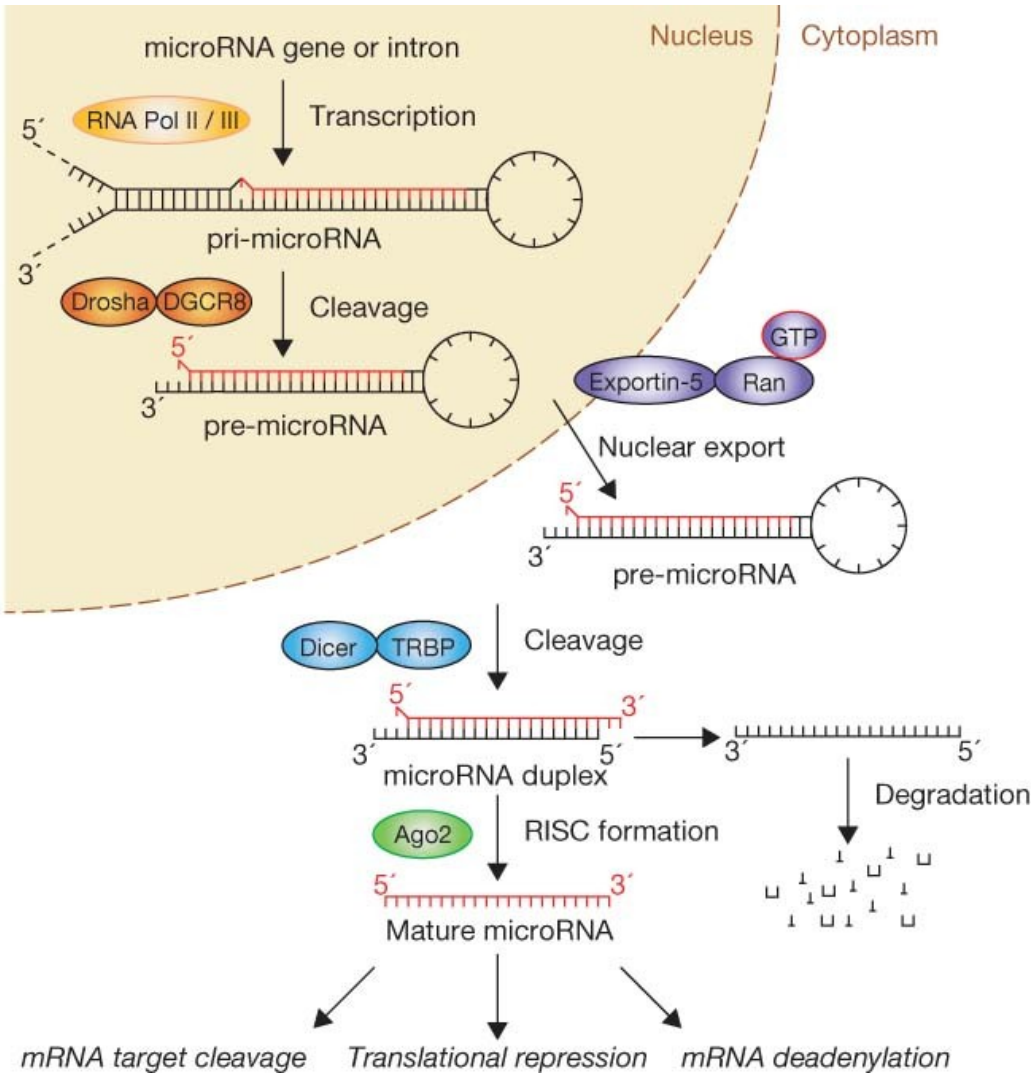

Figure 6. miRNA biogenesis pathways and their regulation. (from J Winter *et al*. Nature Cell Biology 2009; 11:228-234).

All the characterized promoters for the other miRNA genes contain general RNA polymerase II transcriptional regulatory elements previously found in protein-coding genes: this, together with other experimental evidences, strongly suggests

that all miRNAs are pol II products [40]. miRNA gene transcription by pol II produces a pri-miRNA of several hundreds of nts in length, with a 5' cap and a polyadenylated 3', which forms a hairpin stem-loop secondary structure within the nucleus and enters a large complex called microprocessor complex (500–650 kDa). The main components of this complex are Drosha (an RNase III endonuclease) and the essential cofactor DGCR8/Pasha (containing two double-stranded RNA binding domains). Drosha asymmetrically cleaves both strands of the hairpin stem at sites near the base of the primary stem loop thus releasing a 60- to 70-nucleotides pre-miRNA with a 5′ phosphate and a 2-nucleotide 3′ overhang (Figure 6). This process is highly specific and pre determines the sequence of mature miRNA [40]. The pre-miRNAs are then transported to the cytoplasm by Exportin-5 (Exp5) (a member of the Ran transport receptor family): this transport process requires energy, a specific hairpin secondary structure, and is Ran-GTP dependent. When the pre-miRNA reaches the cytoplasm, one of its ends has already been predetermined by Drosha cleavage site selection. Once in the cytoplasm, the pre-miRNAs enters the RISC loading complex (RLC), made by Dicer (a second RNase endonuclease), TRBP (able to bind double stranded RNAs), PACT (protein activator of PKR) and Ago-2 [41-43]. Dicer recognizes the 3' overhangs of the pre-miRNA through the PAZ domain, and its cleavage 22-nt from the end of the substrate releases a mature double-stranded miRNA (miRNA:miRNA* duplex) with 5' phosphates and a 2-nt 3' overhang [44]. Finally, miRNA:miRNA* duplex is unwound by helicase into two single strands: in the majority of cases, miRNA*, which is the less thermodynamically stable strand at 5' end, is degraded, while the leading strand is incorporated into a ribonucleoprotein effector complex known as RNA-induced silencing complex (RISC) which induces gene silence at a post-transcriptional level [36].

Connection between miRNA generating complex and MAPK pathway

It has been widely demonstrated that miRNAs have a master role in many cell related processes; therefore, understanding the relationship between miRNA machinery and the other cellular systems cannot prescind from a deep knowledge of the mechanisms by which miRNA pathway itself is governed. A first demonstration of a direct connection between a cell signaling pathway and the core miRNA machinery was provided by Paroo *et al*, who demonstrated that the ERK pathway enhances the stability of the miRNA-processing complex by phosphorylating TRBP, and that the consequent reprogramming of miRNA expression might mediate ERK signaling [23]. Active TRBP is phosphorylated on Ser142, Ser152, Ser283 and Ser286: it was shown that TRBP and phosphorylated ERK1 and ERK2 interact in vivo, and that recombinant MKK1 and ERK2 are required for the phosphorylation of TRBP in vitro. Furthermore, treatment of cells stably expressing TRBP with a mitogen that induces ERK activation causes the phosphorylation and accumulation of TRBP, and this is blocked by the MKK1 inhibitor U0126. All these evidences strongly suggest that TRBP activation is intimately connected to MAPK pathway [23]. The use of TRBP phospho-mimic is able to induce overexpression of some growth promoting miRNAs, such as miR-17, 92a and 20a, and downregulation of the tumor suppressor let-7a, while an opposite effect is observed in cancer cell lines treated with the inhibitor U0126: this implies that ERK-induced phosphorylation of TRBP and the subsequent alteration in the expression of miRNAs, might actively contribute to the growth-promoting actions of the ERK signaling pathway, and is a potential target of MAPK-targeted therapy [23].

miRNA mediated post-transcriptional repression

After being processed, miRNAs are assembled into ribonucleoprotein complexes called RISC (*RNA-induced silencing complexes*), which identify miRNA targets by the perfect or nearly perfect complementarity between the miRNA and the mRNA. The better characterized components of RISC are Argonaute (AGO) proteins, with PAZ and PIWI domains: in mammals, four AGO proteins (AGO1 to AGO4) function in the miRNA repression but only AGO2 functions in RNA interference (RNAi), which is the process guiding the endonucleolytic cleavage of the target mRNA. Beyond Ago proteins, the complex contains other proteins playing critical roles as regulators of the main effectors of RISC inhibitory functions [45]. The complementary sites for miRNAs associated with RISC reside in the 3'untranslated regions (UTRs) of target mRNAs and are generally present in multiple copies as a necessary condition to reach an efficient translational inhibition [46]. The specific site of mRNA recognition in miRNA molecules is called seed region, and is comprised between nucleotides 2-8; generally, in metazoan miRNAs bind the target mRNA with mismatches and bulges, in contrast, most plant miRNAs bind with near-perfect complementarity to sites within the coding sequence of their targets (Figure 7) [47].

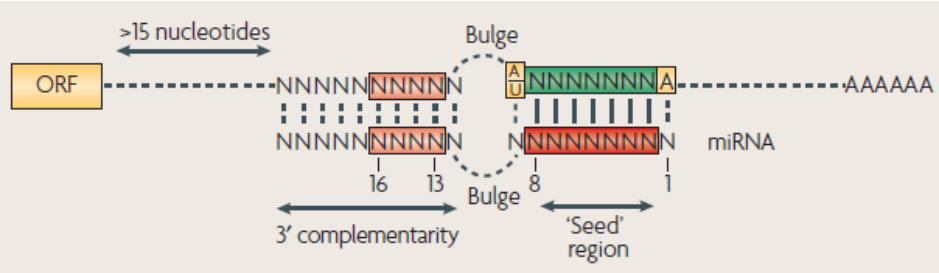

Figure 7. Principles of microRNA–mRNA interactions in metazoan. The base pairing is perfect at the seed region and at miRNA 3' half, while bulges and mismatches can be present in the central region (from W Filipowicz *et al*. Nat Rev Gen 2008; 9:102-114).

Once associated to the target mRNA, RISC inhibitory functions can take place through several possible mechanisms:

- Translational repression, in presence of mismatches in the core part of the seed region;
- mRNA deadenylation and decay in case of perfect complementarity with the target mRNA (Figure 8).

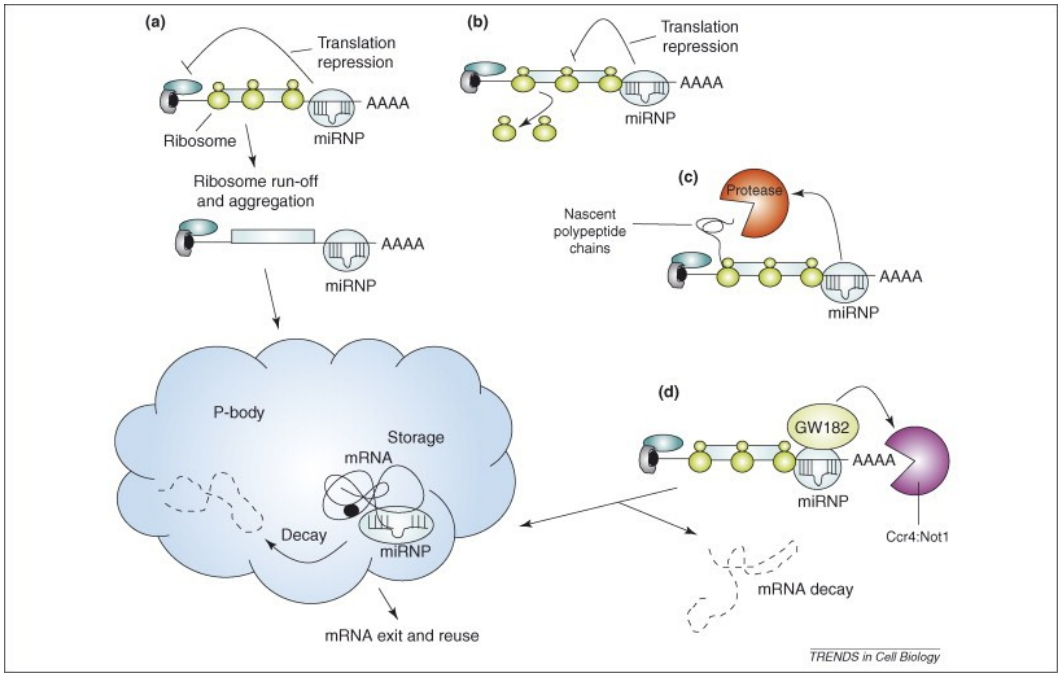

Figure 8. Mechanisms of miRNA-mediated post-transcriptional repression: a) repression of transcription initiation; b) inhibition of protein chain elongation; c) lysis of nascent peptide; d) mRNA deadenilation (from RS. Pillai *et al*. Trends Cell Biol. 2007; 17(3):118-26).

Translational repression can occur at the initiation or at post-initiation steps. Initiation of translation of most cellular mRNAs starts with the recognition of the mRNA 5′-terminal-7-methylguanosine (m^7G) cap by the eukaryotic translation initiation factors (eIF) 4E, 4F and 4G, which together with PAPB1 are responsible

for the association between the mRNA ends, triggering the translation process [48]. Ago 2 and related proteins can compete with eIF4E for m^7G binding, preventing translation. An alternative mechanism of miRNA action was recently proposed at a post-initiation step, since studies with reporter mRNAs targeted by either synthetic or endogenous miRNAs have shown that repressed mRNAs were associated with active polysomes; notwithstanding, how miRNAs could modulate the elongation or termination process remains unclear [49]. In eukaryotes, mRNA degradation can follow two pathways, both of them initiated by a gradual shortening of the mRNA poly(A) tail. The mRNA body can then be degraded by progressive 3′→5′ decay, which is catalysed by the exosome, or by the removal of the cap followed by 5′→3′ degradation, catalysed by the exonuclease XRN1. The final steps of mRNA degradation occur in P-bodies, cytoplasmic structures enriched in proteins participating in miRNA repression functions such as AGO proteins and GW182, and miRNAs themselves [48]. Recent findings demonstrated that lowered mRNA levels account for most (≥84%) of the decreased target's protein production: by using ribosome profiling to measure the overall effects on protein production and compare these to simultaneously measured effects on mRNA levels, Guo *et al.* showed that changes in mRNA levels closely reflect the impact of miRNAs on gene expression and indicate that destabilization of target mRNAs is the predominant reason for reduced protein output [50]. Under certain conditions, or in specific cells, miRNA-mediated repression can be effectively reversed or prevented, and miRNPs or their components can even act as translational activators: this is the case of CAT1, targeted by miR-122 in hepatoma cells, which is released from P-bodies and recruited to polysomes in a process dependent on ELAVL1, or LIMK1 in neurons, repressed by miR-134, which is translated at synapse level [48, 51].

miRNAs and cancer

Like protein coding genes, some miRNAs function as tumor suppressors when their loss of function contributes to the malignant transformation of normal cells; in the same way other miRNAs can function as oncogenes, when their upregulation promotes cancer development or progression. A list of experimentally validated miRNAs acting as tumor suppressor or oncogenes is shown in Table 2.

Table 2. list of validated tumor suppressor or oncogenetic miRNAs in cancer (from R Garzon *et al.* Annu Rev Med 2009; 60:167–179).

MicroRNA	Expression in patients	Confirmed targets	Experimental data	Function
miR-15a miR-16-1	downregulated in CLL[a]	Bcl-2, Wt-1	induce apoptosis and decrease tumorigenicity	TS[a]
let-7 (a,-b,-c,-d)	downregulated in lung and breast cancer	RAS, c-myc, HMGA2	induce apoptosis	TS
miR-29 (a,-b,-c)	downregulated in CLL, AML[a] (11q23), lung and breast cancers, and cholangiocarcinoma	TCL-1, MCL1, DNMT3s	induce apoptosis and decrease tumorigenicity	TS
miR-34a-b-c	downregulated in pancreatic, colon, and breast cancers	CDK4, CDK6, cyclinE2, E2F3	induce apoptosis	TS
miR-155	upregulated in CLL, DLBCL,[a] FLT3-ITD[a] AML, BL,[a] and lung and breast cancers	c-maf	induces lymphoproliferation, pre-B lymphoma/leukemia in mice	OG[a]
miR-17~92 cluster	upregulated in lymphomas and in breast, lung, colon, stomach, and pancreas cancers	E2F1, Bim, PTEN	cooperates with c-myc to induce lymphoma in mice, transgenic miR-17-92 develop lymphoproliferative disorder	OG
miR-21	upregulated in breast, colon, pancreas, lung, prostate, liver, and stomach cancer; AML(11q23); CLL; and glioblastoma	PTEN, PDCD4, TPM1	induces apoptosis and decreases tumorigenicity	OG
miR-372/ miR-373	upregulated in testicular tumors	LATS2	promote tumorigenesis in cooperation with RAS	OG

[a]Abbreviations: CLL, chronic lymphocytic leukemia; AML, acute myeloid leukemia; DLBCL, diffuse large B cell lymphoma; FLT3-ITD, FMS-like tyrosine kinase 3 in tandem duplication mutations; BL, Burkitt lymphoma; TS, tumor suppressor; OG, oncogene.

An example of miRNAs acting as tumor suppressor is given by the cluster of miR-15a and miR-16-1, located at 13q14.2 region, frequently deleted and mutated in CLL patients. Evidence of a tumor suppressor role for this cluster derives from the discovery that the antiapoptotic gene BCL-2, which is widely overexpressed in CLL by unknown mechanisms, is a target of miR-15a/miR-16-1 cluster [52]. Similarly, the let-7 family is downregulated in several tumors: many let-7 members are located in fragile genomic areas associated with lung, breast and cervical cancers, and are involved in the repression of several known oncogenes, such as members of the RAS family, HMGA and MYC, and induce apoptosis and cell cycle arrest when overexpressed in lung and colon cancer [53-55]. Among the oncogenic miRNAs, there is strong evidence of miR-21 playing a role in promoting tumorigenesis: it is upregulated in a wide variety of hematological malignancies as well as solid tumors, including AML, CLL, glioblastoma, and cancers of pancreas, prostate, stomach, colon, lung, breast, and liver, where it plays its main functions through transcriptional repression of three main tumor suppressor genes: PTEN, PDCD4 and TPM1 [55]. Other important oncomiRs are members of miR-17-92 cluster, amplified and overexpressed in many solid tumors, and miR-372 and miR-373, inducing proliferation and tumorigenesis in cooperation with RAS through direct inhibition of the expression of the tumor suppressor gene LATS2 [56, 57]. Since miRNAs play their functions through the spectrum of targets mRNA they interact with, the effect on the processes above mentioned are strongly dependent on the cell type and the cellular context in a given developmental stage of the cell itself; this means that the classification of miRNAs as oncomiRs or tumor suppressors cannot be stated *a priori*, and that a number of miRNAs could play an oncogenic role in one setting but suppress tumor formation in a different scenario [58]. MiRNA expression is tissue specific and strongly dependent on the cellular differentiation stage, that's why the presence of significant alterations of miRNA expression in tumor tissues could be considered a

secondary consequence of processes more deeply implied in tumorigenesis, rather than a direct casual event in tumor progression itself. Since 2002, when it was highlighted for the first time a link between miRNAs and cancer in chronic lymphocytic leukaemia (CLL), several groups have demonstrated that miRNAs are extensively involved in the pathogenesis of many solid tumors, both at steady state and after specific treatments, showing for the most of tumors specific signatures related to tumor classification, diagnosis, and progression [59]. In addition to the identified abnormal levels of specific miRNAs in certain types of human cancers, the biological evidence that miRNAs play important roles in cancer development and progression derives from experimental validations in animal models [58]. A number of cancers with a certain importance, because of their incidence in the population or because of their lethality, are well defined by the presence of highly specific miRNA expression signatures: this is the case of breast, lung, colon, stomach, prostate and pancreatic cancer (Figure 9) [59].

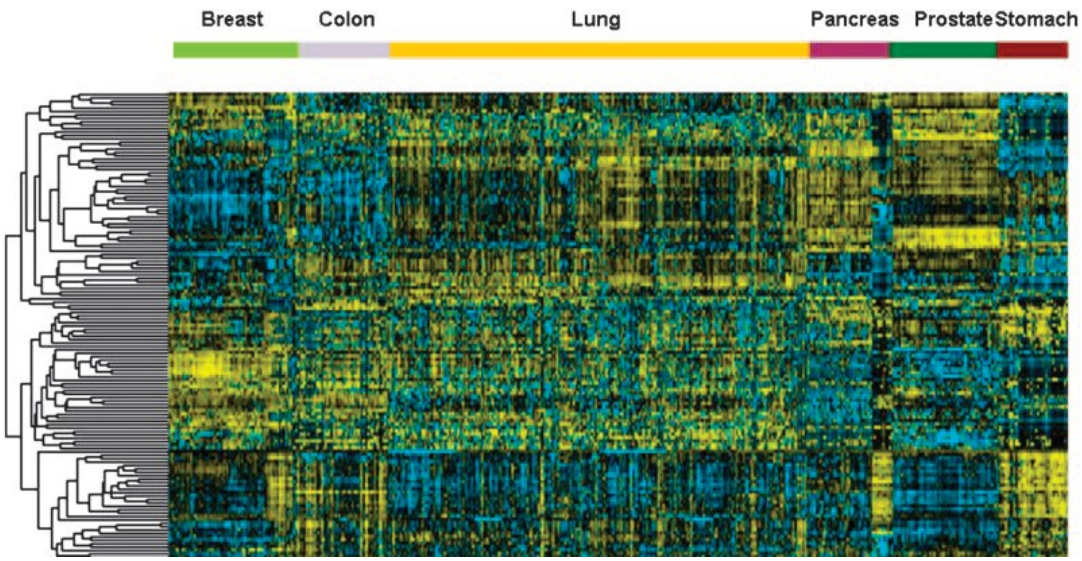

Figure 9. Clustering of miRNA expression profiles derived from 228 miRNAs in 6 solid tumors (from S Volinia *et al*. PNAS 2006; 103(7):2257-61).

Distinguishable abnormalities in miRNA genes and expression patterns were identified in almost all types of cancer, thus providing a strong rationale for the application of miRNAs as diagnostic/prognostic biomarkers. Expression profiles of miRNAs have been found significantly altered in numerous types of human cancers when compared with their corresponding normal tissues, among different subtypes within the same type of cancers, or among individual patients suffering from a same type of cancer but having different prognoses [60, 61].

Circulating miRNAs as a powerful tool for cancer diagnosis

The analyses of miRNA signatures are in general limited to tissue biopsies; however, in the last few years several studies have shown the diagnostic and prognostic usefulness of circulating miRNAs, released by some cell types both under normal and pathological conditions (Table 3) [62]. One of the first studies measuring miRNA levels in serum demonstrated that levels of miR-21 were associated with relapse-free survival in patients with diffuse large B-cell lymphoma [63]. In parallel, many other studies have been published in this field: by measuring the serum levels of miR-141, Mitchell and colleagues could distinguish patients with prostate cancer from healthy subjects; a wider study on miRNA expression profiling in lung cancer, colorectal cancer, and diabetes patients in comparison to related healthy controls found that cancer patients had more elevated serum levels of miR-25 and miR-223 [62, 64]. Currently, one of the most complete studies highlighting the role of circulating miRNAs was carried out on a cohort of 303 non-small-cell lung cancer (NSCLC) patients through Solexa sequencing, and led to the identification of eleven serum miRNAs significantly altered between longer-survival and shorter-survival groups, while some of them were associated to overall survive [65].

Table 3. Serum miRNAs as biomarkers for cancer (from N Kosaka *et al*. Cancer Sci 2010; 101(10):2087-92).

Type of cancer	Biomarker candidate
Diffuse large B-cell lymphoma (DLBCL)	Expression levels of miR-155, miR-210 and miR-21 were higher in DLBCL patient than control sera High miR-21 expression was associated with relapse-free survival
Prostate cancer	Serum levels of miR-141 can distinguish patients with prostate cancer from healthy controls
Ovarian cancer	The levels of the 8 specific miRNAs were similar between cellular and exosomal miRNAs. Exosomal miRNA from ovarian cancer patients exhibited similar profiles, which were significantly distinct from profiles observed in benign disease miR-21, -92, -93, -126 and -29a were significantly overexpressed in the serum from cancer patients compared to controls
Non small cell lung cancer	Eleven serum miRNAs were found to be altered more than 5-fold between longer-survival and shorter-survival groups, and levels of four miRNAs were significantly associated with overall survival
Acute myeloid leukemia (AML) Acute lymphoblastic leukemia (ALL)	miR-92a decreased in the plasmas of acute leukemia patients
Breast cancer	Increased miR-195 levels in patients were reflected in tumors, and circulating levels of miR-195 and let-7a decreased in cancer patients postoperatively, to levels comparable with control subjects miR-155 was differentially expressed in the serum of women with hormone-sensitive compared to women with hormone-insensitive breast cancer
Gastric cancer	The plasma concentrations of miR-17-5p, miR-21, miR-106a, and miR-106b were significantly higher in patients than controls, whereas let-7a was lower in patients
Pancreatic cancer	Circulating miR-210 levels are elevated in pancreatic cancer patients
Pancreatic ductal adenocarcinoma	The combined analyses of four miRNAs (miR-21, miR-210, miR-155, and miR-196a) in plasma can discriminate patients from normal healthy individuals
Squamous cell carcinoma (SCC) of tongue	Plasma miR-184 levels were significantly higher in tongue SCC patients in comparison with normal individuals, and the levels were significantly reduced after surgical removal of the primary tumors
Colorectal cancer	Both miR-17-3p and miR-92 were significantly elevated in the patients, and the plasma levels of these miRNAs were reduced after surgery
Hepatocellular carcinoma (HCC)	An increased amount of miR-500 was found in the sera of the HCC patients, and its levels in sera returned to normal after the surgical treatment

To be able to use circulating miRNAs as a diagnostic marker, we need to gain a better understanding of the mechanisms by which miRNAs are released in the bloodstream. There is evidence that serum miRNAs are particularly resistant to RNases digestion, since they can be detected in this body fluid containing high levels of these enzymes; this implies that they should be released in the blood stream in a form that protects them from degradation. Some hypotheses have proposed that they are secreted in protected protein–miRNA complexes (AGO2,

NPM1, and other RNA binding proteins); another hypothesis is that they are produced as by-products of dead cells [66, 67]. Recent studies have demonstrated a novel mechanism of cell communication using miRNA released in microvesicles (up to 1 μm), or in small membrane vesicles called exosomes (10-100 nm) [68] (Figure 10). Exosomes have been detected in many biological fluids, where they are secreted both under physiological and pathological conditions (e.g. blood plasma, urine and cancerous pleural effusions); besides they are actively produced by many cultured cell types [69]. Among the possible biological functions exerted by exosomes, they have been demonstrated to play a significant role in signalling, immune response, and tumor development [70-72]. The increased levels of tumor-derived exosomes in plasma and malignant effusions of patients with cancer suggest that exosomes can be a rich source for the discovery of blood-based diagnostic biomarkers of disease.

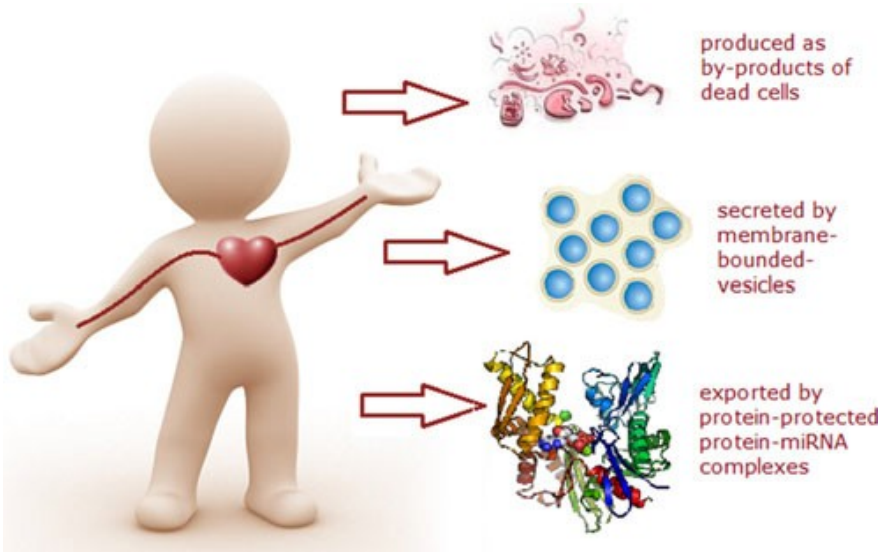

Figure 10. Origin of circulating miRNAs (from J Xu, *et al*. J Mol Med (Berl), 2012; 90(8):865-75).

One of the first reports showing the existence of miRNAs in exosomes was released by Valadi *et al.*, who reported that exosomes released from human and murine mast cell lines contain mRNAs and miRNAs [73]. Since then, many studies started to focus on the expression profiling of miRNAs from exosomes isolated from plasma of diseased patients, in order to identify new miRNA markers that are easily measurable in blood samples. Two pivotal studies led to the identification of eight putative miRNA markers for the diagnosis of ovarian cancer (miR-21, miR-141, miR-200a, miR-200c, miR-200b, miR-203, miR-205, and miR-214) and twelve specific miRNAs (miR-17-3p, miR-21, miR-106a, miR-146, miR-155, miR-191, miR-192, miR-203, miR-205, miR-210, miR-212, and miR-214) for lung cancer, respectively: in both cases it was demonstrated that miRNA profiling could be performed in the absence of tissue and accurately reflects the tumor's profile [74, 75].

miRNAs in CRC

As the result of the numerous alterations involved in CRC pathogenesis, up regulation or reduced expression of several miRNAs, due to transcriptional alterations as well as amplifications, deletions, epigenetic silencing or defects in their biogenesis, have been described in the carcinogenesis of CRC. Two main approaches have been applied to the study of miRNAs involvement in CRC: functional analysis and profiling studies spanning the entire miRNA transcriptome. The first approach is intimately connected to the well-defined alterations leading to impairment of several important cellular pathways in CRC, such as Wnt/βcatenin, MAPK, and P53 pathways (Figure 11).

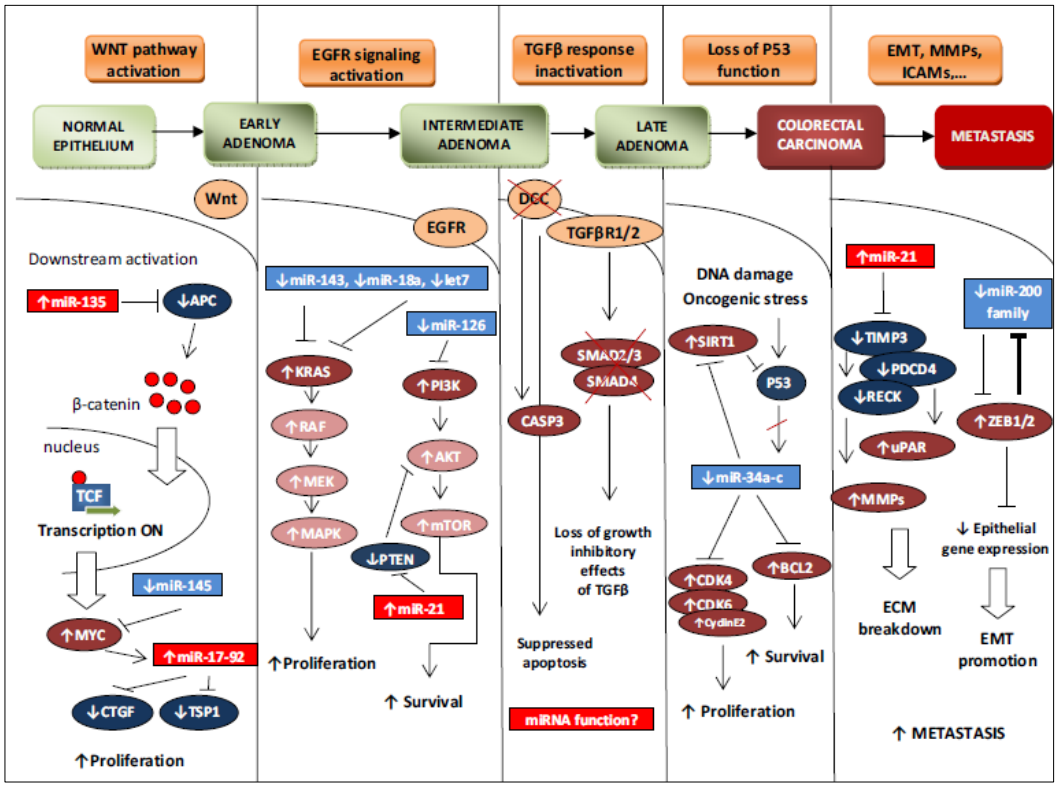

Figure 11. miRNAs involvement in colorectal cancer histopathogenesis (from O Slaby *et al*. Mol Cancer 2009; 14;8:102).

For example, it was recently shown that mir-135 family alterations can be among the early events in CRC pathogenesis: miRNAs belonging to that family are upregulated in CRC, and were demonstrated to target APC tumor suppressor in vivo [76]. EGFR signalling cascades are profoundly associated to miRNA deregulation: KRAS gene, which role in CRC has been widely unveiled, is a direct target of let-7, miR-143 and miR-18a*, which show an inverse expression pattern in CRC samples respect to their target and are significantly down regulated in CRC; loss of miR-126 in CRC is associated with aberrant PI3K signalling, since we assist to accumulation of its target p85β, directly involved in the activation of the pathway [77]. Another important negative regulator of the PI3K pathway is the

tumor suppressor gene PTEN, strongly repressed by miR-21, which is the most frequently upregulated miRNA in CRC [78, 79]. The tumor suppressor gene p53, mutated in 50-70% of CRCs, is a known expression activator, but numerous reports have indicated that p53 also represses the expression of specific genes either directly or indirectly, through molecular mechanism that still need to be characterized: one of these could be the transcriptional activation of miR-34a-c family, which is a well know family of tumor suppressor miRNAs [80]. The study of miRNA connections with cellular pathways led to a better understanding of the role of those signalling pathways in cancer and other diseases, identifying some miRNAs as new potential therapeutic targets, beyond their already established role in diagnosis. Up to some years ago, the most common method for quantification of miRNAs, as well as other types of transcripts, was Northern blot analysis. Over the last years, with the advent of high-throughput (HT) technologies, several new approaches have been developed to screen entire transcriptomes at once: techniques such as cDNA arrays, Real-Time PCR and bead-based miRNA expression rapidly led to the identification of a wide number of putative miRNA markers for CRC. The main advantage of real-time PCR respect to the other techniques is that, since it requires miRNAs amplification, it is more quantitative and more sensitive, allowing the identification of less abundant molecules that couldn't be identified otherwise. The first study of this kind compared the expression of a miRNA set in match paired tumoral and non tumoral tissues from CRC patients and CRC cell lines, leading to the identification of a reliable set of 13 miRNAs significantly deregulated in CRC [78]. The most interesting deregulated miRNAs were miR-31, miR-96, miR-135b, miR-183 (up regulated) and miR-133b, miR-145 (downregulated). These data were also consistent with those obtained by using an experimental approach called miRNA serial analysis of gene expression (miRAGE), which had previously shown a systematic alteration of CRC miRNA expression profiles in CRC. Moreover, it was one of the first

studies on CRC showing that differential miRNA expression between CRC samples could be a link between CRC carcinogenesis and alterations of the RAS/RAF/MEK/ERK pathway. For example, among several proteins with potential oncogenic functions, putative miR-145 targets are MAPK transduction proteins such as MAP3K3 and MAPK4K4, while among targets of miR-133b, the most notable oncogenic target is KRAS [81]. In addition, the expression level of miR-31 was also correlated with the stage of CRC tumor, suggesting that this miRNA could contribute to tumorigenesis and the acquisition of a more aggressive phenotype in CRC, maybe through the inhibition of genes such as FOXC2 and FOXP3, members of the forkhead family of transcription factors which are involved in the silencing of antiapoptotic genes and are known to be modulated, among other pathways, also by ERK/MAPK pathway [82]. In 2005 Volinia *et al*. identified a cancer-specific signature which included significant up regulation of miR-21, miR-17-5p, miR-191, miR-29b, miR-223, miR-128b, miR-24, miR-155, miR-20a, miR-107, miR-32, miR-30c, miR-221 and miR-106a in CRC. Most of these miRNAs have been later confirmed to be up-regulated in CRC by other profiling studies [59]. MiRNA profiling has also been used to classify CRC on the basis of their microsatellite status: Lanza and colleagues showed that microRNA profiling clearly discerned between MSI and microsatellite stable (MSS) tumors [83]. This was subsequently confirmed by another group that also showed the prognostic value of miR-320 and miR-498 in predicting recurrence-free survival [84]. From then, several other studies focused on the use of microRNA profiling to provide prognostic informations and to direct patients to specific treatments. For example, Schetter *et al*. in 2008 confirmed the promising clinical potential of microRNA profiling in clinical management of CRC patients by performing a microRNA microarray expression profiling in more than 200 paired tumor and non-tumor tissues. They found 37 differentially expressed miRNAs in CRC patients, with miR-20a, miR-21, miR-106a, miR-181b, and miR-203 associated

also with poor survival; further validation showed that miR-21 was significantly associated with poor prognosis, and this association was independent of age, sex, and tumor location [79]. This study demonstrated miR-21 role in CRC pathogenesis, showing its involvement in tumor progression and metastasis: it was shown indeed that its expression was progressively increasing in the adenoma-carcinoma sequence. This action can be performed through the modulation of the tumor suppressor genes PDCD4 (that inhibits TPA-induced tumor transformation and progression), which expression resulted inversely correlated with miR-21 in a cohort of 22 CRC patients [85]. The importance on circulating miRNAs in CRC patient screening was first pinpointed on a study by Ng *et al*., in 2009: miR-92 upregulation was identified as one of the best predictive markers for CRC with a sensitivity of 89% and a specificity of 70%, which was demonstrated by strong decrease in its expression after tumor resection [86]. The importance of miR-17-92 cluster, involved in cancer progression through stimulation of proliferation, had been already identified in CRC, through miRNA expression profiling in cancer tissues that identified a significant up regulation of these miRNAs in tumor samples [87]. Similar results were obtained by Huang *et al*., who measured the expression of 12 candidate miRNAs in plasma samples from patients with advanced colorectal neoplasia and healthy controls using real-time RT-PCR. They found that plasma miR-29a and miR-92a have significant diagnostic value for advanced neoplasia [88].

miRNA targeting as a new possible therapeutic approach in CRC

Another important question for management of CRC patients is the possibility of predicting therapy response based on miRNA expression patterns; moreover, it has been shown that specific treatments are able to induce or repress the expression of

miRNAs with a critical role in CRC, suggesting that these changes could be responsible in a direct or indirect way, of the therapeutic effect of certain drugs. For example, treatment with 5-fluorouracil (5-FU) results in a typical miRNA expression pattern in CRC cells: among the 22 miRNAs which expression is influenced by the drug, some of them change their expression in a direction that is opposite to that induced by neoplastic transformation. MiR-200b, targeting mRNA PTPN12 which inactivates products of oncogenes, such as ABL, SRC or KRAS, is overexpressed in CRC, and is significantly down regulated by 5-FU treatment [89]. Another study conducted in vivo analysed miRNA expression changes in CRC patients before and after treatment with capecitabine: two miRNAs, miR-125b and miR-137, showed significant increase in expression levels after two-week therapy [90]. The evidence that miRNAs can be modulated by specific pharmacologic treatments strongly suggests that they could represent a novel class of therapeutic targets themselves: their specific modulation can trigger wider responses through a targeted inhibition/activation of specific mRNA to determine the cellular response to the drug. Overexpression of miRNAs can be induced by using synthetic miRNA mimics or chemically modified oligonucleotides. Conversely, miRNAs can be silenced by antisense oligonucleotides and "antagomirs" (synthetic analogues of miRNAs). It has been shown that inhibition of miR-21 in CRC resulted in the reduction of tumor growth, invasion, angiogenesis and metastasis, while restoration of miR-145 expression has been associated with inhibition of tumor cells growth via down regulation of its target IRS-1 [77]. Notwithstanding, so far, only a limited number of studies have been conducted under *in vivo* conditions in animal models. Gene therapies may be designed to treat CRC and to block the progression of precursor lesions by manipulating the tumor suppressive or oncogenic miRNAs. Such manipulation may control the tumor growth rates and have potential as a new therapy for both early and advanced cancers. To reach this goal, there is need of a definitive mRNA

target validation, the possibility for nonspecific immune activation and it has to be taken in account the lack of a defined, optimal mode of delivery: cross-sensitivity with endogenous miRNAs and lack of specificity for cancer cells can cause nonspecific side effects during miRNA modulation therapy. However, the use of an effective delivery system and less toxic synthetic anti-miRNA oligonucleotides may minimize such side effects. In this regard, exosomes could be considered as a new exiting frontier for miRNA-based therapies: it has been demonstrated that released exosomes contain a specific subsets of cellular mRNA and miRNA that can be transferred to recipient cells, without triggering immune responses, suggesting a new mechanism of cell-to-cell communication via the esRNA (exosomal shuttle RNA) [73]. Further studies demonstrated the importance of exosomes as newly identified vectors for gene therapy [91, 92]. The main advantage revealed by such studies is that exosomes are naturally uptaken by recipient cells without triggering immunogenic responses: the use of these nano-scaled vectors to change the abundance of specific miRNAs within the recipient cells could in some way be used to mimic a given pharmacological treatment, avoiding the problem of both drug toxicity and the already mentioned troubles associated to the classic miRNA-based therapies.

3. MATERIALS AND METHODS

Cell lines

In our studies we used three different CRC cell lines: Caco-2 and HCT-116 cell lines from the Interlab Cell Line Collection (ICLC), and SW-620 cell line from the American Type Culture Collection (ATCC). The first cell line is KRAS wild-type, so the impairment of the cell proliferating pathways is independent from the constitutive activation of KRAS and is sensitive to EGFR-targeting; HCT-116 (established from the primary site of tumor growth) and SW-620 (from a lymph node metastasis), are KRAS-mutated and resistant to EGFR-targeted treatments. Caco-2 cells were cultured in Eagle minimal essential medium (EMEM), supplemented with 20 % fetal bovine serum (FBS), 2 mM L-glutamine, 1% NEAA; HCT-116 cells were cultured in McCoy 5A medium, supplemented with 10 % FBS and 2 mM L-glutamine; SW-620 cells were cultured in Dulbecco modified Eagle medium (DMEM), supplemented with 10 % FBS and 2 mM L-glutamine (Gibco).

Treatments with drugs and inhibitors impairing MAPK pathway

To check the effect of anti-EGFR mAb on Caco-2 and HCT-116 cell lines viability, $5x10^3$ cells per well were seeded in 96-well plates in serum starvation conditions (1% FBS) and treated with 20 μg/mL of cetuximab (Erbitux; Merck KGaA); for the molecular analysis, $1.5x10^6$ cells per flask were seeded into 75 cm^2 flasks. All the experiments were performed in biological triplicates. In order to

evaluate the effect of MAPK inhibition downstream the EGFR receptor, we used three different MAPK/ERK inhibitors on Caco-2, HCT-116 and SW-620 cell lines. U0126 is an adenosine-5′-triphosphate (ATP)-noncompetitive MEK1/2 inhibitor, which specifically prevents in vitro phosphorylation of MEK1/2 by binding to the inactive enzyme and blocking RAF-1 kinase recruitment. FR180204 is an ATP-competitive inhibitor of ERK1 and ERK2 and a weaker inhibitor of the related kinase p38α; it also blocks TGFβ-induced activation of AP-1. WAY265506 is an ATP-competitive inhibitor of MEK1, based on a 4-anilino-3-cyanoquinoline core, not released in commerce yet, and was provided by European Drug Safety and Metabolism Research Center, Wyeth. Besides its affinity for MEK1, it also has a weak effect on ERK2 and several other tyrosine kinases. For each cell line, 3×10^5 cells per well were seeded in six-well plates in serum starvation conditions for 14 h. HCT-116 and SW-620 were separately treated with 25 μM U0126 (MEK 1/2 Inhibitor, Merck), 25 μM WAY265506 (MEK Inhibitor, Pfizer/Wyeth), and 50 μM FR180204 (ERK inhibitor II, Merck); 50 μM of each inhibitor was used for Caco-2 cells. Cells were exposed to inhibitors for 12 h. Control samples were treated with an equivalent volume of DMSO (solvent of the drugs used for treatment). All the experiments were performed in biological triplicates. A schematic representation of anti-EGFR mAb effect is shown in Figure 2, while MAPK/ERK intracellular signaling cascade and the targets of its inhibitors are shown in Figure 12.

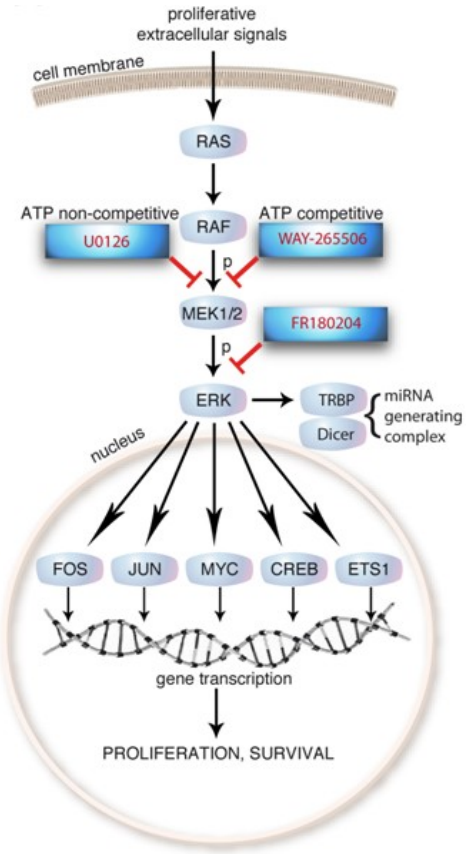

Figure 12. Molecular targets of U0126, WAY-255506 and FR180204 within the MAPK/ERK pathway.

To assess the cell viability after treatment, the MTT assay was performed at 3 time points (24, 48, and 72 hours post treatment) after cetuximab subministration and after 12, 24, 48, and 72h exposure to the three inhibitors of treated cells and their time-matched controls. For each cell line, a 96-well plate was harvested to assess the absorbance values at the starting point (t= 0). Absorbance values were read by using the Multiscan Ascent microplate reader (Thermo Fisher Scientific Inc.).

Western blot analysis of ERK1/2 and pERK1/2

Total protein extracts from Caco-2, HCT-116 and SW-620 after treatment with the MAPK inhibitors were obtained by using the RIPA lysis buffer [2 % protease-inhibitor cocktail (Sigma), 1% of both phosphatase inhibitor cocktail 2, phosphatase-inhibitor cocktail 3 (Sigma)]. Proteins were quantified through Qubit fluorescence quantification system (Invitrogen) and analyzed by SDS-PAGE. Blotting was performed by iBlot Dry Blotting System (Invitrogen). Membranes were probed with monoclonal antibodies to p44/42 MAPK (Erk1/2) and phospho-p44/p42 MAPK (Erk1/2) (Cell Signaling), using β-Actin (Abcam) as loading control. Bound antibodies were detected with peroxidase-labeled goat anti-rabbit IgG-HRP secondary antibody (Santa Cruz). Proteins were detected using the ECL Plus Western Blotting detection (Amersham).

RNA isolation, reverse transcription and miRNA profiling by Real-Time PCR

As a platform for the profiling of miRNA expression in our samples before and after treatment with the mAb cetuximab and the inhibitors of MAPK pathway we chose the TaqMan microRNA low density arrays (TLDA) technology (Applied Biosystems), micro fluidic cards allowing the simultaneous amplification of up to 384 genes per card exploiting the TaqMan assay technology (Figure 13). They are provided as a combination of 2 micro fluidic card set, A and B: the actual version, v3.0, currently contains 754 unique assays specific to human microRNAs updated to capture new content available in Sanger miRBase v14. Each array contains, three selected candidate endogenous control assays (snRNA U6, snoRNA U44 and U48) and one negative control assay (ath-miR-159a). The previous version of these arrays, v2.0, contains assays for 667 miRNAs.

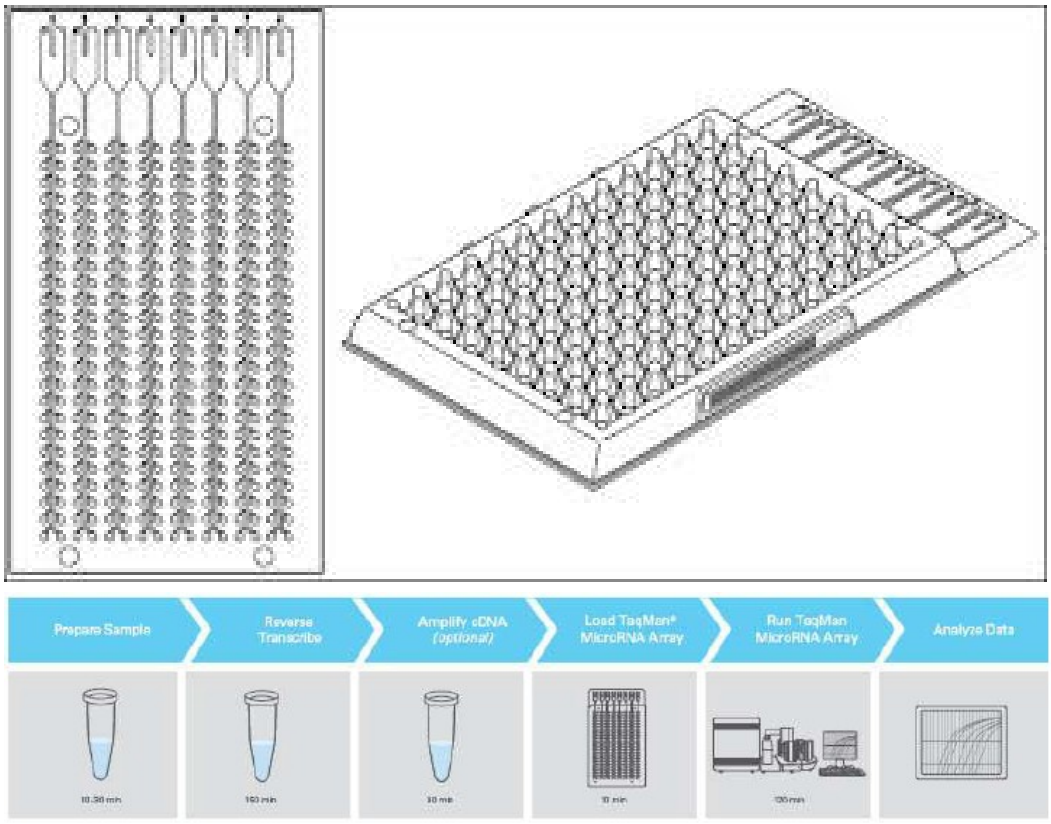

Figure 13. Applied Biosystems 7900HT TaqMan low density array and workflow for the analysis of miRNA transcriptome.

Total RNA from cell lines was extracted using TriZol reagent (Invitrogen), according to the manufacturer's instructions, and quantified by Qubit (Invitrogen). One microgram of total RNA from Caco-2 and HCT-116 treated with cetuximab and related controls was retrotranscribed using the TaqMan MicroRNA Reverse Transcription Kit and Megaplex Primer Pools A and B (Applied Biosystems), according to the Megaplex Protocol, while 100 ng of total RNA from Caco-2, HCT-116 and SW-620 treated with the MAPK inhibitors were first retrotranscribed and subsequently pre-amplified with TaqMan PreAmp Master Mix Kit (Applied Biosystems). Six microliters of megaplex and preamp products, respectively, from both primer pools were mixed up with TaqMan Universal PCR

Master Mix (Applied Biosystems) and loaded into the microfluidic cards TaqMan Human MicroRNA Array v2.0 or v3.0 A and B (Applied Biosystems). All reactions were performed in a 7900HT Fast Real Time PCR system (Applied Biosystems). All the experiments were performed in biological triplicates. Result validation was performed by single TaqMan assays (Applied Biosystems) according to manufacturer's instructions.

Expression data analysis

Cetuximab treated samples

We applied 2 different methods for data normalization. First, we calculated the relative levels of miRNA expression through the $2^{-\Delta\Delta Ct}$ method, using snRNA U6 and snoRNA U48 as endogenous controls. The values of Ct greater than 35 were treated as 35, whereas undetermined Ct values were treated as 40. We accepted as reliable only fold change values concordant in both endogenous controls. Expression data in Results section are shown as natural logarithm (ln) of relative quantity (RQ) of miRNAs, normalized with respect to snRNA U6 from a calibrator sample (the time-matched untreated controls). To identify differentially expressed miRNAs, we applied a paired t test (or t test between subject in the comparison between cell lines) among ΔCt by using the following parameters: assumption of equal variance; a (overall threshold P value) = 0.01; the P value was based on permutation; the significance was determined by the adjusted Bonferroni correction. We considered as up- or downregulated those genes having a natural logarithm of expression fold change of ≥ 1 or ≤ -1, respectively. We excluded those miRNAs having undetermined Ct or Ct values greater than 35 in both sample and calibrator. We also performed a second normalization with the global median normalization method. Similar to microarray analysis, for each sample, Ct values

were normalized with respect to the median of Ct of the array [78]. Data about the relative abundance of miRNAs in cell lines, before and after treatment, were displayed with MeV04 (http://www.tm4.org/mev.html).

MAPK Inhibitors treated samples

Given the relative instability of standard endogenous controls (eg, snRNA U6, snoRNA U48) in CRC, as reported by Chang *et al*. [93], we identified the most reliable genes to be used as normalizators within the arrays for the three cell lines for all the treatments to gain an accurate miRNA expression profiling. We applied two different methods for the identification of the most stable expressed genes: we first used DataAssist v.3 software (Applied Biosystems), which calculates the relative stability of candidate endogenous controls for all samples, calculating a score based on the Ct values for a given gene among all samples. This led to the identification of about 15 candidate endogenous controls, that we further filtered by applying the geNorm Algorithm, a Visual Basic Application (VBA) for Microsoft Excel, that calculates the gene expression stability among a set of control genes through an M-value: less stable genes are eliminated, leading to a step-by-step recalculation of the M-value for the remaining genes [94]. By this procedure we identified the following endogenous controls for each of the three cell lines, for both arrays: miR-532-5p, mir-130b and miR-26a for Array A, and miR-31*, miR-378, miR-151-3p and miR-126* for Array B, respectively. To identify miRNAs differentially expressed after treatment we applied the $2^{-\Delta\Delta Ct}$ method: data normalization was performed by using each of the six genes above-mentioned as endogenous controls. We accepted as reliable only fold change values concordant by using all endogenous controls. To evaluate miRNA expression variation we considered two different comparisons: a) each cell line after exposure to all inhibitors respect to their matched untreated controls (by this approach we obtained cell line-specific Differentially Expressed miRNAs (DE

miRNAs) after ERK pathway inhibition); b) all cell lines after a specific treatment respect to all untreated controls (to evaluate the drug-specific dysregulated miRNAs). RQ values < 1 were converted in negative fold changes by following formula: -1/RQ. The identification of DE miRNAs was performed by SAM (Significance of Microarrays Analysis), applying a Two-class paired test among ΔCt by using a p-value based on permutation (100 permutations); Imputation Engine: K-nearest neighbors (10 neighbors); False Discovery rate < 0.15. We accepted as reliable only those DE miRNAs concordant by using all endogenous controls. We excluded as DE miRNAs those having either undetermined Ct or Ct values > 35 in both sample and calibrator. The computation of SAM was obtained by using MeV04 software.

Tissue samples

CRC samples used in this study were collected as part of standard clinical care activity. Formalin-fixed, paraffin-embedded (FFPE) samples from CRC patients were obtained from the Unit of Pathology, Azienda Policlinico, University of Catania, and were analyzed in accordance with the policies of the institutional review board of the hospital. All the specimens were from surgical resection and verified by histopathologic confirmation of neoplastic phenotype. For DNA and total RNA isolation, 20-μm tissue sections were used. Total DNA and RNA from FFPE samples were extracted by using QIAamp DNA Kit (Qiagen, Hilden Germany) and RecoverAll Total Nucleic Acid Isolation Kit (Ambion, Applied Biosciences, Austin, TX), respectively, following the manufacturer's instructions.

Detection of KRAS mutations and miRNA expression assays in FFPE CRC samples

KRAS mutational status in FFPE samples was assessed by using real-time PCR allelic discrimination. DNA from each sample was analysed by TaqMan MGB custom assays (Applied Biosystems) discriminating the 7 most common mutations in codons 12 and 13 of KRAS [95]. In particular, we screened the following mutations: Gly12Ser (GGT>AGT), Gly12Arg (GGT>CGT), Gly12Cys (GGT>TGT), Gly12Asp (GGT>GAT), Gly12Ala (GGT>GCT), Gly12Val (GGT>GTT), Gly13Asp (GGC>GAC). All the PCR reactions were performed (in triplicates) on 7900HT Fast Real Time PCR System (Applied Biosystems) by using TaqMan Genotyping Master Mix (Applied Biosystems). Each mutation was assayed by using in the same reaction two different TaqMan probes, one probe for each allele in a two-allele system (wild type and mutated one). Each probe consists of an oligonucleotide with a 5′-reporter dye [FAM (allele1) and VIC (allele2)] and a 3′-quencher dye (TAMRA). Expression analysis of miRNAs from FFPE CRC was performed by TaqMan MicroRNA Assay (Applied Biosystems). Differential expression of miRNAs in CRC patients and normal colon epithelial tissue controls was evaluated by the Wilcoxon rank sum test ($P<0.05$).

miRNA target prediction and gene ontology term analysis

The analysis on DE miRNAs targets was carried out by using a combination of several approaches to obtain a short list of reliable mRNA targets. A first list of predicted and experimentally validated targets of DE miRNAs was extracted from miRecords, by interpolation between the highest number of the 11 prediction tools (http://mirecords.biolead.org).

Cetuximab treated samples

To improve the first list of predicted targets we used anticorrelation data between miRNAs and mRNAs or miRNAs and proteins [96, 97] and (http://discover.nci.nih.gov/cellminer/home.do). This additional filtering was also performed by using the Hoctar database for intronic miRNAs (http://hoctar.tigem.it). Standard Pearson correlation test was performed to verify the negative correlation between miRNAs and mRNAs by using $P < 0.05$. The Gene Ontology (GO) functional classification of miRNA targets was performed by using the cytoscape plug-in BINGO (http://www.psb.ugent.be/cbd/papers/BiNGO/Home.html). The analysis of statistically significant GO differences between time points was performed by using Babelomics tool FatiGO (http://babelomics3.bioinfo.cipf.es).

MAPK Inhibitors treated samples

To improve our prediction, we also used expression anticorrelation between miRNAs and their putative mRNAs targets: data were retrieved from http://mirgator.kobic.re.kr and other datasets. An additional filtering was performed by using starBase (sRNA target Base), a database for the exploration of miRNA–target interaction maps from a combination of CLIP-Seq and Degradome-Seq data, allowing the identification of the sites of Argonaute interactions and miRNA cleavage sites, respectively (http://starbase.sysu.edu.cn). CLIP-Seq experiments are based on crosslinking between RNA and proteins, followed by immunoprecipitation coupled with high-throughput sequencing, while degradome sequencing is a modified version of 5' RACE, used to analyze patterns of RNA degradation: the combination of these techniques is useful for the identification of miRNA-targets interactions. We improved the target list by the Gene Ontology (GO) functional classification of miRNA targets, by using DAVID Functional Classification tool (http://niaid.abcc.ncifcrf.gov/gene2gene.jsp): this led us to

focus on mRNA among our list, specifically involved in biological processes related to MAPK pathway (e.g. signal transduction, proliferation, cell cycle regulation, migration, adhesion). Finally, we filtered the list of predicted targets by excluding those that are not expressed in normal colon epithelium or in CRC (www.cgl.ucsf.edu/Research/genentech/genehub-gepis/index.html). Statistically validated expression values of miRNA targets from HT experiments in cancer models were from Oncomine repository (www.oncomine.org). We enriched our targets list by retrieving specific information about validated miRNA targets from literature (Figure 14).

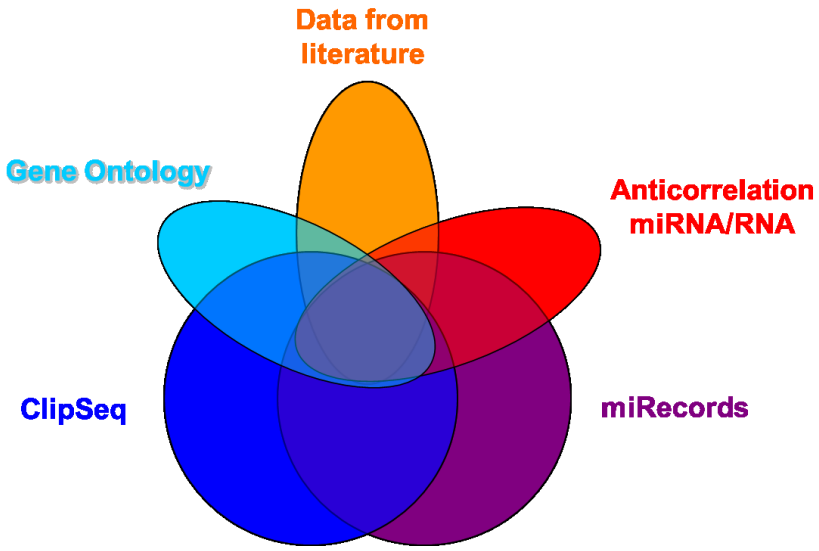

Figure 14. Diagram showing the overlapping between the different prediction methods used for target analysis.

The expression of putative targets after modulation of miRNA expression and after drug treatment was evaluated by Fast SYBR Green RT-PCR, according to the manufacturer instructions (Applied Biosystems). Primers for their amplification,

designed with Primer-BLAST (http://www.ncbi.nlm.nih.gov/tools/primer-blast/), are shown in Table 4.

Table 4. Primers designed for the expression analysis of DE miRNAs target genes.

GENE	Fw SEQUENCE	Rev SEQUENCE	AMPLIMER LENGTH (bp)
ARFIP2	CACGGGAACGGCGAAGCCAG	CGGCCAGACCCTGTGGGGAT	158
BNIPL	TTTGAGTGGAGGCACAAGCAGGG	GGGCTCGCAGGTTTTTCCGT	101
BUB3	TGGGTTACGTGCAGCAGCGC	CTCAACTGCCACTCGGCCTTCA	119
CABLES1	TGCGGCAACACGATACCAGGAA	ACTGTCGCGATACGGCAGCAC	95
CAMTA1	AAGAGAGGCACCGCTGGAACAC	GTGGTCTTGTCTTAGGGGAGGTGGT	102
CCND2	CACCTGGATGCTGGAGGTCTGTGA	CGGGACCCCAGCCAAGAAACG	97
CDKN1A	GCACTCAGAGGAGGCGCCATGT	GCAGCCCGCCATTAGCGCAT	141
CFL2	TTCTTAATCGCCTGTATGGTGGT	GCCGAAACTGTTACCTGTCTC	140
CREB5	AGCATCATGGGGATGCAAGGTCC	GGCAGCAGGGTGGTGAGTCAA	120
CREBL2	GAAGAGTTGGTATCCAGTCGAGA	GGGCCTTTATTTCAGAAGGGATT	118
DCN	GGTGGGCTGGCAGAGCATAAGT	CTGGACCGGGTTGCTGAAAAGAC	150
DMBT1	GGCCAGGGCTCAGGACCCATTG	ATGCATGTGAGGTCGGCCAAGT	190
FOXO3	AGCAACAGCTCTGCCGGCTG	GGGCTTTTCCGCTCTTCCCCC	142
GAS7	ACCCAGACACGATGCCGGAACA	AGTTCAAACCCAGCCACGGTGC	118
GRB2	AGCTACTGCAGACGACGAGCTG	GCCGTCTTTTCCATTAAGCTCTGCC	109
LATS2	CAGCAGGAGCATCGAGGCCG	CTCCGCGTCACTGGGGTTGG	135
LFNG	GGGAAGATGAGGCCCTGGCCAG	CGTAGTTGTCATCGTCCACGTGGC	162
LIMK1	AGGTGACACACCGTGAGACA	CCAGGCATCGCATGACCTT	111
NAPEPLD	CACAGCAGTGTTCCAAGTTCT	GTCCCAGCCATGTGACTCTT	127
PDCD4	ACCACAGTTGGTGGGCCAGTTT	ACGGTAGCCTTATCCAGAGCAGCT	129
PTEN	AATGTTCAGTGGCGGAACTTGCA	CGTCGTGTGGGTCCTGAATTGGA	90
RAB5C	AGCACAATTGGAGCGGCCTTCC	GGGCCAGGCTGTGATACCGC	109
SCRIB	GCGACACCCTCACCGTGCTG	CTGTTCCGGTGGCCGATGCC	118
SLC2A1	GGCATGGCGGGTTGTGCCAT	ATGGGATGGGGCCAGGACCC	136
SOCS5	TCCCGCCCCTCTAAAGCCCTG	ACGGCTTCCTCCCTCATGACCGA	127
SOCS5	GCAGGTGCCCTGGATGAGGCC	ACTACGGCTTCCTCCCTCATGACCG	133
SOX6	ATGGACCTTGCTCGCCAACAGC	TGAGCGGAGGCATGTGACCC	124
SRF	GCAAGCGTCTCCCTCCCGTG	ACGTCATGATGGTGGCGGGC	89
TBC1D4	TCCTGGCGGCAGCGCATTTT	GGGGACAGTGGCAGCAGCTC	110
TICAM1	AACTCCGCAGAAGCCCCAGC	TGCAGGAGCTGCCCAAGCAG	91
TMEM178	TCTCAGCCCATCCGCTTGCGAA	GCCGCAGAGAAGGACGGCTAC	135
TMEM52	TGCGACGTGGCAGTCATCCC	TACTGCACGGAGCTGTAGGAGGT	77
TRIP10	CTGAACTCCGAGGCCCGGGT	TGCTGCTCTGGGGGCAAGTG	106
TXNIP	CATCCAGCATGGCCAGCCGAA	TAGCAGGGAGGAGCTTCTGGGGTA	85
ZNF512B	GGTGCTGCTGACCAGGTCGG	TGGGCAGGTGTCCAGGCTGT	94
ZWINT	GCTGAACTCGGCGCCTGGAAA	ATGCCTGCCACCTCAGCCAG	87
Endogenous control: PPIA	TCGTGCCGTTTTGCAGACGC	CAAACAGCTCAAAGGAGACGCGG	127

Computational genomic analysis

To evaluate the regulatory networks in which DE miRNAs are involved, we computationally identified transcription factors (TFs) potentially regulating them. Predicted evolutionarily conserved and validated Transcription Factor Binding Sites (TFBS) were retrieved from TransMir (http://202.38.126.151/hmdd/mirna/tf), PuTmiR (www.isical.ac.in/~bioinfo_miu), mirGen 2.0 (http://diana.cslab.ece.ntua.gr/mirgen), CircuitsDB (http://biocluster.di.unito.it/circuits), and ECR Browser (http://ecrbrowser.dcode.org). The prediction of transcription factors was improved by verifying the correlation of expression (positive or negative) between the predicted couples miRNA/TF by using Multiexperiment Matrix (http://biit.cs.ut.ee/mem).

Network analysis

Cetuximab treated samples

The biological networks of miRNA target genes were built by retrieving the corresponding interactome data through cytoscape plug-in APID2NET (http://bioinfow.dep.usal.es/apid/apid2net.html). They include validated differentially expressed miRNA targets, predicted targets from our anticorrelation analysis, and first neighbors of the targets. The analysis of network centrality was performed using the plug-in Network Analyzer (http://med.bioinf.mpi-inf.mpg.de/netanalyzer). Data on functional relationship between genes and drugs were extracted from the PharmGKB (http://www.pharmgkb.org/index.jsp) and Comparative Toxicogenomics Database (http://ctd.mdibl.org/), whereas the information about cancer involvement was obtained from Database of Functional

Census of Human Cancer Genes (http://bioinfo.hrbmu.edu.cn/fcensus/Home.jsp), miR2Disease database, and literature (http://www.mir2disease.org).

MAPK Inhibitors treated samples

The biological network of miRNAs, TFs, target genes was built by retrieving the corresponding interactome data through Cytoscape NCBI Entrez EUtilities Web Service Client (www.pathwaycommons.org/pc/cytoscape.do). Network centrality analysis was performed through the plug-in Network Analyzer. The enrichment of nodes from the MAPK pathway was performed by using DAVID Functional Classification Tool.

In vitro modulation of miRNA expression

Caco-2, HCT-116 and SW-620 cell lines were transfected with 17.5 to 60 pmoles of anti-miR-92a-1*, 1226*, 372, 135b*, miR-720 and relative negative controls, and 15 pmoles of pre-miR-663b and relative negative control (Ambion, Austin, TX, USA), respectively. Transfection experiments were performed by using the reverse transfection protocol, according to the manufacturer's instructions. Briefly, siPORT NeoFX Transfection Agent (Ambion) was diluted in optiMEM mediun (Gibco). Anti-miRNAs and relative negative controls were diluted in optiMEM. The diluted transfection reagent was combined with each of the diluted anti-miRNAs, pre-miR-663B and relative negative controls, followed by incubation at 20°C for 10'. The mixture was dispensed into 24 well plates, and $6x10^4$ cells were seeded per well. All the experiments were performed in biological triplicates. Total RNA was extracted at different time points (24, 48, 72h post-transfection, PT) and used for both confirming transcription efficiency (>70%) and performing expression analysis of putative targets by RT-PCR.

Cell viability and apoptosis assays

For MTT assay and apoptosis detection after miRNAs modulation, we transfected the three cell lines by seeding 1.2×10^4 cells per well in 96-well plates and appropriately scaling the amount of transfection reagents. The MTT assay was performed, as previously discussed, to assess cell viability at 24, 48, and 72 h PT. Apoptosis was analyzed with the APOPercentage apoptosis assay kit (Biocolor). This assay is a detection and measurement system that monitors the occurrence of apoptosis in anchorage-dependent cells during *in vitro* culture. The maintenance of phospholipids asymmetry is essential for normal transmembrane function, and disruption of this asymmetry is associated with cell activation or pathologic conditions. The process is regulated by 'flippases', which catalyze the active transport of aminophospholipids from the outer to inner monolayer. In cells undergoing apoptosis, flippase is overwhelmed by the action of another enzyme, termed 'floppase' or 'scramblase', which randomizes the distribution of newly synthesized lipids [98]. The transfer of phosphatidylserine to the outside of the membrane, which is one of the earliest apoptotic events, permits the transport of the APOPercentage dye into the cell. The uptake of the dye is unidirectional, leading to dye accumulation within the cell (Figure 15).

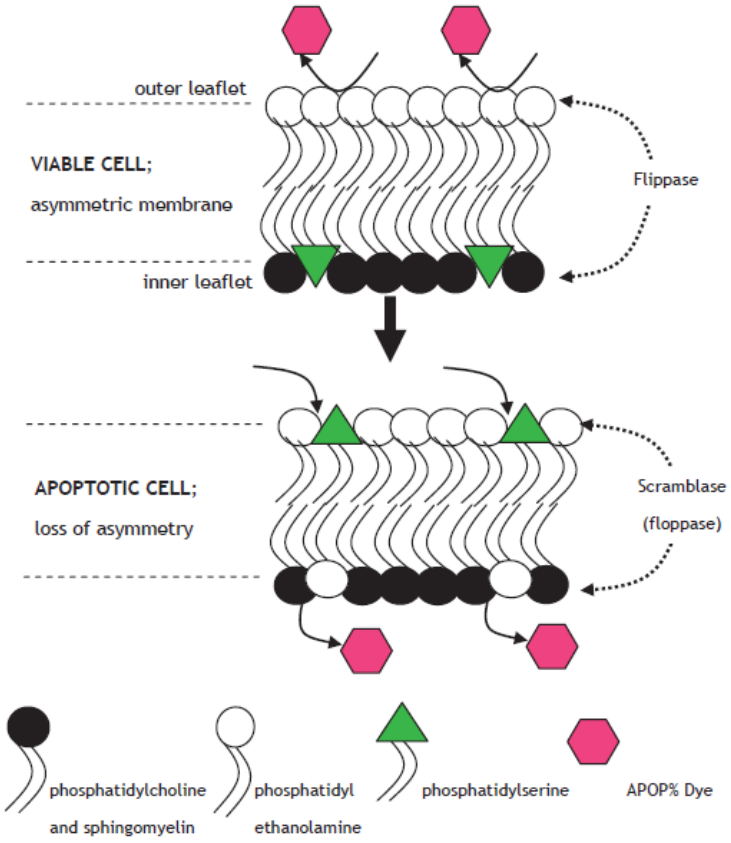

Figure 15. Principle of APOPercentage assay: the dye enters the cell when asymmetric phospholipid composition of mammalian cell membrane is lost.

We evaluated apoptosis rates at 24 and 48 h PT, according to manufacturer's instructions. Thirty minutes prior to the end of the incubation period for the transfections, the apoptosis specific purple dye was added to each well. Cells were then washed twice with PBS and photographed with an Olympus BX50 fluorescence microscope equipped with a Leica DC500 digital colour camera. Apoptosis was quantified by counting dye-positive cells in each well. All the experiments were performed in six biological replicates. Similar experimental

procedures were used to assay apoptosis 12, 24, and 48 h after treatment with the three specific inhibitors of MAPK pathway.

Cell migration assay

Migration rates after transfection were evaluated by Oris™ Universal Cell Migration Assembly Kit (Platypus Technologies, LCC) according to the manufacturer's instructions.

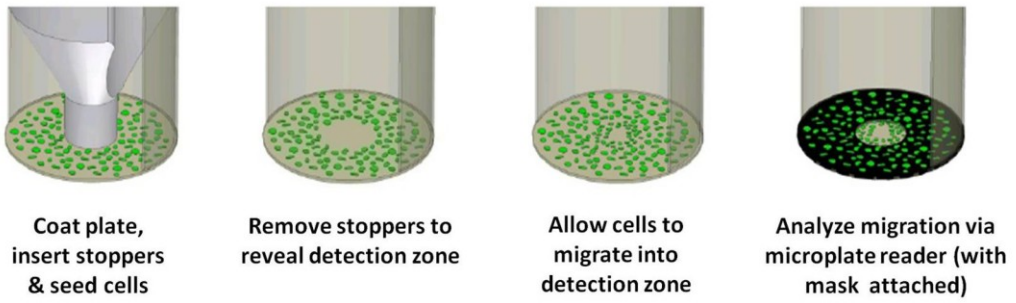

Figure 16. Schematic representation of Oris cell migration assay.

Briefly, Caco-2, HCT-116 and SW-620 cells, transfected with pre-miRNA, anti-miRNAs and their negative controls, were seeded into 96 well plates at $8x10^4$, 1 and $1.2x10^5$ cells per well, respectively, after insertion of Oris™ Cell Seeding Stoppers (Platypus Technologies) (Figure 16). To create the detection zone to the centre of the well, the stoppers were removed at 24h post-transfection (0h), and, after washing cells with PBS, fresh culture medium was added. Endpoint detection of cell migration into detection zone was performed at 24h after the stoppers

removal using Giemsa (Invitrogen) colorimetric stain. The detection zones for each well were photographed with a microscope Zeiss Axioplan at 0h (pre-migration reference wells) and 24h. The cells migrated into detection zone were quantified by converting digital images into pixel numbers with GIMP (GNU Image Manipulation Program) software. All the experiments were performed in biological triplicates. Similar experimental procedures were followed to assay cell migration after drug treatment.

4. RESULTS

ALTERATIONS OF miRNA TRANSCRIPTOME AND GLOBAL NETWORK STRUCTURE IN COLORECTAL CARCINOMA AFTER CETUXIMAB TREATMENT

Sensitivity of colon cancer cells to cetuximab treatment

To test the sensitivity of CRC cell lines to cetuximab, Caco-2 and HCT-116 viability after drug treatment was analyzed along a time course of 72 hours by using the MTT assay. Cetuximab had an evident negative time dependent effect on Caco-2 cell line viability. On the other hand, as expected based on KRAS mutation present in HCT-116 genome, the MTT assay showed no appreciable effects on HCT-116 viability (Figure 17).

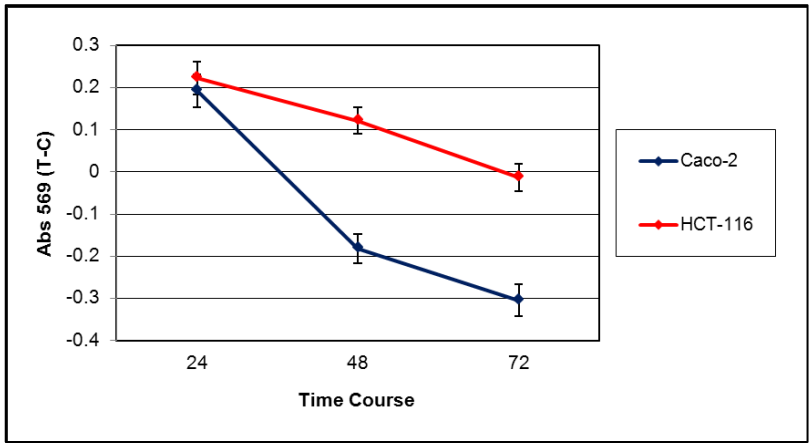

Figure 17. MTT viability assay on Caco-2 and HCT-116 cell lines after cetuximab treatment. Abs= absorbance values at 569 nm. T= treated; C= control.

The aim of this research was the identification of a specific set of differentially expressed miRNAs that can be ascribable to the different genomic features of these two cell lines, which reflect in some way (with all the limitations associated to the use of *in vitro* models) the situation of colorectal cancer patients respect to the possibility of being treated or not with mAbs targeting EGFR.

Analysis of miRNA transcriptome after cetuximab treatment

We performed the expression profiling of 667 miRNAs in Caco-2 and HCT-116 cell lines, 24 and 48 hours after cetuximab treatment, by using TaqMan low density array (TLDA) technology. To assess the reproducibility of TaqMan TLDA we computed the Pearson correlation (r; $P < 0.01$) among the ΔCt of biological replicates of treated and untreated cell lines. We found a high concordance between the 3 biological replicates for each sample (mean of $r > 0.87 \pm 0.07$) (Figure 18).

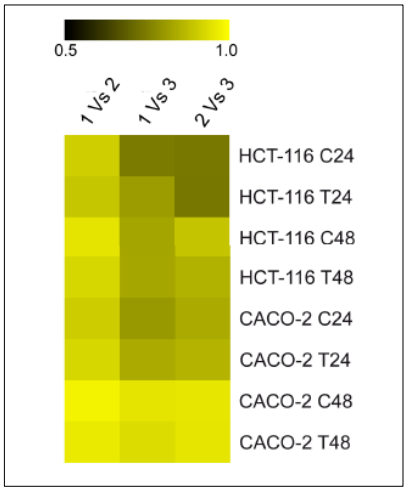

Figure 18. Matrix of r values calculated for each possible combination of the three biological replicates (P value < 0.01; N=673). 1, 2, 3 = biological replicates.

The results obtained using the two different normalization methods ($2^{-\Delta\Delta Ct}$ and global median normalization, see Materials and Methods) are comparable with each other; however, we selected the $2^{-\Delta\Delta CT}$ method for further analysis, as it was shown to be more stringent. After 24 hours of cetuximab treatment, we found 12 differentially expressed miRNAs (6 downregulated and 6 upregulated) in Caco-2 cells, and 16 differentially expressed miRNAs (11 downregulated and 5 upregulated) in HCT-116. After 48 hours incubation with cetuximab, we observed 10 deregulated miRNAs in Caco-2 (8 downregulated and 2 upregulated), and 6 differentially expressed miRNAs in HCT-116 (5 downregulated and 1 upregulated) (Table 5).

Table 5. miRNAs differentially expressed after 24 and 48 hours of cetuximab treatment.

Caco-2				HCT-116			
miRNA differentially expressed after 24 h of cetuximab treatment	**Average ln**	**miRNA differentially expressed after 48 h of cetuximab treatment**	**Average ln**	**miRNA differentially expressed after 24 h of cetuximab treatment**	**Average ln**	**miRNA differentially expressed after 48 h of cetuximab treatment**	**Average ln**
hsa-miR-18a*	0.92	hsa-miR-17*	−2.45	hsa-let-7b	−1.97	hsa-miR-146a	1.15
hsa-miR-122	1.94	hsa-miR-107	−0.93	hsa-let-7e	−1.37	hsa-miR-152	−3.10
hsa-miR-124	−2.66	hsa-miR-122	−1.28	hsa-miR-17*	3.15	hsa-miR-223	−1.54
hsa-miR-330-5p	3.66	hsa-miR-133b	−2.76	hsa-miR-148a	−3.38	hsa-miR-323-3p	−2.53
hsa-miR-486-5p	3.82	hsa-miR-144*	−3.49	hsa-miR-181c*	4.76	hsa-miR-503	−4.75
hsa-miR-512-3p	3.53	hsa-miR-146b-3p	4.7	hsa-miR-193b*	2.74	hsa-miR-597	−1.74
hsa-miR-517c	−2.18	hsa-miR-219-1-3p	−3.54	hsa-miR-202	−3.89		
hsa-miR-523	3.11	hsa-miR-499-5p	−2.68	hsa-miR-219-1-3p	−2.34		
hsa-miR-545	−2.4	hsa-miR-576-3p	2.56	hsa-miR-330-3p	−1.34		
hsa-miR-610	−1.73	hsa-miR-610	−3.48	hsa-miR-330-5p	4.88		
hsa-miR-622	−1.05			hsa-miR-423-5p	−1.04		
hsa-miR-636	−1.06			hsa-miR-509-5p	3.37		
				hsa-miR-542-3p	−2.05		
				hsa-miR-542-5p	−2.54		
				hsa-miR-610	−5.83		
				hsa-miR-708	−4.04		

NOTE: miRNA expression is reported as average Ln of relative quantity of treated samples with respect to their time matched controls.

Interestingly, the sets of differentially expressed miRNAs in the two cell lines at both time points is not overlapping, confirming that the 2 cell lines respond differently to cetuximab, as already shown by MTT experiments, with some exceptions: miR-610 is generally downregulated in both cell lines along the time course (except for HCT-116 at 48 hours); miR-219-1-3p was downregulated in Caco-2 and HCT-116 24 and 48 hours after treatment, respectively; miR-330-5p, upregulated in both cell lines at 24 hours post treatment. About 35% of the differentially expressed miRNA genes in Caco-2 and HCT-116 showed the same expression trend in the two time points, suggesting that the miRNA regulation processes triggered by cetuximab start in early phases after drug subministration but keeps going during the time course (Figure 19).

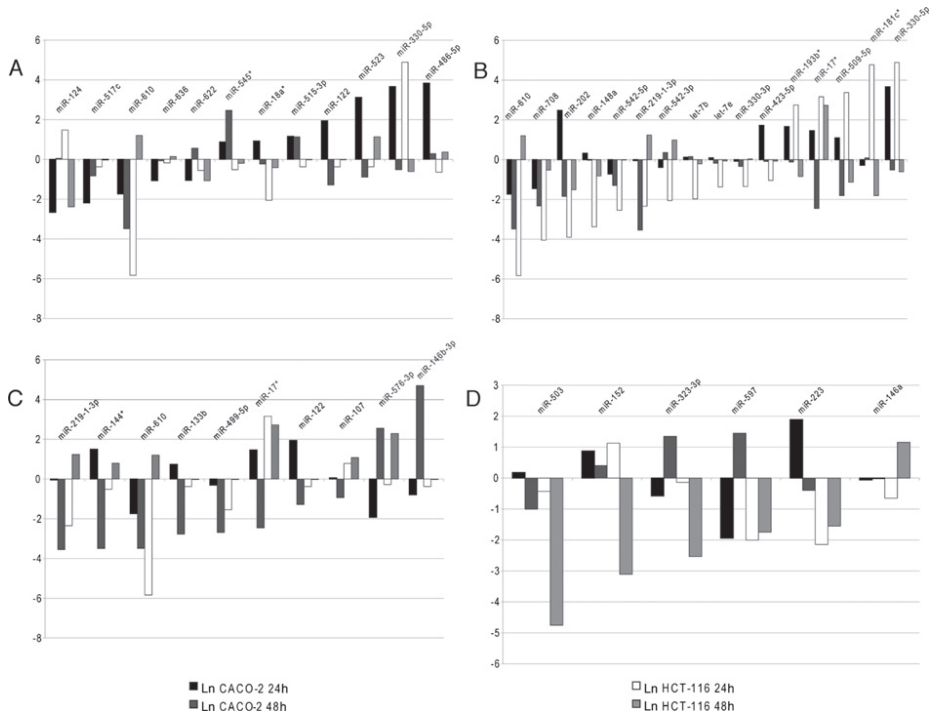

Figure 19. Differentially expressed miRNAs after cetuximab treatment in (A) Caco-2 at 24h, (B) HCT-116 at 24h, (C) Caco-2 at 48h, (D) HCT-116 at 48h (paired t test, $P < 0.01$). Data are shown as average natural logarithm (ln) of relative quantity of miRNAs in treated cells with respect to the time-matched untreated control.

On the other hand, some miRNAs show opposite expression patterns in the two cell lines after treatment: miR-17*, upregulated in HCT-116 at 24 hours, was downregulated in Caco-2 at 48 hours post treatment. Finally, miR-122 is overexpressed in Caco-2 after 24 hours but reduced its expression at 48 hours. These peculiarities in miRNA expression changes after 24 and 48 hours of cetuximab treatment in the two cell lines could suggest a role of these miRNAs within the signaling cascade triggered by this drug. We finally compared the RQ values of miRNAs at steady state in both cell lines, finding that about 7% of all miRNAs analyzed had different basal expression levels in the 2 cell lines. This suggests that the corresponding molecular networks at steady state may be differentially prone to respond to EGFR inhibitors. Furthermore, about 8% (let-7b, miR-146a, miR-330-3p, and miR-486-5p) of differentially expressed miRNAs in treated Caco-2 and HCT-116 also seemed to be differentially expressed in the 2 cell lines at steady state.

Correlation between KRAS mutational status and miRNA expression in FFPE CRC samples

In our cohort of CRC patients we found 14 KRAS wild-type and 11 KRAS mutated. We have chosen a set of 10 miRNAs to be tested in these patients among differentially expressed miRNAs (5 differentially expressed after treatment, and 5 miRNAs with unchanged expression as a control): miR-17a, miR-19a*, miR-99b, miR-146b-3p, miR-194, miR-219-1-3p, miR-330-5p, miR-486-5p, miR-497, and miR-708. Our data indicated that, while the expression of the most of analyzed miRNAs is not substancially different between patients with wild-type or mutated KRAS, miR-146b-3p and miR-486-5p had expression levels significantly elevated in KRAS mutated CRC samples when compared with KRAS wild-type ones (Wilcoxon rank sum test: $P < 0.03$ and $P < 0.006$, respectively; Figure 20).

Moreover, miR-486-5p was also more expressed in HCT-116 than Caco-2 cell line, while both miRNAs were upregulated in Caco-2 after cetuximab treatment.

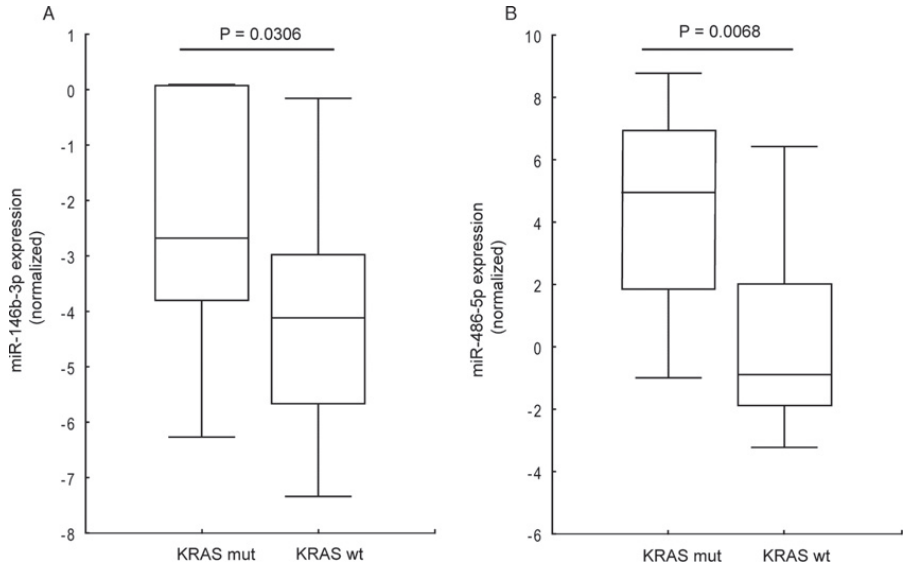

Figure 20. Box and Whisker plot showing miR-146b-3p (A) and miR-486-5p (B) expression in formalin-fixed, paraffin-embedded tissue samples from CRC patients. Expression values are shown as ΔCt normalized using snRNA U6 and multiplied by -1.

Identification of putative conserved TFBS for co-regulated miRNAs

To find common regulatory mechanisms controlling miRNA expression after treatment, we searched for validated or predicted TFBSs in genomic regions upstream of miRNA genes and evaluated the expression correlation between transcription factors and miRNAs. We found TFBSs for 203 transcription factors, focusing on 25 based on the number of occurrences and their involvement in CRC pathogenesis and in pharmacologic response (Table 6). As expected, many

differentially expressed miRNAs are controlled by CRC related transcription factors: MYC, amplified and overexpressed in CRC; TCF3, controlled by the WNT pathway; YY1 and ZEB1 overexpressed in CRC; HAND1 and PAX6, frequently hypermethylated in CRC; JUN, activated by KRAS cascade; MYB, activated in CRC; and TP53, deleted or mutated in CRC. Interestingly, we found that some of the genes, controlled by KRAS pathway and involved in cetuximab response, potentially control the expression of differentially expressed miRNAs. For instance, ELK1 putatively regulates miR-193b* and miR-523 and is positively correlated to their expression; STAT1, activated by EGF signaling, could be responsible for miR-146b-3p abundance in KRAS–mutated FFPE samples; in KRAS wild-type cell line, where miR-145 (targeting STAT1) is downregulated, STAT1 potentially activates miR-146b-3p after 48 hours of cetuximab exposure. By mining TransMir, we found that MYC represses expression of let-7b and let-7e (their pre-miR also had anticorrelated expression with MYC) and could be responsible for downregulation of these miRNAs 24 hours after treatment. Finally, miR-17* expression during cetuximab treatment in Caco-2 and HCT-116 could be due to the regulation of miR-17-92 cluster by MYC and NK-like family of homeobox genes (NKX2-5, TLX1, and TLX3). We filtered and validated the data on TFBSs through the analysis of expression correlation among transcription factors and miRNAs: HNF4A, RUNX1, and TCF3 are the TFs controlling the highest number of differentially expressed miRNAs (≥15) in both cell lines after treatment. TFs with functions related to organ development or involved in different cancers (i.e., FOXD3, GATA1, HNF1A, MAF, NKX2-5, PAX4, and POU2F1), had a high occurrence of TFBS and were correlated with the expression of differentially expressed miRNAs. Based on these findings, we hypothesize their potential involvement also in CRC response to cetuximab.

Table 6. List of the main miRNA-regulating transcription factors.

TF OFFICIAL GENE SYMBOL	LOCUS	MIRNA	TRANSMIR VALIDATED PMID	EXPRESSION CORRELATION	CRC-RELATED PUBMED ID	EGFR PATHWAY-RELATED KEGG ID
CUX1	miR-152	miR-152		correlated		
CUX1	miR-148a	miR-148a		correlated		
CUX1	miR-219-1	miR-219-1-3p		correlated		
CUX1	miR-107	miR-107		anticorrelated		
CUX1	miR-423	miR-423-5p		anticorrelated		
ELK1	miR-523	miR-523		correlated		ko04012
ELK1	miR-193b	miR-193b*		correlated		ko04012
FOXA2	miR-122	miR-122		correlated	17283222	
FOXA2	miR-107	miR-107		anticorrelated	17283222	
FOXA2	miR-124-3	miR-124		anticorrelated	17283222	
FOXA2	miR-152	miR-152		anticorrelated	17283222	
FOXA2	miR-323	miR-323-3p		anticorrelated	17283222	
FOXD3	miR-146a	miR-146a		correlated		
FOXD3	miR-146b	miR-146b-3p		correlated		
FOXD3	miR-122	miR-122		correlated		
FOXD3	miR-124-1	miR-124		anticorrelated		
FOXD3	miR-124-3	miR-124		anticorrelated		
FOXD3	miR-330	miR-330-5p		anticorrelated		
FOXD3	miR-330	miR-330-3p		anticorrelated		
FOXD3	miR-17	miR-17*		not analyzed		
FOXD3	miR-517c	miR-517c		anticorrelated		
FOXD3	miR-152	miR-152		anticorrelated		
FOXD3	let-7e	let-7e		anticorrelated		
FOXJ2	miR-133b	miR-133b		not analyzed		
FOXJ2	miR-146b	miR-146b-3p		anticorrelated		
FOXJ2	miR-148a	miR-148a		anticorrelated		
FOXJ2	let-7e	let-7e		correlated		
GATA1	miR-144	miR-144*	18303114	correlated		
GATA1	miR-523	miR-523		correlated		
GATA1	miR-124-1	miR-124		correlated		
GATA1	miR-133b	miR-133b		correlated		
GATA1	miR-152	miR-152		anticorrelated		
GATA1	miR-181c	miR-181c*		anticorrelated		
HAND1	miR-499	miR-499-5p		correlated	19723660	
HAND1	miR-107	miR-107		correlated	19723660	
HAND1	miR-219-1	miR-219-1-3p		anticorrelated	19723660	
HAND1	let-7b	let-7b		anticorrelated	19723660	
HAND1	miR-181c	miR-181c*		anticorrelated	19723660	
HNF1A	miR-133b	miR-133b		correlated		
HNF1A	miR-107	miR-107		correlated		
HNF1A	miR-122	miR-122	19617899	correlated		
HNF1A	miR-423	miR-423-5p		anticorrelated		
HNF1A	miR-17	miR-17*		anticorrelated		
HNF1A	miR-503	miR-503		anticorrelated		
HNF1A	miR-146b	miR-146b-3p		anticorrelated		
HNF4A	miR-144	miR-144*		correlated		
HNF4A	miR-18a	miR-18a*		correlated		
HNF4A	miR-202	miR-202		correlated		
HNF4A	miR-517c	miR-517c		correlated		
HNF4A	miR-107	miR-107		correlated		
HNF4A	miR-181c	miR-181c*		correlated		
HNF4A	miR-330	miR-330-5p		correlated		
HNF4A	miR-330	miR-330-3p		correlated		
HNF4A	miR-323	miR-323-3p		correlated		
HNF4A	miR-17	miR-17*		not analyzed		
HNF4A	miR-499	miR-499-5p		correlated		

HNF4A	let-7e	let-7e		anticorrelated		
HNF4A	miR-124-2	miR-124		anticorrelated		
HNF4A	miR-124-3	miR-124		anticorrelated		
HNF4A	miR-148a	miR-148a		anticorrelated		
HNF4A	miR-503	miR-503		anticorrelated		
HNF4A	miR-146b	miR-146b-3p		anticorrelated		
HNF4A	miR-193b	miR-193b*		anticorrelated		
HNF4A	miR-219-1	miR-219-1-3p		anticorrelated		
HNF4A	let-7b	let-7b		anticorrelated		
JUN	let-7e	let-7e		correlated	20395206	
JUN	let-7b	let-7b		correlated	20395206	
JUN	miR-219-1	miR-219-1-3p		correlated	20395206	
JUN	miR-323	miR-323-3p		correlated	20395206	
JUN	miR-181c	miR-181c*		correlated	20395206	
JUN	miR-148a	miR-148a		anticorrelated	20395206	
MAF	miR-499	miR-499-5p		correlated		
MAF	miR-146b	miR-146b-3p		correlated		
MAF	miR-330	miR-330-5p		correlated		
MAF	miR-330	miR-330-3p		correlated		
MAF	miR-122	miR-122		correlated		
MAF	miR-124-1	miR-124		anticorrelated		
MAF	miR-219-1	miR-219-1-3p		anticorrelated		
MAF	let-7b	let-7b		anticorrelated		
MYB	miR-523	miR-523		correlated	18574464	
MYB	miR-148a	miR-148a		correlated	18574464	
MYB	miR-124-2	miR-124		correlated	18574464	
MYB	miR-124-3	miR-124		correlated	18574464	
MYB	miR-17	miR-17*		anticorrelated	18574464	
MYB	miR-202	miR-202		anticorrelated	18574464	
MYB	miR-193b	miR-193b*		anticorrelated	18574464	
MYC	miR-17	miR-17*	17943719, 19066217	not analyzed	20029424	ko04012
MYC	let-7e	let-7e	19211792	anticorrelated	20029424	ko04012
MYC	miR-499	miR-499-5p		anticorrelated	20029424	ko04012
MYC	let-7b	let-7b	19211792	anticorrelated	20029424	ko04012
MYOG	miR-133b	miR-133b		correlated		
MYOG	miR-17	miR-17*		anticorrelated		
MYOG	miR-499	miR-499-5p		anticorrelated		
MYOG	miR-219-1	miR-219-1-3p		anticorrelated		
NKX2-5	miR-193b	miR-193b*		anticorrelated		
NKX2-5	miR-133b	miR-133b		correlated		
NKX2-5	miR-499	miR-499-5p		correlated		
NKX2-5	miR-17	miR-17*		not analyzed		
NKX2-5	miR-423	miR-423-5p		anticorrelated		
NKX2-5	miR-219-1	miR-219-1-3p		anticorrelated		
PAX4	miR-499	miR-499-5p		correlated		
PAX4	miR-133b	miR-133b		correlated		
PAX4	miR-330	miR-330-5p		correlated		
PAX4	miR-330	miR-330-3p		correlated		
PAX4	miR-323	miR-323-3p		anticorrelated		
PAX4	miR-17	miR-17*		anticorrelated		
PAX4	miR-152	miR-152		anticorrelated		
PAX4	miR-219-1	miR-219-1-3p		anticorrelated		
PAX4	miR-122	miR-122		anticorrelated		
PAX6	miR-503	miR-503		correlated	10344734	
PAX6	miR-323	miR-323-3p		correlated	10344734	
PAX6	miR-148a	miR-148a		anticorrelated	10344734	
PAX6	miR-133b	miR-133b		not analyzed	10344734	
PAX6	miR-146a	miR-146a		anticorrelated	10344734	
PAX6	miR-219-1	miR-219-1-3p		anticorrelated	10344734	
PAX6	miR-146b	miR-146b-3p		anticorrelated	10344734	
POU2F1	miR-144	miR-144*		correlated		

POU2F1	miR-18a	miR-18a*		correlated		
POU2F1	miR-517c	miR-517c		correlated		
POU2F1	miR-523	miR-523		correlated		
POU2F1	miR-133b	miR-133b		correlated		
POU2F1	miR-17	miR-17*		correlated		
POU2F1	miR-330	miR-330-5p		correlated		
POU2F1	miR-330	miR-330-3p		correlated		
POU2F1	miR-148a	miR-148a		anticorrelated		
POU2F1	miR-152	miR-152		anticorrelated		
POU2F1	miR-193b	miR-193b*		anticorrelated		
POU2F1	miR-219-1	miR-219-1-3p		anticorrelated		
PPARG	miR-107	miR-107		correlated	18391483	
PPARG	miR-144	miR-144*		anticorrelated	18391483	
REL	miR-133b	miR-133b		correlated		
REL	miR-17	miR-17*		anticorrelated		
REL	miR-193b	miR-193b*		anticorrelated		
RUNX1	miR-107	miR-107		correlated		
RUNX1	miR-18a	miR-18a*		correlated		
RUNX1	miR-523	miR-523		correlated		
RUNX1	miR-223	miR-223		correlated		
RUNX1	miR-122	miR-122		correlated		
RUNX1	miR-181c	miR-181c*		correlated		
RUNX1	miR-124-1	miR-124		correlated		
RUNX1	miR-124-2	miR-124		correlated		
RUNX1	miR-124-3	miR-124		correlated		
RUNX1	miR-17	miR-17*		not analyzed		
RUNX1	miR-499	miR-499-5p		correlated		
RUNX1	miR-133b	miR-133b		correlated		
RUNX1	miR-202	miR-202		anticorrelated		
RUNX1	miR-193b	miR-193b*		anticorrelated		
RUNX1	miR-219-1	miR-219-1-3p		anticorrelated		
TCF3	miR-486	miR-486-5p		correlated	11326276	
TCF3	miR-144	miR-144*		correlated	11326276	
TCF3	miR-523	miR-523		correlated	11326276	
TCF3	miR-107	miR-107		correlated	11326276	
TCF3	let-7b	let-7b		correlated	11326276	
TCF3	miR-124-1	miR-124		correlated	11326276	
TCF3	miR-124-2	miR-124		correlated	11326276	
TCF3	miR-124-3	miR-124		correlated	11326276	
TCF3	miR-330	miR-330-5p		not analyzed	11326276	
TCF3	miR-330	miR-330-3p		not analyzed	11326276	
TCF3	miR-17	miR-17*		anticorrelated	11326276	
TCF3	miR-181c	miR-181c*		anticorrelated	11326276	
TCF3	miR-193b	miR-193b*		not analyzed	11326276	
TCF3	miR-202	miR-202		anticorrelated	11326276	
TCF3	miR-499	miR-499-5p		anticorrelated	11326276	
TCF3	miR-512-2	miR-512-3p		anticorrelated	11326276	
TCF3	miR-517c	miR-517c		anticorrelated	11326276	
TCF3	miR-146b	miR-146b-3p		anticorrelated	11326276	
TCF3	miR-323	miR-323-3p		anticorrelated	11326276	
TCF3	miR-219-1	miR-219-1-3p		anticorrelated	11326276	
TP53	miR-202	miR-202		correlated	16172461	
TP53	miR-107	miR-107	20308559	correlated	16172461	
TP53	miR-223	miR-223		anticorrelated	16172461	
YY1	miR-107	miR-107		correlated	19360355	
YY1	let-7e	let-7e		correlated	19360355	
YY1	miR-181c	miR-181c*		correlated	19360355	
ZEB1	miR-517c	miR-517c		correlated	17486063	
ZEB1	miR-423	miR-423-5p		anticorrelated	17486063	

MiRNA targets and biological networks

To evaluate the biological significance of the differentially expressed miRNAs we have identified in this study, we searched for their involvement in human cancer and in CRC, finding that 67% of them are involved in cancer, and around 20% are specifically related to CRC. Interestingly, 50% of miRNAs showing a different abundance in the sensitive and resistant cell lines at steady state are involved in CRC, suggesting that the basal differential expression of these miRNAs could be responsible for the different response of these cells to the drugs, being related to their different mutational status altering MAPK pathway-related processes. We identified DE miRNA molecular targets (validated and predicted), overlapping two different methods in order to increase the stringency of our results (see Materials and Methods): this led us to identify 513 miRNAs targets (226 experimentally validated and 287 predicted). We kept only those predicted targets having a negative Pearson coefficient in the correlation analysis with miRNA expression ($P < 0.05$). About 30% of the cancer-related targets we identified were involved in CRC. Moreover, we found that about 36% of targets had been previously reported to be involved in CRC response to drugs and 11 targets had been previously reported to be involved in the cetuximab pathway (Table 7). We built the networks of differentially expressed miRNAs after treatment, in both cell lines for each time point, by retrieving protein–protein and DNA–protein interactions of their targets and first neighbors. Interestingly, we found that AKT1, GRB2, MYC, NFKB2, PLCG1, RAF1, and SP1, all related to the cetuximab pathway, are present in all networks and, in most of cases, are also the network hubs (>90 interactions); moreover, around 7% of genes in each of the four networks are involved in several types of cancer, including CRC, and ≥20% of these genes are involved in CRC response to drug treatment.

Table 7. miRNA targets involved in cetuximab pathway, CRC, and CRC response to drugs.

	Target genes	DE miRNAs targeting mRNAs	Caco-2 expression	HCT-116 expression
miRNA targets involved in the cetuximab pathway	C18orf37	hsa-miR-124	Down, 24h PT	
	CCND1	hsa-let-7b		Down, 24h PT
	FAM57A	hsa-miR-124	Down, 24h PT	
	MAP2K4	hsa-miR-576-3p	Up, 48h PT	
	M-ras	hsa-miR-330-5p	Up, 24h PT	Up, 24h PT
	N-ras	hsa-let-7b		Down, 24h PT
	PIK3R1	hsa-mir-486-5p	Up, 24h PT	
	PRKCA	hsa-miR-330-5p	Up, 24h PT	Up, 24h PT
	SP1	hsa-miR-124	Down, 24h PT	
	STAT5A	hsa-miR-509-5p		Up, 24h PT
	VEGFA	hsa-miR-330-3p		Down, 24h PT
	VEGFA	hsa-miR-330-5p	Up, 24h PT	Up, 24h PT
miRNA targets involved in CRC	ABCA1	hsa-miR-152		Down, 48h PT
	BCL9	hsa-miR-330-3p		Up, 24h PT
	EYA4	hsa-miR-124	Down, 24h PT	
	PRKCB1	hsa-miR-330-3p		Down, 24h PT
	PRKD1	hsa-miR-124	Down, 24h PT	
	PTEN	hsa-mir-486-5p	Up, 24h PT	
	PTPN12	hsa-mir-486-5p	Up, 24h PT	
	PTPN12	hsa-miR-124	Down, 24h PT	
	TRIM33	hsa-miR-512-3p	Up, 24h PT	
	CCND1	hsa-let-7b		Down, 24h PT
	MAP2K4	hsa-miR-576-3p	Up, 48h PT	
	N-ras	hsa-let-7b		Down, 24h PT
	PIK3R1	hsa-mir-486-5p	Up, 24h PT	
	PRKCA	hsa-miR-330-5p	Up, 24h PT	Up, 24h PT
miRNA targets involved in CRC response to drugs	CASP3	hsa-let-7b		Down, 24h PT
	CCND1	hsa-let-7b		Down, 24h PT
	RELA	hsa-miR-124	Down, 24h PT	
	VEGFA	hsa-miR-330-3p		Down, 24h PT
	VEGFA	hsa-miR-330-5p	Up, 24h PT	Up, 24h PT
	GADD45A	hsa-miR-152		Down, 48h PT
	CYP1B1	hsa-miR-124	Down, 24h PT	
	AHR	hsa-miR-124	Down, 24h PT	
	IL1A	hsa-miR-146b-3p	Up, 48h PT	
	CYP19A1	hsa-let-7b, hsa-let-7e		Down, 24h PT
	ESR1	hsa-miR-330-3p		Down, 24h PT
	ESR1	hsa-miR-152		Down, 48h PT
	SLC16A1	hsa-miR-124	Down, 24h PT	
	SP1	hsa-miR-124	Down, 24h PT	
	CDK4	hsa-miR-124	Down, 24h PT	
	MAPK14	hsa-miR-124	Down, 24h PT	
	PRKCA	hsa-miR-330-5p	Up, 24h PT	Up, 24h PT
	ABCC5	hsa-let-7e		Down, 24h PT
	CTGF	hsa-miR-124	Down, 24h PT	
	PTEN	hsa-mir-486-5p	Up, 24h PT	
	TOB1	hsa-mir-486-5p	Up, 24h PT	
	CAV1	hsa-miR-124	Down, 24h PT	
	CXCR4	hsa-miR-146a		Up, 48h PT
	ITGB1	hsa-miR-124	Down, 24h PT	
	NR1I2	hsa-miR-148a		Down, 24h PT
	RUNX2	hsa-miR-636	Down, 24h PT	
	ALDOA	hsa-miR-122	Up, 24 h PT Down, 48 h PT	
	CDK6	hsa-let-7b		Down, 24h PT
	CDK6	hsa-miR-124	Down, 24h PT	
	CEBPA	hsa-miR-124	Down, 24h PT	
	COL6A3	hsa-miR-330-3p		Down, 24h PT
	ID2	hsa-miR-330-3p		Down, 24h PT
	LMNB1	hsa-miR-124	Down, 24h PT	
	NGFR	hsa-miR-330-5p	Up, 24h PT	Up, 24h PT
	SLC2A1	hsa-miR-152		Down, 48h PT

The analysis of network centrality showed that EEF1A1, GRB2, and UBC (direct interactors of miRNA targets) are amongst the proteins with the highest degree (a network parameter based on the number of direct connections of a node within a network) in all networks. Interestingly, GRB2 is involved in cetuximab response and, more generally, in CRC response to drugs [99]. EEF1A1 is considered to be a regulator of cell growth and cytoskeletal network; its expression is elevated in tumors (including CRC) and it was reported to be involved in CRC response to drugs [100, 101]. UBC is a component of the ubiquitin proteasome system playing a key role in the regulation of colorectal epithelial cells proliferation, and is implicated in colorectal carcinogenesis [102]. We determined the statistically overrepresented GOs in the 4 networks, focusing on the comparisons between the 2 cell lines on a given time point. This analysis highlighted a high occurrence of common processes such as regulation of transcription and cell proliferation, cell motility and angiogenesis, regulation of mitogen-activated protein kinase (MAPK) activity, apoptosis at 24 hours post treatment; at 48 hours, the 2 cell lines share only general processes as transcription, regulation of cell proliferation, and apoptosis (hypergeometric test, Benjamini adjusted $P \leq 0.00005$). Interestingly, we observed that at 24 hours Caco-2 network is enriched in proteins related to the activation of apoptosis, differentiation, and negative regulation of cell growth and migration, regulation of MAPK activity, Wnt and Notch pathways and vascular endothelial growth factor (VEGF) activity with respect to HCT-116, which instead has overrepresented GOs related to angiogenesis. At 48 hours, HCT-116 network is enriched in proteins involved in differentiation, positive regulation of cell growth, migration, epithelial to mesenchymal transition, regulation of MAPK cascade, angiogenesis, EGFR and VEGF pathways (hypergeometric test, Benjamini FDR adjusted $P < 0.05$; Figure 21).

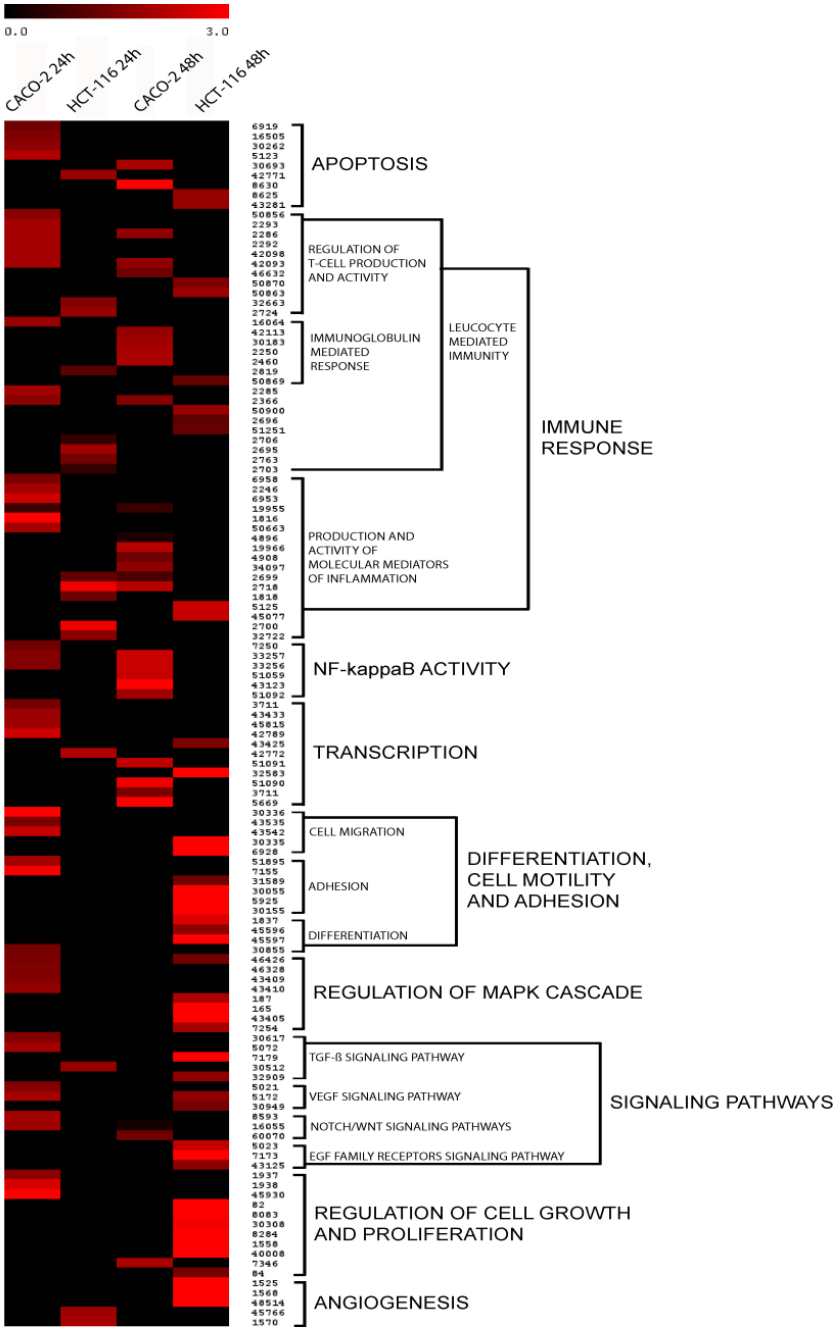

Figure 21. Matrix of the differences of Gene Ontology among networks based on differentially expressed miRNA target.

The processes correlated to immunity are extensively represented in our GO analysis. With respect to HCT-116, Caco-2 is enriched in proteins involved in the activation of the molecular mediators of inflammation both at 24 and 48 hours post-treatment. Moreover, in Caco-2 at 24 and 48 hours post-treatment, we found several GOs related to NF-kB activity that are absent in HCT-116 (Figure 21). We identified the statistically significant differences in GO terms between 24 and 48 hours post-treatment. In Caco-2 cells at 24 hours we found a high occurrence of biological processes and molecular functions related to signal transduction, transmembrane receptor activity, and G-protein–coupled receptor protein signaling pathway in comparison with 48 hours post-treatment (Fisher exact test, adjusted $P < 0.05$).

ALTERATIONS OF miRNA TRANSCRIPTOME AND GLOBAL NETWORK STRUCTURE IN COLORECTAL CARCINOMA AFTER TREATMENT WITH MAPK/ERK INHIBITORS

Effects of FR180204, U0126, WAY265506 on CRC cells

We evaluated the effect of the three specific MAPK inhibitors at 12 h post treatment by MTT assay, showing a significant decrease of cell viability in the three CRC cell lines (markedly in HCT-116 and SW-620) (Figure 22A). Western blot analysis at 12 h proved that FR180204, U0126, and WAY265506 reduced ERK1/2 phosphorylation, confirming the negative modulation of the pathway: specifically, U0126 and WAY265506 lowered ERK phosphorylation to undetectable levels in HCT-116 and SW-620 cells at a concentration of 25 μM, while it was necessary to raise the concentrations up to 50 μM to obtain comparable results in Caco-2 (Figure 22B). A possible explanation to this behavior

is that the two cell lines harboring a mutated KRAS (HCT-116 and SW-620) have an aberrant activity of ERK, which is more prone to inhibition by drugs [103]. Finally, by performing RT-PCR we observed a significant reduction of GRP78 (involved in unfolded protein response and transcriptionally induced by p-ERK) expression following the treatments in all cell lines through RT-PCR (Figure 22C) [104].

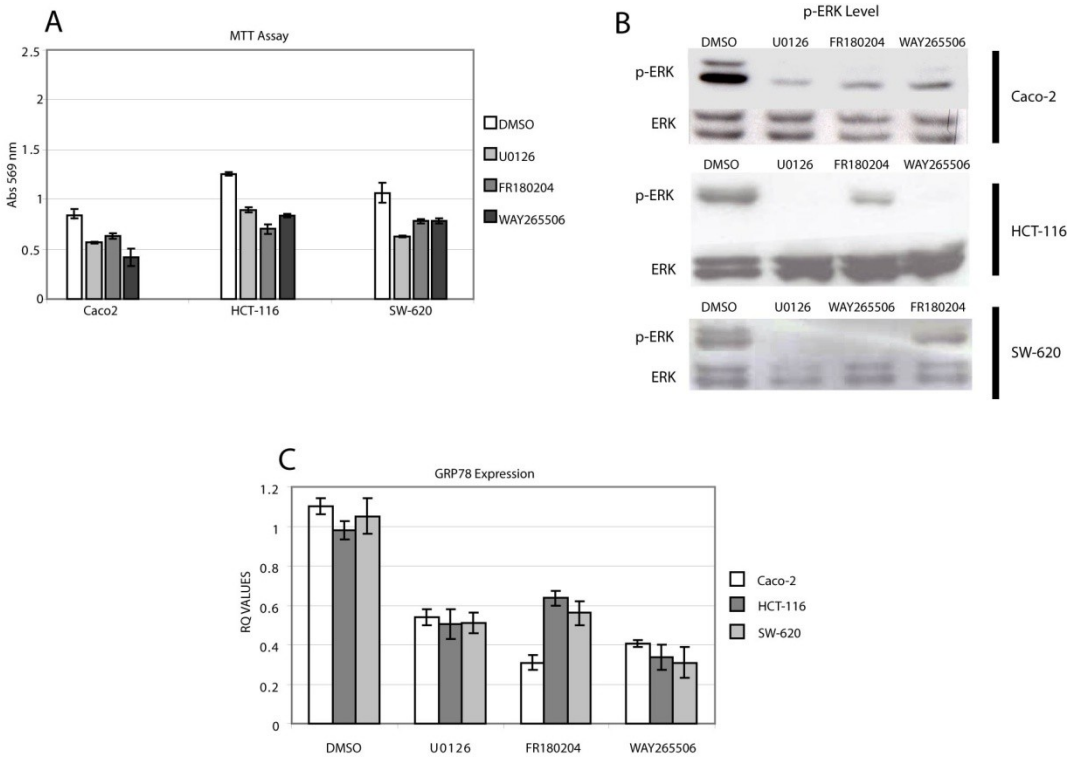

Figure 22. Effects of MAPK inhibitors in CRC cell lines. A) MTT assay 12h after treatment with MAPK/ERK inhibitors (U0126, FR180204, WAY265506); DMSO was used as control. B) Western Blot analysis of phospho-ERK p44/42 and total ERK levels. β-actin was used as mass loading control (not shown). C) RT-PCR analysis of GRP78 in CRC cell lines, 12h PT with the indicated inhibitors. DMSO, solvent only control.

Alterations of miRNA profile in CRC after treatment with MAPK/ERK inhibitors

We profiled the expression of 745 miRNAs in Caco-2, HCT-116, and SW-620 cells 12h after treatment with MAPK/ERK inhibitors. We assigned differentially expressed miRNAs to two classes: (1) common DE miRNAs for all inhibitors in a specific CRC cell line; (2) common DE miRNAs for all cell lines relative to a specific inhibitor. Through the first comparison, we pinpointed 15 miRNAs in Caco-2 cells (nine downregulated and six upregulated), 10 miRNAs in HCT-116 (seven downregulated and three upregulated), 10 miRNAs in SW-620 (nine downregulated and one upregulated; Table 8). The second type of comparison brought to the identification of two DE miRNAs for FR180204 (both downregulated), seven DE miRNAs for U0126 (five downregulated, two upregulated), 27 DE miRNAs for WAY265506 (14 downregulated, 13 upregulated; Table 9). Interestingly, most of the differentially expressed miRNAs were downregulated: this is not surprising, since it has been demonstrated that MAPK/ERK pathway is able to positively regulate the miRNA generating complex through the phosphorylation of TRBP [23].

Table 8. miRNA commonly deregulated in a specific colon cancer cell line after treatment with all the MAPK/ERK inhibitors.

	miRNAs	U0126 Avg FC	FR180204 Avg FC	WAY265506 Avg FC	Literature Data About CRC and Other Cancer
CACO-2	hsa-miR-9	-1.55	-2.16	-2.33	Methylated in CRC. Colorectal cancer cell lines with KRAS mutations showed an over-expression of miR-9.
	hsa-miR-19b-1*	-1.66	-1.93	-1.21	MiRNA belonging to oncogenic cluster 17-92.
	hsa-miR-92a-1*	-1.84	-1.53	-1.66	MiRNA belonging to oncogenic cluster 17-92.
	hsa-miR-142-5p	2.37	4.41	2.15	Downregulated in lung cancer.
	hsa-miR-203	-1.14	-1.46	-2.14	Overexpression of miR-203 decreased Bcl-xL expression and increased Bax and active caspase-3 levels.
	hsa-miR-212	-1.65	-2.23	-1.39	miR-212 is increased in pancreatic cancer and targets RB.
	hsa-miR-296-3p	1.94	1.42	3.63	Tumor suppressor in breast cancer.
	hsa-miR-302a	-1.35	-2.22	-1.11	miR-302s were downregulated in irradiated breast cancer cells.
	hsa-miR-302b	-1.26	-2.17	-1.64	miR-302b maintains “stemness” of human embryonal carcinoma cells.
	hsa-miR-331-3p	1.02	-2.01	-2.12	miR-331-3p targets E2F1 and induces growth arrest in human gastric cancer.
	hsa-miR-450b-5p	2.62	3.39	1.89	
	hsa-miR-615-5p	-3.64	-2.53	-2.14	/
	hsa-miR-664	1.56	2.11	4.16	/
	hsa-miR-1260	1.43	2.19	3.08	/
	hsa-miR-1291	2.04	1.75	9.82	/
HCT-116	hsa-miR-20a*	-1.62	-1.2	-1.47	/
	hsa-miR-135b*	-2.11	1.68	-2.39	/
	hsa-miR-190	1.75	1.37	1.36	Downregulated in CRC and glioblastoma.
	hsa-miR-210	1.96	-1.36	2.19	miR-210 regulates cancer cell proliferation through targeting FGFRL1.
	hsa-miR-222*	-1.41	-1.36	-2.69	/
	hsa-miR-329	7.69	-1.54	3.71	Downregulated in Uterus/Endometrial_cancer.
	hsa-miR-362-3p	-1.65	-1.94	-1.58	Upregulated in Grade 3 vs Grade 1/2 Breast cancer.
	hsa-miR-374a*	-2.64	-1.16	-4.01	/
	hsa-miR-545	-2.07	-1.64	-1.32	/
	hsa-miR-671-3p	-1.84	-1.65	-2.27	Upregulated in Breast cancer.
SW-620	hsa-miR-10a	-1.11	-1.66	-3.02	miR-10a was found overexpressed in CRC.
	hsa-miR-19a*	-1.97	-1.91	-2.67	Mir belonging to oncogenic cluster 17-92.
	hsa-miR-19b-1*	-1.66	-1.17	-2.38	Mir belonging to oncogenic cluster 17-92.
	hsa-miR-92a-1*	-2.79	-1.08	-3.69	Mir belonging to oncogenic cluster 17-92.
	hsa-miR-29b	-2.26	-3.05	-2.94	MicroRNA-29 family (a, b, c) is down-regulated in lung cancer.
	hsa-miR-150	-2.03	-1.56	-1.32	EGR2 is a direct target of miR-150.
	hsa-miR-210	1.83	2.16	1.39	miR-210 regulates cancer cell proliferation through targeting FGFRL1.
	hsa-miR-720	-3.08	-3.93	-3.29	/
	hsa-miR-886-3p	-2.44	-2.83	1.09	miR-886-3p down-regulates CXCL12 expression in human marrow stromal cells.
	hsa-miR-1244	-5.68	-3.45	-1.33	/

Table 9. miRNA commonly deregulated in all colon cancer cell lines after treatment with a specific MAPK/ERK inhibitor.

	miRNAs	Caco2 Avg FC	HCT-116 Avg FC	SW-620 Avg FC	Literature Data About CRC and Other Cancer
U0126	miR-19b-1*	-1.66	-2.05	-1.66	Mir belonging to oncogenic cluster 17-92.
	miR-92a-1*	-1.84	-2.39	-2.8	Mir belonging to oncogenic cluster 17-92.
	miR-135b*	-1.2	-2.1	-1.92	/
	mir-210	1.27	1.96	1.83	miR-210 regulates cancer cell proliferation through targeting FGFRL1.
	miR-222*	-1.14	-1.4	-2.49	/
	mir-328	1.35	1.8	3.16	Downregulated in CRC.
	miR-1226*	-2.49	-2.44	-2.64	/
FR180204	miR-222*	-1.52	-1.36	-2.19	/
	mir-372	-3.41	-1.32	-3.19	miR-372 promoted invasiveness of lung cancer cell lines and metastasis in CRC.
WAY-265506	let-7g*	3.4	1.6	3.29	/
	mir-15b	-2.17	-1.27	-1.58	miR-15b is overexpressed in CRC patients and may be associated with the development of the disease.
	miR-17*	-3.53	-1.56	-1.76	Mir belonging to oncogenic cluster 17-92.
	miR-20a*	-1.11	-1.47	-1.62	/
	miR-22*	-1.04	-1.65	-1.7	/
	mir-27a	1.49	1.78	2.19	miR-27a is linked to oncogenic transformation.
	miR-27a*	-1.13	-2.05	-2.98	/
	miR-30a-3p	1.03	-1.33	-1.75	downregulated in CRC.
	miR-92a-1*	-1.66	-2.29	-3.69	Mir belonging to oncogenic cluster 17-92.
	miR-191*	5.11	1.55	2.88	/
	miR-200a*	-1.07	-3.56	-1.29	/
	miR-200b*	-11.62	-1.47	-2.59	/
	miR-222*	1.08	-2.69	-1.52	/
	mir-324-3p	2.83	1.59	1.51	Downregulated in invasive pancreatic cancer.
	miR-374a*	-1.5	-4	-2	/
	miR-425*	3.99	-1.1	5.68	/
	miR-483-3p	-2.57	-1.78	-1.89	Several solid cancers has high levels of miR-483-3p.
	mir-483-5p	1.39	5.95	3.85	Marker of Malignancy, 483-5p is downregulated in adrenocortical carcinoma respect to adenomas.
	miR-572	3.79	3.05	1.52	Upregulated following hypoxia in SCC cells.
	miR-622	14.65	4.21	13.8	Downregulated miRNA in ovarian cancer tissues and cell lines.
	miR-625*	-1.03	-2.62	-1.6	/
	miR-663B	16.92	12.25	11.12	Downregulated in breast cancer following aberrant hypermethylation.
	miR-664	4.16	1.44	1.57	/
	miR-1285	6.67	1.93	2.6	miR-1285 inhibits the expression of p53 and p21. Its expression levels increased after proton beams treament.
	miR-1290	7.55	5.08	6.09	When miR-1290 is upregulated a decrease in pAkt expression and inhibition of cell growth is observed.
	miR-1291	9.82	2.73	5.12	/
	miR-1300	7.09	2.46	4.93	/

We confirmed TLDA data on miR-17*, miR-19a*, mir-19b-1*, miR-92a-1*, mir-135b*, mir-210, mir-372, mir-374a*, mir-483-3p, mir-663b, mir-720, mir-1226*, mir-1290 by Single TaqMan Assays (STAs). As previously done for TLDA normalization procedure, we used the more stable miRNAs (miR-26a, miR-31*, miR-532-5p) as normalizators for STAs. The trend of expression fold changes from TLDAs and STAs was consistent, but the specific quantification differed due to protocol and stoichiometry differences (i.e., samples, probes, preamplification of TLDA samples). To evaluate the consistency of the expression trend between data from TLDA and from single assays, respectively, we calculated Pearson correlation of the datasets and obtained r=0.93 (two-tailed p value <0.0001), showing that the data from the two different systems are concordant. For nearly 50 % of DE miRNAs, we were unable to find previous studies on their biological role, including CRC and MAPK/ERK pathway. Since our aim was to enrich the knowledge on the possible involvement of miRNAs in MAPK pathway functions and impairment in cancer, particularly in CRC, among the list of differentially expressed miRNAs we focused on six of them, based on their elevated fold change and on the absence of relevant data on their biological role. These selected miRNAs were representative of each of the two classes mentioned before: 3 miRNAs (miR-92a-1*, miR-135b*, miR-720) specifically dysregulated in Caco-2, HCT-116 and SW-620, respectively, after all the treatments, and 3 miRNAs (miR-1226*, miR-663b, miR-372) commonly dysregulated in all the three cell lines after treatment with U0126, WAY265506 and FR180204, respectively (Tables 8 and 9). Literature mining demonstrated that almost all downregulated miRNAs in our study are related to oncogenic pathways in CRC or other cancers, while upregulated miRNAs are involved in antioncogenic activities or are downregulated in CRC and other tumors. Many downregulated miRNAs (i.e., miR-17*, miR-19a*, mir-19b-1*, miR-20a*,miR-92a-1*) belong to the oncogenic cluster 17–92, which is known to be amplified and over expressed in B-cell lymphomas and solid

tumors including CRC (see Introduction for more details) [105]. Following treatment with WAY265506, miR-17* was downregulated in all cell lines, especially in Caco-2. Notably, we had also shown that this miRNA is downregulated in the same cell line also after cetuximab treatment (Table 5). Moreover, though each of the six miRNAs was representative of each comparison class we established, some of them are widely dysregulated in our cell models (in more than one cell line and after treatment with more than one specific inhibitor), suggesting a stronger general correlation both with CRC and with MAPK pathway, rather than a specific connection with one given cell type or a specific inhibitor: for example, miR-92a-1* was downregulated after treatment with all inhibitors in Caco-2 and SW-620, and in all cell lines after U0126 and WAY-265506 administration; miR-135b* was downregulated in HCT-116 after treatment with all inhibitors and in the three cell lines after U0126; miR-720, downregulated in SW-620 after all treatments, is also downregulated in HCT-116 after U0126 subministration.

Correlation between KRAS mutational status and miRNA expression in FFPE CRC samples

We compared the expression of the six miRNAs previously chosen (miR-92a-1*, miR-135b*, miR-372, miR-663b, miR-720, and miR-1226*) in 22 CRC samples (11 KRAS wild-type and 11 KRAS mutated) respect to five normal controls, and in KRAS wild-type patients respect to those with mutated KRAS. The results indicate that miR-92a-1*, miR-135b*, miR-372, and miR-720 are significantly overexpressed in CRC samples than in normal controls, and in CRC patients with mutated KRAS than in wild-type ones (Wilcoxon rank sum test: $p<0.031$, $p<0.019$, $p<0.014$, $p<0.046$, respectively; Figure 23). These data are consistent

with our starting hypothesis that the miRNAs we have chosen for our analysis are controlled by MAPK/ERK pathway: if this is true, it is not surprising that the constitutive activation of KRAS in CRC mutated patients could lead to miRNAs overexpression. On the contrary, the expression of miR-663b and miR-1226* is not significantly different in both comparisons (Wilcoxon rank sum test: $p<0.15$ for miR-663b, $p<0.19$ for miR-1226*).

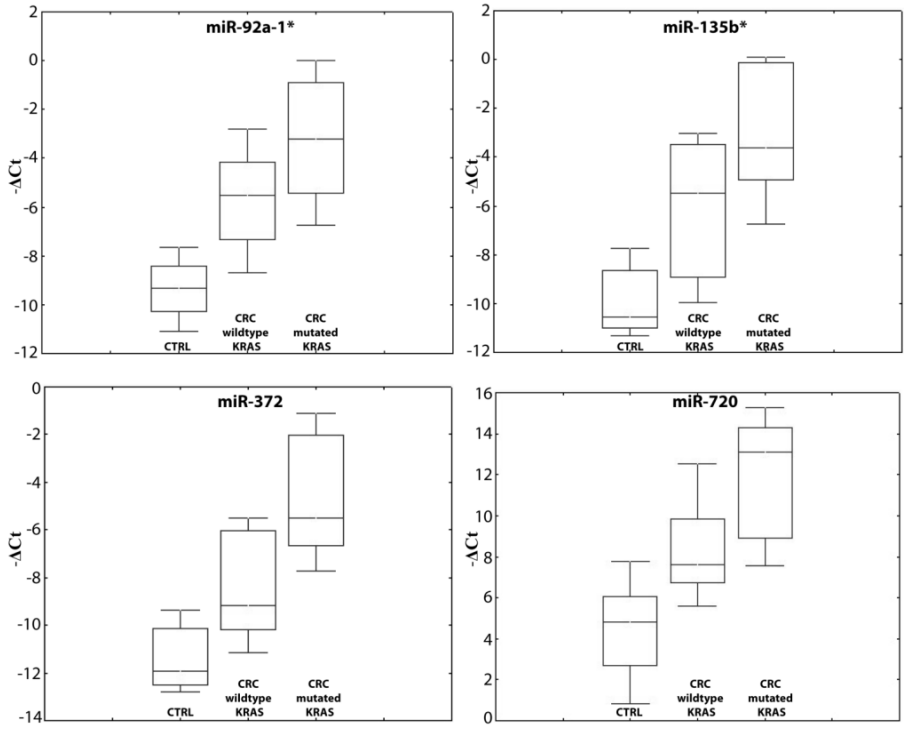

Figure 23. Box and Whisker plot of miR-92a-1*, miR-135*, miR-372, and miR-720 expression in formalin-fixed, paraffin-embedded tissues from CRC patients. Expression values are shown as ΔCt normalized to snRNA U6 and multiplied by −1. Differential expression of miRNAs in patients with wild-type or mutated KRAS, respect to normal FFPE controls, was evaluated by the Wilcoxon rank sum test ($P<0.05$).

Analysis of miRNA targets

To evaluate the biological functions of the six miRNAs analyzed in this study, we computationally searched their validated or predicted targets (Table 10).

Table 10. List of validated and predicted targets for the six DE miRNAs.

Target	MIRNA	Evidence*	Featured Biological Function
ARFIP2	miR-720	Anticorrelation; ClipSeq (8); Structural Prediction (2)	Cell Motion
BNIPL	miR-720	Anticorrelation; Structural Prediction (3)	Positive regulation of apoptosis
BUB3	miR-135b*	Structural Prediction (2)	M phase
CABLES1	miR-135b*	Structural Prediction (2)	G1/S transition of mitotic cell cycle
CABLES1	miR-372	Anticorrelation; ClipSeq (1); Structural Prediction (2)	G1/S transition of mitotic cell cycle
CAMTA1	miR-135b*	Anticorrelation; Structural Prediction (2)	Transcription regulator activity
CAMTA1	miR-372	Anticorrelation; ClipSeq (30); Structural Prediction (6)	Transcription regulator activity
CAMTA1	miR-92a-1*	Anticorrelation; Structural Prediction (2)	Transcription regulator activity
CCND2	miR-663B	ClipSeq (10); Structural Prediction (3)	G1/S transition of mitotic cell cycle
CDKN1A	miR-372	Validated	Negative regulation of cell cycle
CFL2	miR-372	Anticorrelation; ClipSeq (20); Structural Prediction (6)	Regulation of actin cytoskeleton
CREB5	miR-1226*	Anticorrelation; Structural Prediction (2)	Regulation of transcription
CREB5	miR-372	Anticorrelation; ClipSeq (1); Structural Prediction (5)	Regulation of transcription
CREBL2	miR-720	ClipSeq (1); Structural Prediction (3)	Regulation of transcription
DCN	miR-1226*	Anticorrelation; Structural Prediction (2)	Extracellular matrix organization
DMBT1	miR-135b*	Anticorrelation; Structural Prediction (2)	Positive regulation of epithelial cell differentiation
FOXO3	miR-372	Anticorrelation; ClipSeq (1); Structural Prediction (3)	Positive regulation of apoptosis
GAS7	miR-1226*	Anticorrelation; Structural Prediction (2)	Actin filament organization
GRB2	miR-663B	ClipSeq (1); Structural Prediction (3)	MAPK signaling pathway
LATS2	miR-135b*	Anticorrelation; Structural Prediction (2)	Negative regulation of cell cycle
LATS2	miR-372	Validated	Negative regulation of cell cycle
LATS2	miR-92a-1*	Anticorrelation; Structural Prediction (2)	Negative regulation of cell cycle
LFNG	miR-92a-1*	Anticorrelation; Structural Prediction (2)	M phase
LIMK1	miR-663B	ClipSeq (2); Structural Prediction (2)	Regulation of cell growth
NAPEPLD	miR-372	Anticorrelation; ClipSeq (15); Structural Prediction (6)	Phospholipid metabolic process
PDCD4	miR-135b*	Anticorrelation; Structural Prediction (2)	Negative regulation of cell cycle
PDCD4	miR-372	Anticorrelation; ClipSeq (1); Structural Prediction (2)	Negative regulation of cell cycle
PTEN	miR-372	Anticorrelation; Structural Prediction (2)	Cell Motion, positive regulation of apoptosis
PTEN	miR-92a-1*	Anticorrelation; Structural Prediction (2)	Positive regulation of apoptosis
RAB5C	miR-663B	ClipSeq (44); Structural Prediction (2)	Small GTPase mediated signal transduction
SCRIB	miR-720	ClipSeq (1); Structural Prediction (3)	Cell Motion, Negative regulation of cell cycle
SLC2A1	miR-663B	ClipSeq (1); Structural Prediction (3)	Carbohydrate transport, Pathways in cancer
SOCS5	miR-372	Anticorrelation; Structural Prediction (4)	Epidermal growth factor receptor signaling pathway
SOCS5	miR-92a-1*	Anticorrelation	Epidermal growth factor receptor signaling pathway
SOX6	miR-1226*	Anticorrelation	Negative regulation of transcription
SRF	miR-663B	ClipSeq (5); Structural Prediction (2)	Cell Motion, MAPK signaling pathway
TBC1D4	miR-135b*	Anticorrelation; Structural Prediction (2)	Small GTPase mediated signal transduction
TICAM1	miR-92a-1*	Anticorrelation; Structural Prediction (2)	Positive regulation of apoptosis
TMEM178	miR-92a-1*	Anticorrelation; Structural Prediction (2)	Cell junction
TMEM52	miR-92a-1*	Anticorrelation; Structural Prediction (2)	Cell junction
TRIP10	miR-663B	ClipSeq (6); Structural Prediction (2)	Actin cytoskeleton organization
TXNIP	miR-372	Anticorrelation; ClipSeq (264); Structural Prediction (6)	Positive regulation of apoptosis
ZNF512B	miR-372	ClipSeq (4); Structural Prediction (6)	Transcription / Cell division and chromosome partitioning
ZWINT	miR-92a-1*	Anticorrelation; Structural Prediction (2)	M phase

*: values between brackets show i) number of reads generated by CLIP-Seq (ClipSeq), and ii) number of consistent tools of miRNA target prediction (Structural Prediction).

Interestingly, CDKN1A and LATS2 are validated miR-372 targets in human gastric adenocarcinoma; CABLES1, CAMTA1, CREB5, LATS2, PDCD4, PTEN, SOCS5 are putative targets of at least two different miRNAs. To verify the putative interactions among miRNAs and the putative targets we have identified, as well as their biological role within MAPK/ERK pathway, we evaluated whether *in vitro* modulation of miRNA expression and MAPK inhibitors treatment were able to affect the target genes expression.

Alteration of targets expression after miRNA modulation

We performed transient transfection with anti-miRs for miR-92a-1*, miR-135b*, miR-372, miR-720, miR-1226*, and pre-miR-663b in the three CRC cell lines, with a 75% transfection efficiency at 24h after transfection (AT). We analyzed target expression at 24, 48, and 72 h AT to determine the kinetics of transcript variations (Figure 24). This led us to importantly shorten the list of putative targets to focus on, since we considered as reliable only those targets which expression was consistent with miRNA knock-down or knock-in in at least two cell lines. PTEN, SOCS5, TMEM52 were upregulated after knockdown of miR-92a-1* in Caco-2 and HCT-116, while knockdown of miR-135b* resulted in upregulation of LATS2 in Caco-2 and SW-620. In all cell lines, downregulation of miR-372 increased the expression of TXNIP, which had the highest number of reads (264) in Clip-Seq experiments related to this miRNA (Table 10). Interestingly, the enforced expression of miR-663b led to downregulation of three important cell cycle regulators in all cell lines: CCND2, GRB2, and SRF. Knockdown of miR-720 caused an evident upregulation of ARFIP2 (typically downregulated in CRC) in HCT-116 and a modest increment of BNIPL in all cell lines.

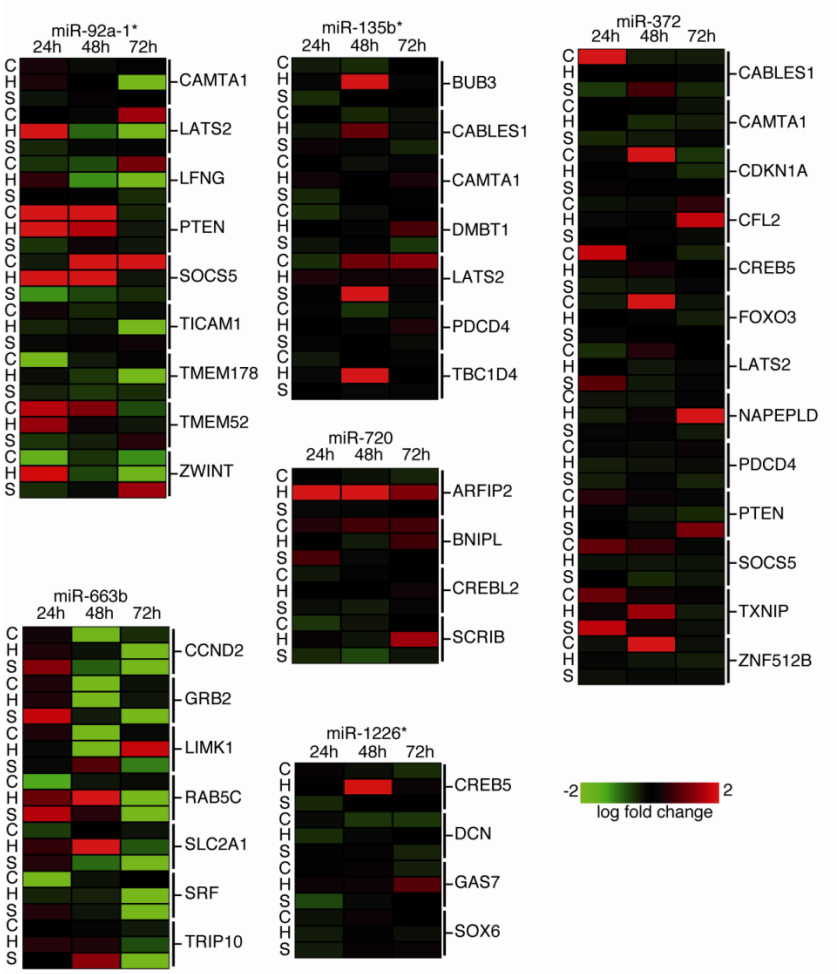

Figure 24. Expression matrix of miRNA targets at 24, 48 and 72h after transient transfection of CRC cell lines with anti-miR-92a-1*, anti-miR-135b*, anti-miR-372, anti-miR-720, anti-miR-1226* and pre-miR-663b. C= Caco-2; H= HCT-116; S= SW-620. Data are shown as log2 of RQ of target genes in treated cells, relative to the time-matched negative control. Up regulated genes are shown in red, down regulated genes in green.

Interestingly, the enforced expression of miR-663b led to downregulation of three important cell cycle regulators in all cell lines: CCND2, GRB2, and SRF. Knockdown of miR-720 caused an evident upregulation of ARFIP2 (typically downregulated in CRC) in HCT-116 and a modest increment of BNIPL in all cell lines. Down modulation of miR-1226* caused overexpression of CREB5 in HCT-

116 cells. The kinetics of target modulation was different among CRC cell lines and targets: for some miRNA targets the expression regulation started in early stages after miRNA modulation, and was concluded at later time points; other targets have an opposite behavior. This could have several possible explanations: miRNA targeting is more or less peculiar of a given cell type, since based on the molecular patterns and stage of a given cell type, several different RNAs could compete for miRNA binding. Moreover, it is known that mRNA:miRNA interaction is not an exclusive binding, and a specific mRNA can be regulated simultaneously by different miRNAs [106-108]. Moreover, mRNA isoform heterogeneity in different molecular contexts could result in cell-specific modulation of miRNA targets [109]. Finally, transfection efficiency varies among different cells types due to their genotypes and molecular phenotypes.

Alteration of targets expression after treatment with MAPK inhibitors

We determined the expression levels of miRNA targets we had pinpointed after miRNAs knock-down/in after treatment with the MAPK inhibitors modulating their putative controlling miRNAs. This led us to further reduce the list of reliable targets: our data show that the expression levels of PTEN and SOCS5 (putative targets of miR-92a-1*) increased after drug treatments in Caco-2 and HCT-116, while miR-92a-1* decreased in the same experimental conditions. LATS2 (miR-135b* putative target) was upregulated in all cell lines after treatment with U0126, and in Caco-2 and SW-620 after exposure to WAY265506. TXNIP was overexpressed after FR180204 treatment in all cell lines, while its regulator, miR-372, was downregulated. CCND2 (putative target of miR-663b) resulted downregulated after treatment with WAY265506 in all cell lines, while miR-663b was overexpressed (Figure 25). It is interesting to note that we couldn't identify reliable targets for two of the six miRNAs analyzed in this study based on the transcriptional analysis we have performed: this doesn't exclude that for these

miRNAs some targets could be subjected to translational regulation, though it has been demonstrated that miRNAs predominantly act to decrease target mRNA levels [50].

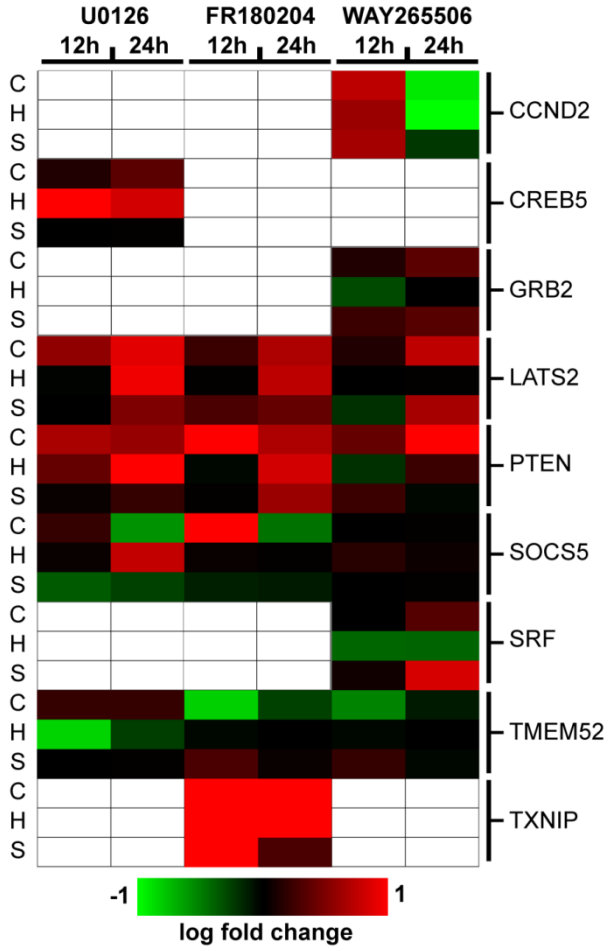

Figure 25. Expression matrix of target genes 12 and 24h after treatment with the three MAPK inhibitors. C= Caco-2; H= HCT-116; S= SW-620. Data are shown as log2 of RQ of target genes in treated cells, relative to the time-matched negative control. Up regulated genes are shown in red, down regulated genes in green.

Intriguingly, through mining of large epidemiology datasets from Oncomine database, we found that CCND2 (miR-663b target) is upregulated, while PTEN, LATS2, TXNIP (targets of miR-92a-1* and miR-372) are significantly downregulated in CRC. These findings are in agreement with the results on the expression of their candidate controlling miRNAs from our cohort of CRC samples (Figure 23).

Identification of transcription factors regulating differentially expressed miRNAs and correlation of their expression with miRNA targets

We have identified a set of 51 TFs putatively controlling the expression of the six miRNAs we analyzed in this study: interestingly, all of them are directly or indirectly regulated by MAPK/ERK pathway (e.g., by phosphorylation) (Table 11). Ideally, if a TF positively regulates a given miRNA, we should expect an inverse correlation with the targets of that miRNA, and *viceversa*, TFs acting as miRNA repressors should be positively correlated with its targets [110, 111]. Based on this assumption, we analyzed the expression correlation of couples TF/miRNA targets for those mRNAs which expression was antithetic to that of their putatively controlling miRNAs after *in vitro* modulation of their expression by anti-miRs or pre-miR (Figure 26). We found a high anticorrelation score between a set of putative TFs for miR-92a-1* (E2F1, HNF1A, MYCN, NKX2-5, PAX4, TLX1, TLX2, TLX3) and PTEN and SOCS5, which are targets of this miRNA. LATS2 (target of miR-135b*) was positively correlated to DDIT3 and anticorrelated to BACH2 and CEBPA. TXNIP (target of miR-372) was positively correlated to HIF1A, IRF1, IRF2, STAT1, STAT3, RELA and negatively correlated to ARNT2, E2F1, E2F3, PAX4, TFDP1.

Table 11. Transcription factors potentially controlling DE miRNAs expression and their involvement in MAPK/ERK pathway.

TRANSCRIPTION FACTOR[a]	microRNA	EVIDENCE[b]	TF INVOLVEMENT IN MAPK PATHWAYS
ARNT2*	miR-372	1	MAPKs modulate AhR/Arnt transactivation function
BACH2*	miR-135b*	3-4	Potentially phosphorylated by MAPK-dependent kinases s6ks
CEBPA*	miR-135b* / miR-663B	2-4 / 2	Phosphorylated by ERK
DDIT3*	miR-135b*	2-4	Transcriptionally activated by MEK/ERK
E2F1*	miR-92a-1* / miR-372	2-3-4/ 1	Increases indirect p38 phosphorylation and activation
E2F3* - E2F4	miR-372	1	Generally involved in MAPKs regulation
EGR1 - EGR2	miR-372	1	Regulated by MAPKs
ELK1	miR-372	1	Phosphorylated and activated by MAPKs
ETS1*	miR-720 / miR-372	1	Phosphorylation, activation and translocation into the nucleus by ERK/RAS-dependent hyperactivation
ETV4	miR-720	1	Activated by ERK
GATA2	miR-372	1	Phosphorylation and regulation by MAPKs
HIF1A*	miR-372	3-2	MAPKS act indirectly on the positive regulation of HIF1A transactivation activity
HNF4A	miR-372	1	Its DNA affinity is inhibited by MAPKs phosphorylation
HSF1*	miR-663B	2	Its DNA affinity is inhibited by MK2 kinase
IRF1*-IRF2*-IRF9/IRF7*	miR-372 / miR-135b*	1 / 3-4	Regulated by p38 MAPK
JUN*	miR-1226*	2	Phosphorylated by MAPKs
MAF	miR-372	1	Transcriptionally regulated by MAPKs
MYC*	miR-92a-1*/miR-372/miR-135b*	2-3-4/ 1 / 3-4	Regulated by ERK activity
MYCN*	miR-92a-1*	2-3-4	Block of its degradation by RAS activity
MYOG	miR-372	1	Its transcription regulation involves p38 MAPK
NANOG	miR-372	1	Transcriptionally downregulation by ERK1/2
NKX2-1 / NKX2-5* / NKX3-1	miR-372 / miR-92a-1* / miR-1226*	1 / 2-3-4 / 2	Regulated by MAPKs
PPARA	miR-1226*	2	Activated by p38 MAPK
PPARG	miR-1226*	2	Inhibitory phosphorylation by MAPKs
PRDM1	miR-720	1	Expression activated by ERKs
RELA*	miR-372	1	Phosphorylated by p38 MAPK
RUNX1*	miR-1226*	2	Regulated by ERK1/2
SMAD1	miR-372	1	Phosphorylated by ERK
SP3	miR-372	1	Activated by p38 MAPK
SPI1	miR-372	1	Potentially phosphorylated by MAPK to regulate its stability
STAT1*-STAT3* / STAT5A	miR-372 / miR-1226*	1 / 2	Phosphorylated by MAPKs
STAT2 / STAT6*	miR-372 / miR-720	1	Regulated by MAPKs
TBX5	miR-372	1	Potentially phosphorylated by FGF/MAPK pathways
TCF3	miR-372	1	Phosphorylated by MAPKs to decrease its proteasomal degradation
TFDP1*	miR-372	1	It eterodimerizes with E2F proteins that interacts with MAPKs
TP53*	miR-1226*	2	Regulation of activation and protein accumulation dependent on ERK1/2
TWIST1	miR-372	2-3	Stabilized by phosphorylation dependent on MAPKs
WT1	miR-372	1	Transactivates MAPKs regulators Sprouty1 and MKP3
YY1*	miR-720	1	Downregulated after p38 MAPK pathway inhibition
ZEB1	miR-372	1	MAPKs inhibition determines its suppression
ZNF143	miR-372	1	Its levels are regulated by MAPKs

[a]**:** The Transcription Factors marked by an asterisk showed a statistically significant correlation with targets of putatively controlled miRNAs.

[b]**:** The sources of data about prediction TF-miRNA couples.

1: ECR browser; 2: Putmir; 3: Transmir; 4: FF

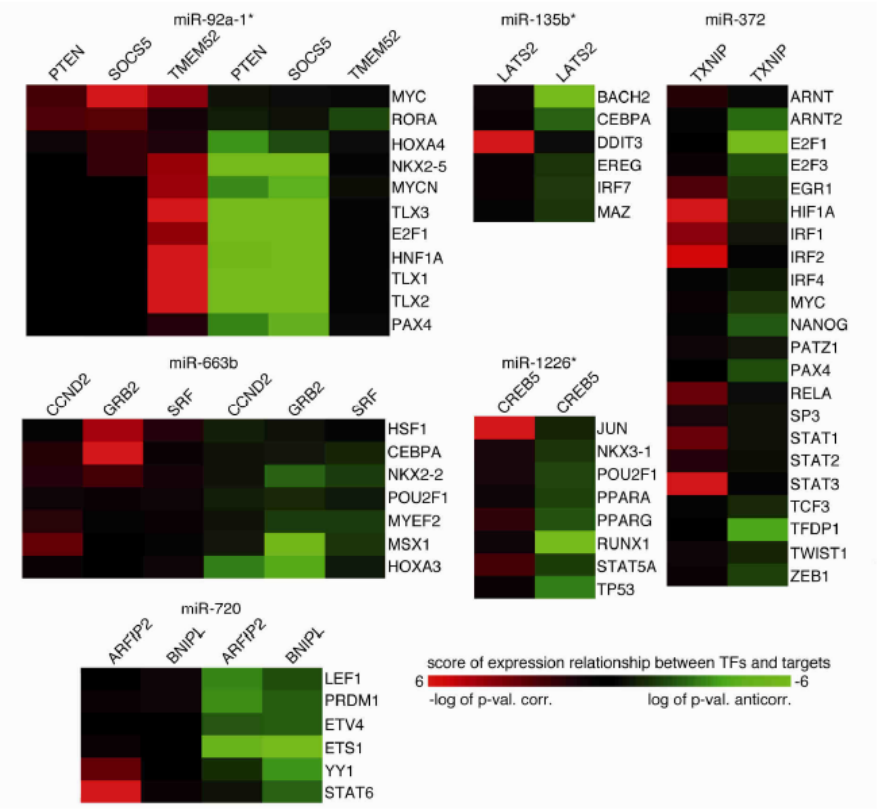

Figure 26. Heat map showing the anticorrelation/correlation scores of TF-target pairs for specific miRNAs. Data are shown as -log10 of P-value for correlation (red) and log10 of P-value for anticorrelation (green).

The expression of CEBPA, HSF1, MSX1 (putative TFs for miR-663b) was positively correlated to the expression of two miR-663b targets: CCND2, GRB2; GRB2 expression was anticorrelated to HOXA3, another putative TF for miR-663b. ARFIP2 (target of miR-720) was positively correlated to STAT6 and YY1 and negatively to ETS1 and LEF1; interestingly, the expression of ETS1 was also anticorrelated to BNIPL, another miR-720 target. Finally, CREB5 (target of miR-1226*) was positively correlated to JUN and anticorrelated to RUNX1 and TP53. Taken together, these data confirm the molecular relationship among TFs, which regulate miRNA expression, and miRNA targets. Otherwise, these correlations

could also result from positive or negative feedback loops involving TFs, miRNAs, other structural RNAs and target proteins through complex molecular signaling circuits, still poorly characterized [112].

Network based on TFs regulating miRNAs and their targets

We built a cellular network comprising miR-92a-1*, miR-135b*, miR-372, miR-663b, miR-720, miR-1226* by retrieving the known protein–protein and DNA–protein interactions among their TFs, relative targets, and their first neighbours (Figure 27A). The generated network, consisting of 985 nodes and 3,453 edges, is topologically centered on E2F1, EGFR, GRB2, JUN, MAPK1, MAPK3, MYC, RELA, STAT3, and TP53. Interestingly, the entire MAPK/ERK pathway (from EGF receptor to MYC) is comprised within the network. To statistically analyze the enrichment of nodes involved in MAPK pathway, we compared the KEGG ontologies of all nodes within the network against the entire genome by using DAVID Functional Classification Tool. We found that MAPK pathway is the most represented biological pathway in our network with corrected enrichment *P* values (modified Fisher's exact test) = 01.2×10^{-31}. In particular, 45 and 10% of miRNA-TFs pairs and miRNA targets, respectively, are directly linked to MAPK/ERK pathway, while 50 and 75% are indirectly connected to the pathway through one neighbour. About 6% of targets (e.g., GRB2) and 3% of TFs (e.g., MYC) are established members of the MAPK/ERK pathway. Altogether, these data convincingly show that the signaling circuits, controlled by miR-92a-1*, miR-135b*, miR-372, miR-663b, miR-720, and miR-1226* overlap with the MAPK/ERK pathway.

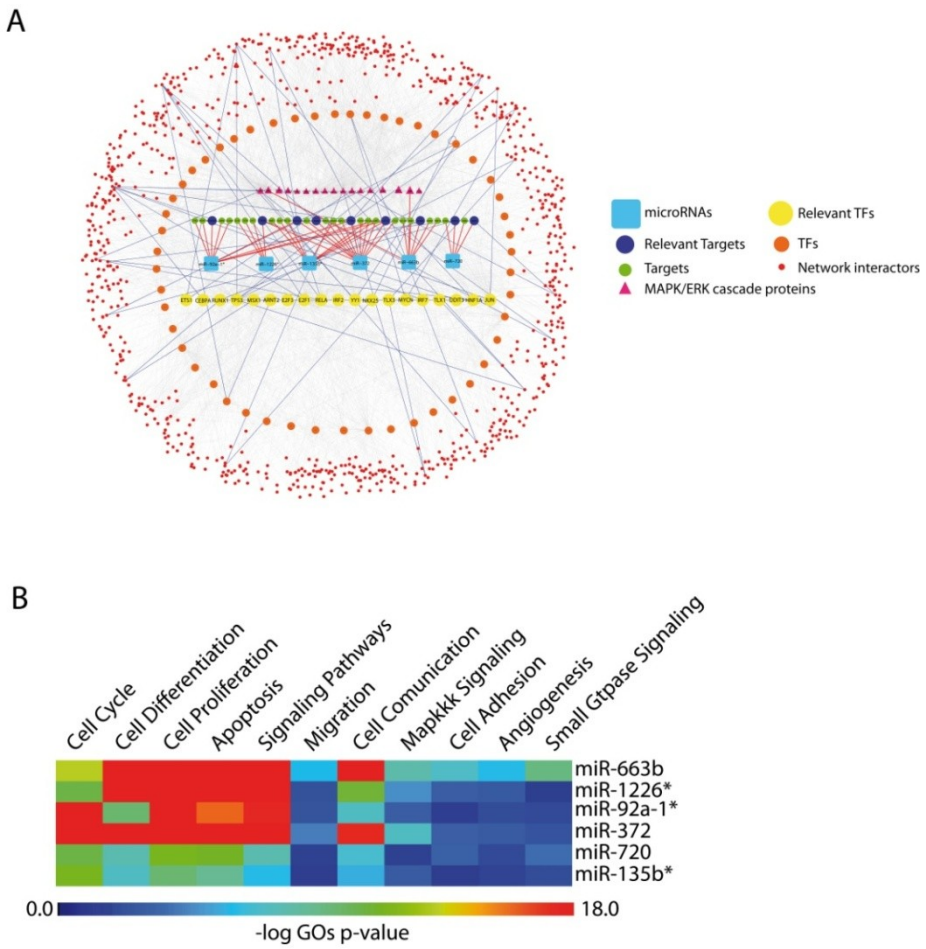

Figure 27. DE miRNAs network analysis. (A) Network built on TFs regulating miRNAs and miRNA targets: the connections spotlighted in the center of the network are comprised within the MAPK/ERK pathway. (B) Overrepresented GO, related to MAPK-ERK pathway, in the sub-networks centered on each of the six DE miRNAs. Data are shown as – log10 of p-values for each GO. Relevant targets: putative miRNA targets, which expression was inversely modulated after transfection experiments. Relevant TF: transcription factors showing significant expression correlation with miRNA targets.

We determined the statistically overrepresented GOs from the subnetworks centered on each DE miRNA (TFs, targets and their first neighbours for each DE miRNA), and found that all DE miRNAs had connections with proteins involved in several MAPK/ERK-related biological processes: cell proliferation,

differentiation, apoptosis, communication, adhesion, migration, angiogenesis (Hypergeometric test; Benjamini and Hochberg FDR correction; $p \leq 0.01$) (Figure 27B).

Effects of drug treatments and DE miRNAs modulation on cell proliferation, migration, apoptosis

Based on the experimental and computational data obtained for miR-92a-1*, miR-135b*, miR-720, miR-1226*, miR-663b, and miR-372, relative to their expression, putative mRNA targets and regulating TFs, which generally suggest their putative involvement in the main processes regulated by MAPK/ERK pathway, we decided to perform some functional analysis to experimentally demonstrate whether these miRNAs can be considered as new possible plugs for a better understanding of the functioning of this important pathway in colorectal cancer. We analyzed three main processes regulated by MAPK/ERK pathway, which are strongly impaired in all cancers, including CRC, such as cell proliferation, apoptosis and cell migration and invasiveness in the three cell lines used in this study after treatment with the three inhibitors and after *in vitro* modulation of the six miRNAs expression.

Analysis of cell proliferation

The MTT assay was performed at 12, 24, 48, and 72 h after treatment with the three inhibitors, and at 24, 48, and 72 h after transfection. All drugs had a linear strong negative effect on cell proliferation respect to the relative negative controls (DMSO treated samples), due both to the block of cell cycle caused by the direct inhibition impairing MAPK pathway, and to a subsequent involvement of apoptotic processes in later time points (Figure 28A).

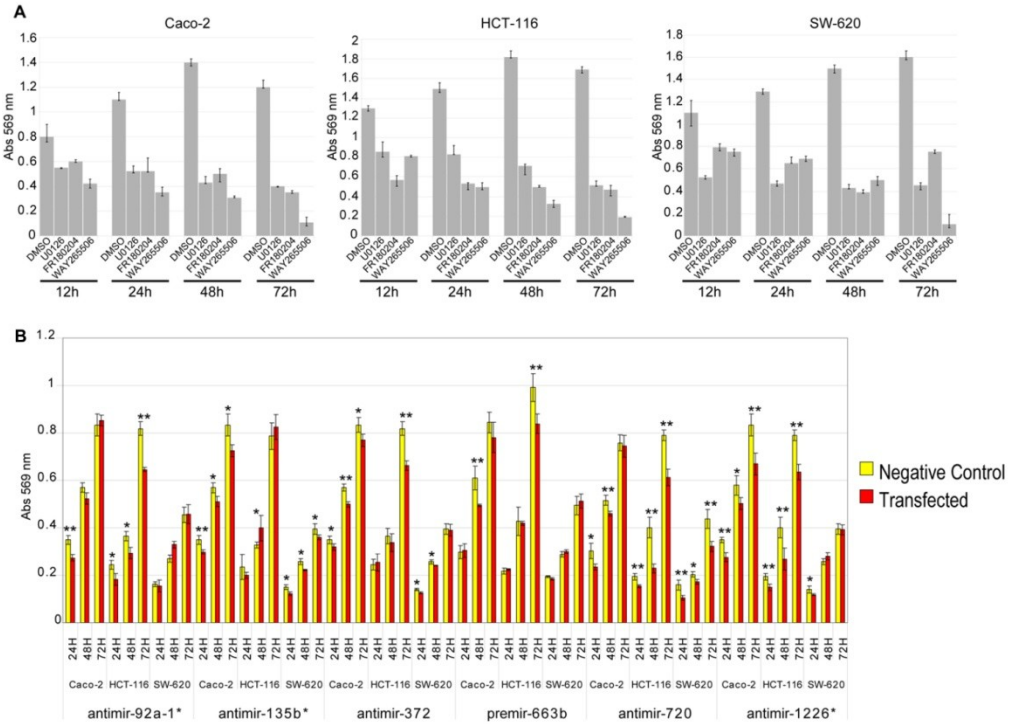

Figure 28. MTT assay on CRC cell lines after (A) treatment of Caco-2, HCT-116, and SW-620 with the drugs and DMSO control for 12, 24, 48, 72 h, and (B) after transient transfection with the indicated anti/pre-miRs for 24, 48, and 72h. Negative control, cells transfected with irrelevant oligonucleotides for pre/anti-miRs. Experiments were performed in six biological replicates. T-test paired, *P≤0.05, **P≤0.01.

Modulation of miRNA expression had a similar but more moderate effect on cell proliferation: this is not surprising, since the effect of the drugs certainly involves the synergic effect of much more different mechanisms and the impairment of several molecular pathways than the *in vitro* alteration of a single miRNA. The results of miRNA modulation effects on cell proliferation are shown in Figure 28B**.** Knockdown of miR-372, miR-720, miR-1226* resulted in a decrease of proliferation in all CRC cell lines, even though in different temporal windows for each miRNA. Caco-2 and HCT-116, but not SW-620 were significantly affected in their proliferation rates by downregulation of miR-92a-1* and upregulation of

miR-663b. MiR-135b* knockdown had a negative effect on Caco-2 and SW-620 proliferation, but caused a slight increase of proliferation in HCT-116 at 48 h. It is interesting to note that in some cases the decrease of proliferation was observed up to 72 h after miRNA knockdown. This could suggest, as for the MAPK inhibitors, a significant long-lasting biological effect (caused by modulation of these miRNAs) due to the arising of apoptosis at specific time points, besides a variation of viability or a cell number decrease. MTT assay, indeed, only identifies metabolically active cells within a cell population; any possible explanation of the reduced number of viable cells has to be investigated by further assays.

Analysis of apoptosis

We performed the analysis of apoptosis by using APOpercentage assay (see Materials and Methods, Figure 15). We evaluated apoptosis rates after 12, 24, and 48 h after treatment with the three MAPK/ERK inhibitors, showing that apoptosis progressively increased in all cell lines during drug treatments with respect to controls, especially for WAY265506 (Figure 29).

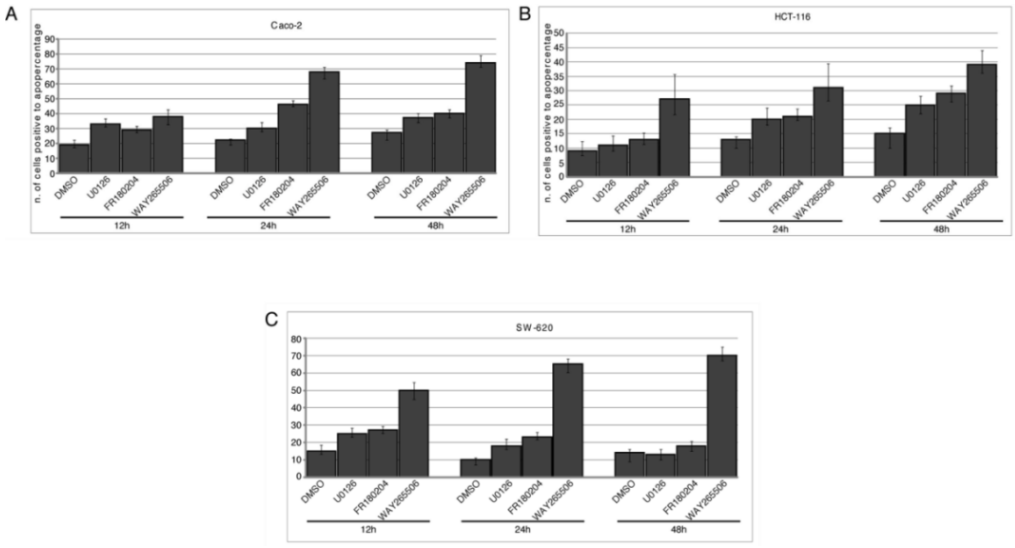

Figure 29. Analysis of apoptosis after 12, 24, and 48h of treatment with the three MAPK/ERK inhibitors and DMSO control for (A) Caco-2, (B) HCT-116, (C) SW-620.

Apoptosis was evaluated at 24 and 48 h after transfection with anti/pre-miRs: knockdown of miR-135b*, miR-372, miR-720 increased apoptosis in all CRC cell lines, while down modulation of miR-92a-1* increased apoptosis only in HCT-116 and SW-620 (Figure 30). Knockdown of miR-1226* increased apoptosis levels only in SW-620 cells. Gain of function experiments for miR-663b showed no appreciable variation of apoptosis in all cell lines. In some cases the functional analysis showed asynchronous results in viability and apoptosis assays (e.g., anti-miR-372 induced significant increase in apoptosis in HCT-116 cells, both at 24 and 48 hours, but an appreciable decreasing of viability was shown at 72 hours) (Figures 28B and 30)**.** This could be due to methodological and biological reasons. It is well-known that the colorimetric assays as MTT are able to measure cell viability, based on the ability of functional mitochondria to metabolize various tetrazolium salts; apoptosis is an active mode of cell death that requires, at least in early stages, metabolically active cells. In other words, cells in early stages of apoptosis may be considered viable; moreover, early apoptosis is believed to be reversible if the conditions inducing apoptosis are removed. Although silencing of miR-135b* induced apoptosis in HCT-116, it also caused a modest increment of proliferation in the same cells at 48 h. These data are only apparently in contrast, since a cell population with high levels of apoptosis tends to counterbalance the decrease of viable cells by increasing proliferation rates [113]. Moreover, many cell cycle genes (as p53, RB, E2F, MYC) can have a dual role: based on the molecular context, they may regulate both cell cycle progression and apoptosis [114]. Accordingly, it is not surprising that we found miRNAs with similar features.

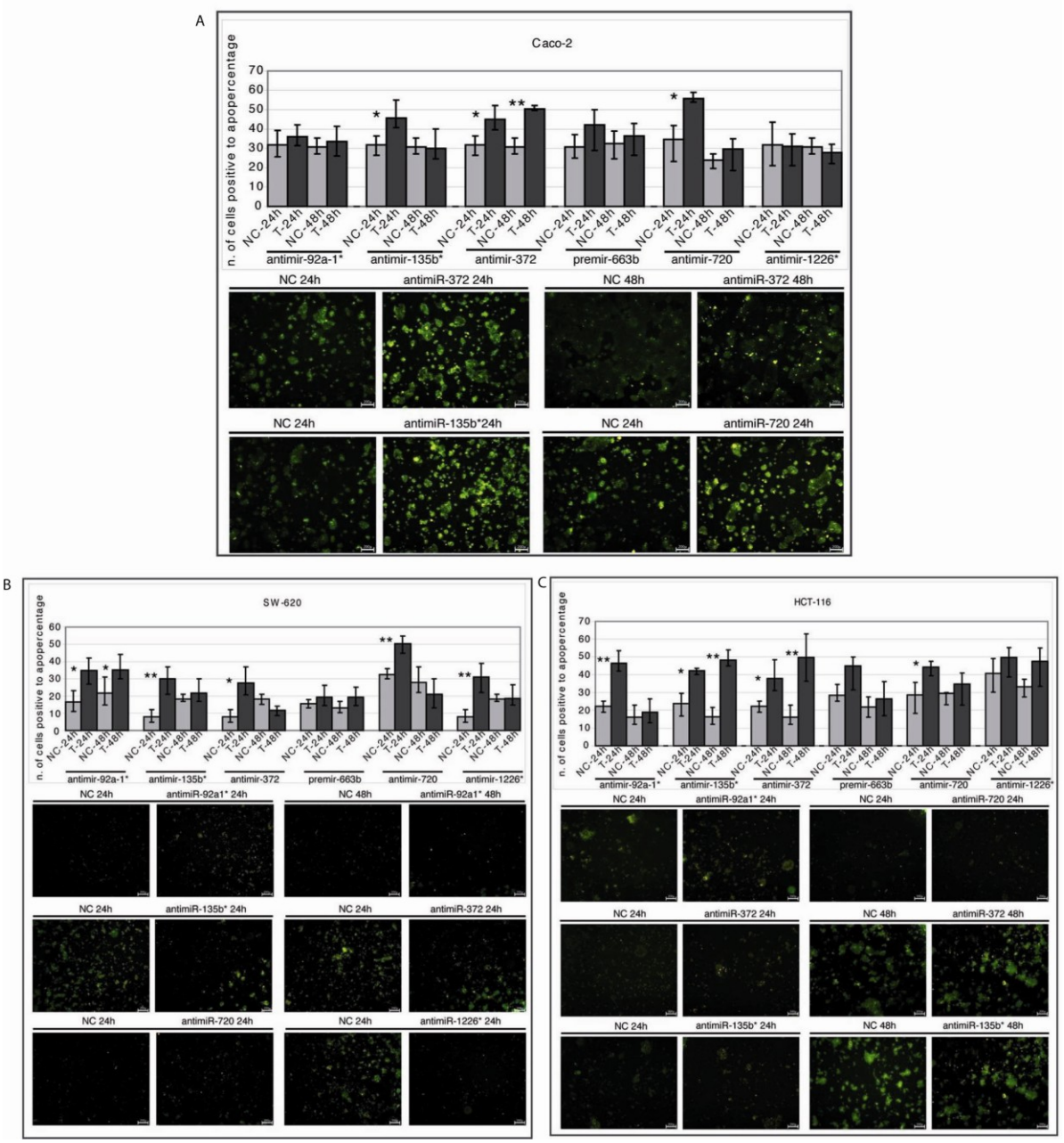

Figure 30. Analysis of apoptosis after 24 and 48h transient transfection with indicated anti-miRs and pre-miR of (A) Caco-2, (B) HCT-116, and (C) SW-620. Results are expressed as total number of stained cell in the whole well of six replicates. T test paired, *P≤0.05, **P≤0.01. In photomicrographs, cells were treated with APOPercentage Dye after transient transfection (magnification 4X). Apoptotic cells are depicted in yellow–orange.

Analysis of cell migration

We evaluated cell migration at 12, 24 and 48 h after treatment with the three inhibitors respect to DMSO negative controls, and 48 h after transfection by using the 24 h time point as pre-migration reference (Figure 31). U0126 and FR180204, but not WAY265506, caused a decrease of cell migration in Caco-2 and HCT-116 cell lines respect to controls.

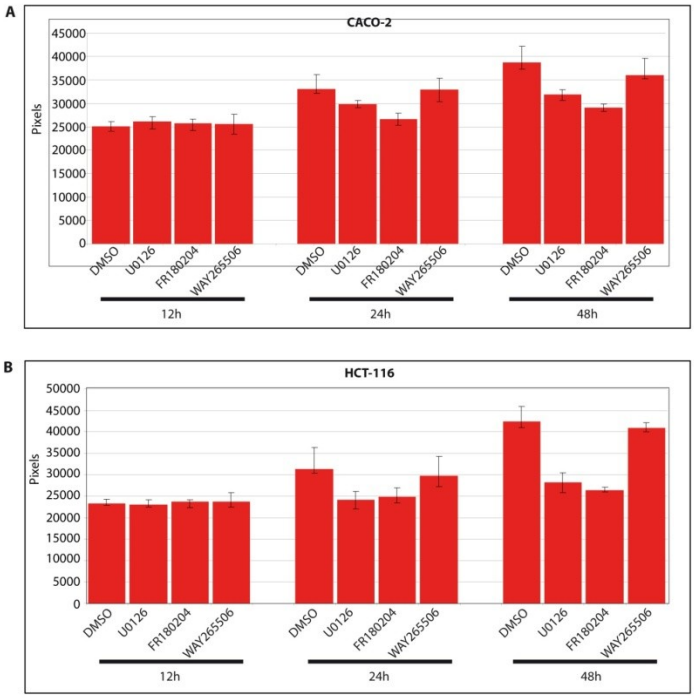

Figure 31. Detection of CRC cells migration after treatment with MAPKs inhibitors. Graphs show the pixel counts within the detection zone at 12, 24, and 48 h AT of (A) Caco-2, (B) HCT-116 with the indicated inhibitors and DMSO control.

Following miR-720 knockdown, we observed a lower number of Caco-2 and HCT-116 cells into the detection zone respect to negative controls: this suggests a decreased migration efficiency of these cells. The same effect was observed in HCT-116 cells after down modulation of miR-92a-1* and miR-372 (Figure 32A and B). In our experimental system, we found no appreciable alterations of migration properties for SW-620 cell line, both after MAPK inhibition and after transient transfection for all miRNAs: this could be explained by basal low expression levels of CD44, which is possibly responsible for their low spontaneous migration [115, 116].

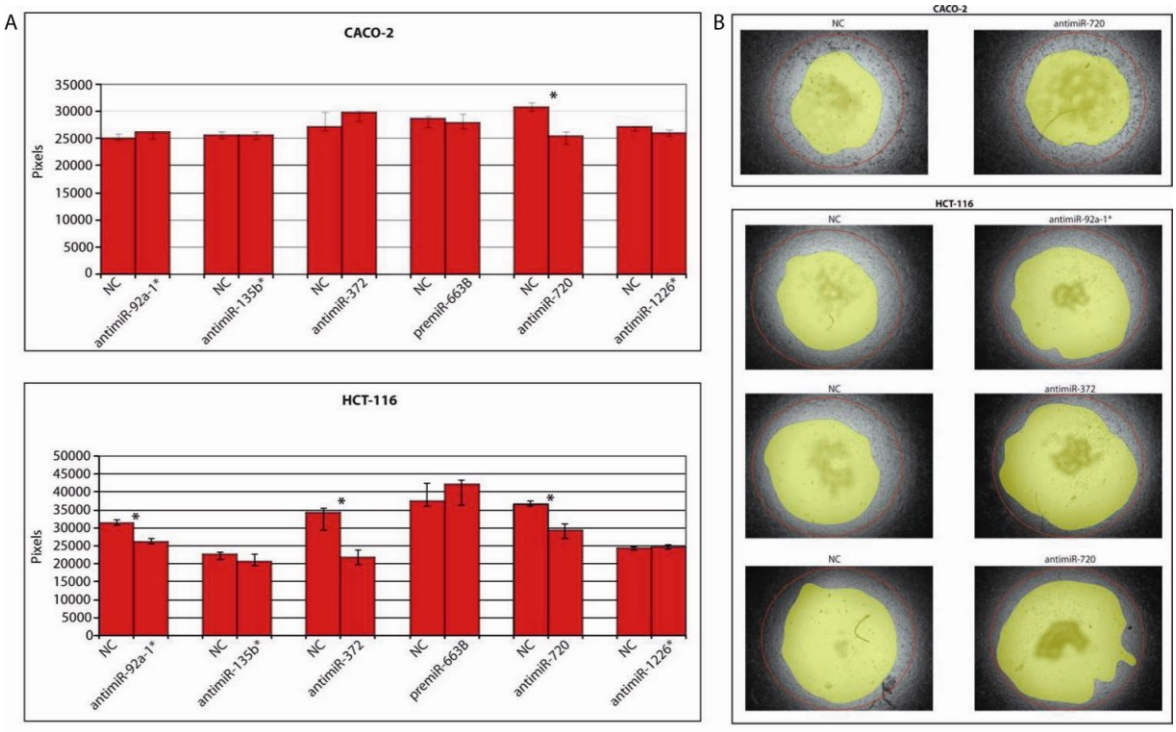

Figure 32: Detection of CRC cells migration after transient transfection. (A) Graphs showing the pixel count within the detection zone at 48 h AT of Caco-2 and HCT-116. (B) HCT-116 with anti-miRs and pre-miR. (B) Photomicrographs showing the fronts of cell migration in Caco-2 (e) and HCT-116 (f), transfected with anti-miRs and negative controls. The red circle shows the cell migration boundary when the stopper was removed (t0), the yellow area shows detection zone free from cells at t24. T test paired, *P≤0.05.

5. DISCUSSION

Studies performed during this last decade have demonstrated the complex structure of cellular networks and their fine regulation [117]. One of the major cellular pathways involved in cell proliferation, which impairment is observed in many, if not all, human cancers, is MAPK/ERK pathway, located downstream of several growth-factor receptors, including EGFR. Overexpression and activation of this receptor are commonly detected in CRC, and several lines of evidence indicate that hyperactivation of ERK/MAPK pathway plays an important role in progression of this cancer [24]. Moreover, it has been widely uncovered the relationship between MAPK pathway and miRNAs, which, together with other ncRNAs, are known to perform a prominent role in the regulation of cellular processes [118, 119]. Moreover, their expression is strongly implicated in CRC tumorigenesis and progression [120]. For all these reasons, the key components of MAPK pathway represent good putative targets for pharmacological treatment. The molecular bases of response to cancer therapeutics are complex because they involve multiple processes and corresponding cellular pathways and networks [121, 122]. The new generation of targeted therapies has been conceived to affect specific molecular processes that control tumor growth, survival, and apoptosis. Several antitumor agents, interfering with the EGFR pathway, have been developed. Among them, cetuximab is used for CRC treatment either as a single agent or in combination with chemotherapy [17]. On the other hand, the quest of highly specific inhibitors for downstream effectors of EGFR, with the aim of gaining a strong effect on specific sub-pathways with the maximum reduction of side effects, is currently taking place. Genome-wide expression profiling of

mRNAs after specific treatments has been used to understand the regulatory circuits triggered by drugs, and have shown that the levels of mRNAs and the encoded proteins are often not overlapping. This could have a number of causes, such as post-transcriptional regulation. In this context, miRNAs could have a critical role in controlling the complex signaling activated by internal and external stimuli, including antitumor therapeutic strategies [123]. Accordingly, it is likely that they could incisively affect the response to specific inhibitors of EGFR-related pathways, such as treatment with cetuximab, and specific inhibitors of MAPK/ERK pathway. Our experimental approach, based on miRNA profiling in CRC cell lines after specific treatments, aims at exploring miRNAs global involvement in MAPK/ERK pathway in CRC. By using the HT approach, we could identify miRNAs activated in CRC within the pathway and miRNAs negatively regulated in CRC. The analysis of miRNA expression was performed 24 h and 48 h after cetuximab treatment and 12 h after treatment with the three inhibitors. These differences depend on the different chemical properties of the molecules we used: cetuximab is a mAb acting at the cell surface, which effects at intracellular level are predominantly visible starting from 24 h after treatment, while MAPK specific inhibitors, DMSO soluble, directly enter the cell to act on the key players of MAPK pathway; their effect is extremely precocious, starting already a couple of hours after their subministration. In our experimental model, we show that cetuximab treatment, as well as treatment with three specific inhibitors of MAPK/ERK signaling downstream the EGFR (U0126, FR180204 and WAY265506), were able to induce important miRNA transcriptome alterations both in KRAS mutated and wild-type CRC cells (Tables 5, 8 and 9). We compared the miRNA transcriptome of 2 CRC cell lines, Caco-2 (sensitive) and HCT-116 (resistant) after cetuximab treatment, to identify putative miRNAs possibly involved in the different response of CRC patients to EGFR inhibition, based on their genotypic features. Since the set of differentially expressed

miRNAs in the 2 cell lines was almost entirely not overlapping, with exclusion of miR-219-1-3p, miR-330-5p, and miR-610 (Table 5), we suppose a different miRNA transcriptome organization in the 2 model systems because of the specific and expected genome individuality that they mirror. Unsurprisingly, let-7b and let-7e are downregulated in HCT-116 after cetuximab treatment. The members of let-7 family are known to target KRAS and, recently, their involvement in cetuximab response has been reported [124]. The downregulation of KRAS negative regulators (let-7 family) could be a mechanism positively selected in resistant cells, where KRAS downstream signaling remains activated even after treatment, to contribute to cetuximab resistance. It is notable that miR-17* (previously known as miR-17-3p), a CRC marker found to be abundant in biopsies and plasma of patients and positively regulated by MYC, is upregulated in the resistant cell line and downregulated in the sensitive one after cetuximab treatment. This antithetic modulation of miR-17* could represent one of the discriminating molecular mechanisms of resistance or sensitivity. Interestingly, miR-17* is also strongly downregulated in Caco-2 cell line after direct inhibition of ERK with FR180204: a more moderate downregulation of this miRNA was also observed in the KRAS mutated cell lines, with border line FC values, that could be ascribed to the general reduction on miRNA levels after inhibition of ERK phosphorylation. Indeed, about 70 % of DE miRNAs were downregulated after treatment: this would confirm that MAPK/ERK pathway downregulation also negatively modulates the miRNA generating complex and that miRNAs are globally involved in MAPK cascade [23]**.** The different miRNA transcriptomes in the 2 cell lines after cetuximab treatment could be the outcome of transcription factors involved in the response to cetuximab or in related pathways. On the basis of our data, we found 25 putative miRNA-controlling transcription factors for both cell models (e.g., HNF4A, RUNX1, TCF3), 17 of which had been previously reported to be involved in CRC (e.g., MYC, TCF3) [125, 126]. Some of these transcription factors could

specifically control the expression of differentially expressed miRNAs, determining the variation of miRNA transcriptome after cetuximab treatment [127]. We found a similar behavior in the three CRC cell lines treated with the three inhibitors for the same pathway: miRNA profiles in Caco-2, HCT-116 and SW-620 (another KRAS mutated CRC cell line which differs from the other because it derives from a metastasis) were generally unique, with some exceptions. This is not surprising, since the compounds have different molecular targets (Figure 12) and distinct mechanisms of actions. We also failed to find miRNAs commonly altered in all cell lines for all treatments, except for miR-222*, which was slightly, but reproducibly, downregulated in all our experimental conditions. Again, this evidences the strong genomic individuality of the cell lines. We focused our attention on those miRNAs, which were shown to be commonly altered in: (1) all cell lines after a specific treatment (class A); (2) a specific cell line after all treatments (class B). This approach allowed us to identify sets of miRNAs involved in the regulation of cellular functions by MAPK/ERK in CRC. We focused on six miRNAs, miR-92a-1*, miR-135b*, miR-720 for class A, and miR-1226*, miR-663b, and miR-372 for class B, based on their FC values and on the lack of information about their biological role. It is to note that none of the differentially expressed miRNAs after MAPK inhibition showed high fold change values (i.e., FC>3). This suggests that within the MAPK/ERK pathway miRNAs may act cooperatively, rather than individually: they may be involved in the fine tuning of gene expression centered on ERK signaling. By overlapping different computational approaches we identified a reliable set of mRNA targets of differentially expressed miRNAs both after cetuximab treatment and after treatment with the three MAPK/ERK inhibitors. Target analysis may provide further insight into the molecular mechanisms and biological pathways responsible for sensitivity/resistance to therapy, or MAPK pathway activation within a given cellular context (Tables 7 and 10). Intriguingly, all the selected mRNA targets had

trends of expression opposite to their putatively regulating miRNAs (negative Pearson coefficient). This suggests that these miRNA–mRNA couples may correspond to biological relevant regulatory circuits in our models [128]. Among the mRNA targets identified for differentially expressed miRNAs after cetuximab treatment, we found a significant amount of genes involved in CRC pathogenesis, cetuximab pathway, and most interestingly, in the CRC response to drugs (Table 7). On the other hand, several mRNAs targets identified in this study are targeted by several differentially expressed miRNAs having well-established CRC associations (i.e., let-7, miR-17*, miR-18a*, miR-107, miR-133b, miR-223) and some of them are known to be involved in the cetuximab pathway (let-7b, let-7e). From the list of computationally identified targets for the six differentially expressed candidate miRNAs after treatment with MAPK inhibitors, we focused on a limited number of mRNAs based on confirmation of their antithetic expression respect to their putatively regulating miRNAs after their modulation in the cell lines, and verifying that their expression is regulated after treatment with MAPK inhibitors. PTEN, SOCS5, LATS2, TXNIP, CCND2 are known to be deregulated in CRC: in particular, PTEN, LATS2 and TXNIP (targets of upregulated miRNAs after treatment) are all strongly downregulated in CRC, while CCND2 (target of a downregulated miRNA), is overexpressed. Moreover, they are all involved in the regulation of MAPK related processes like cell proliferation, apoptosis and cell migration [129-132]. Our HT expression data demonstrate that many molecular features of MAPK pathway are shared among different cell lines and stimuli; others, instead, are the outcome of specific cell phenotypes/genotypes or specific treatments: likely, this mirrors the clinical heterogeneity that is to be expected within patients' cohorts; unsurprisingly, we found that some miRNAs had a different abundance in CRC patients based on their KRAS mutational status (Figures 20 and 23). The higher levels of miR-146b-3p and miR-486-5p in KRAS mutated samples, with respect to wild-type ones,

could be the indirect result of constitutional activation of KRAS signaling (Figure 20). Almost 80% of the miR-486-5p targets are negative regulators of cell proliferation or involved in apoptosis. Among miR-486-5p targets, PIK3R1 is upregulated in responsive patients after cetuximab treatment [133]. MiR-146b-3p has been reported to be an unfavorable cancer prognostic marker for patients with squamous cell lung cancer or papillary thyroid carcinoma [134, 135]. Interestingly, its upregulation is statistically associated with BRAF mutation in papillary thyroid carcinoma. Moreover, indirect evidence in breast cancer would suggest that miR-146a and 146b target EGFR [136]. Accordingly, profiling of these miRNAs in CRC patients could complement KRAS–based diagnosis to predict sensitivity to cetuximab. The upregulation of miR-92a-1*, miR-135b*, miR-372, miR-720 in CRC patients, respect to normal controls, confirms their oncogenetic role (Figure 23): this is what we expected to find, based on the assumption that these miRNAs, deregulated after treatment with some specific inhibitors of MAPK pathway, are regulated by this pathway. Furthermore and notably, the expression levels of these miRNAs were significantly higher in mutated KRAS samples than in wild type ones. Taken together, these data suggest that the upregulation of miR-146b-3p, miR-486-5p, miR-92a-1*, miR-135b*, miR-372, and miR-720 in CRC patients with mutated KRAS would be a downstream molecular effect of hyperproliferative stimuli triggered by KRAS mutations or in other nodes from the same pathway. To determine the main biological and molecular functions affected by differentially expressed miRNAs in our studies, we performed the network analysis on the main targets of deregulated miRNAs after cetuximab and MAPK inhibitors treatments. Unsurprisingly, the 4 networks of the targets of differentially expressed miRNA after cetuximab treatment and their first interactors are centered on the same hubs, EEF1A1, GRB2, and UBC. Although the role of EEF1A1 in CRC remains unsatisfactorily characterized, the involvement of GRB2 and UBC in the regulation of EGFR pathway has been proved [102, 137]. In particular, GRB2 is a

critical link between cell surface growth factor receptors and the RAS signaling pathway, participating in EGFR internalization and its subsequent ubiquitylation [137]. Moreover, the ubiquitin complex regulates other key molecules in CRC carcinogenesis and components of the KRAS pathways. This would mean that the regulatory circuits spreading from differentially expressed miRNAs focus on key molecules, playing a central role in proper signaling transmission from EGFR and in its internalization and turnover. These findings are well inserted in the scenario of the downstream effects of cetuximab. Indeed, it has been shown that cetuximab also induces EGFR internalization and ubiquitin-mediated degradation. We analyzed the statistically overrepresented GO terms within the networks. We observed that differentially expressed miRNAs in Caco-2 both at 24 and 48 hours post-treatment preferentially target genes involved in the regulation of Notch and Wnt pathways, whereas the set of differentially expressed miRNAs in HCT-116 may control the signaling pathways of EGFR at 48 hours post treatment (Figure 21). In intestinal crypts, the canonical Wnt pathway inhibits the b-catenin destruction complex [138]. The processes related to immunity are extensively represented in our GO analysis. We noticed that Caco-2 cells, with respect to HCT-116, are enriched in proteins involved in the activation of the molecular mediators of inflammation (Figure 21). It has been reported that cetuximab treatment of CRC patients increases the expression of proinflammatory proteins and that host response to therapy could be a potential prognostic factor in CRC. Moreover, in Caco-2 at 24 and 48 hours post-treatment, we found several GOs related to NF-kB activity, which are absent in HCT-116 (Figure 21). Expression of this transcription factor, also activated by the EGFR downstream signaling pathway, has been associated with prognosis and resistance to antitumor treatments in CRC and other solid tumors [139]. These data stress as different responses to cetuximab are related to different sets of differentially expressed miRNAs and, accordingly, to different molecular signaling. Finally, we identified

statistically significant differences in GO terms between 24 and 48 hours post-treatment in our model cell lines. This indicates that the regulation of the molecular cascade, controlling the EGFR mediated pathway, represents an early effect of cetuximab administration in the sensitive cell line. We performed a similar analysis for the six miRNAs which expression is altered after treatment with the three MAPK inhibitors: it is interesting to note that within the network including miRNAs, their targets and targets' first interactors, and miRNA regulating TFs, the whole MAPK pathway, from EGFR to MYC, was included within the network (Figure 27A and B). These data are concordant with our starting hypothesis that these six miRNAs are intimately involved in the regulatory circuits spreading from activated EGFR and are likely to be regulated themselves by this important signaling pathway. Moreover, when analyzing the GOs of the single subnetworks from each of the six miRNAs, we could observe that three out of the main biological processes regulated by MAPK pathway, which are also strongly implicated in tumorigenesis, are statistically overrepresented in all of them. To experimentally verify what we have computationally inferred, we modulated the expression of the six miRNAs to reproduce the same kind of dysregulation found in our cell lines after drug treatment. As hypothesized, all miRNAs analyzed were able to affect at least one of the major biological processes investigated (proliferation, migration, apoptosis), in at least two of the three cell lines (Figures 28-32). MiRNAs modulated in a specific cell line after treatment (i.e., miR-92a-1*, miR-135b*, miR-720 in Caco-2, HCT-116, SW-620, respectively), caused variations in proliferation, apoptosis, migration also when down modulated in the other cell lines (Figures 28-32). This demonstrates that their functional role is maintained in different genomic contexts. Based on the computational analysis and experimental evidences we have produced in our study, we could propose a model for the involvement of at least four of the six

miRNAs in MAPK/ERK pathway, including the role of their main targets in its signaling circuits (Figure 33).

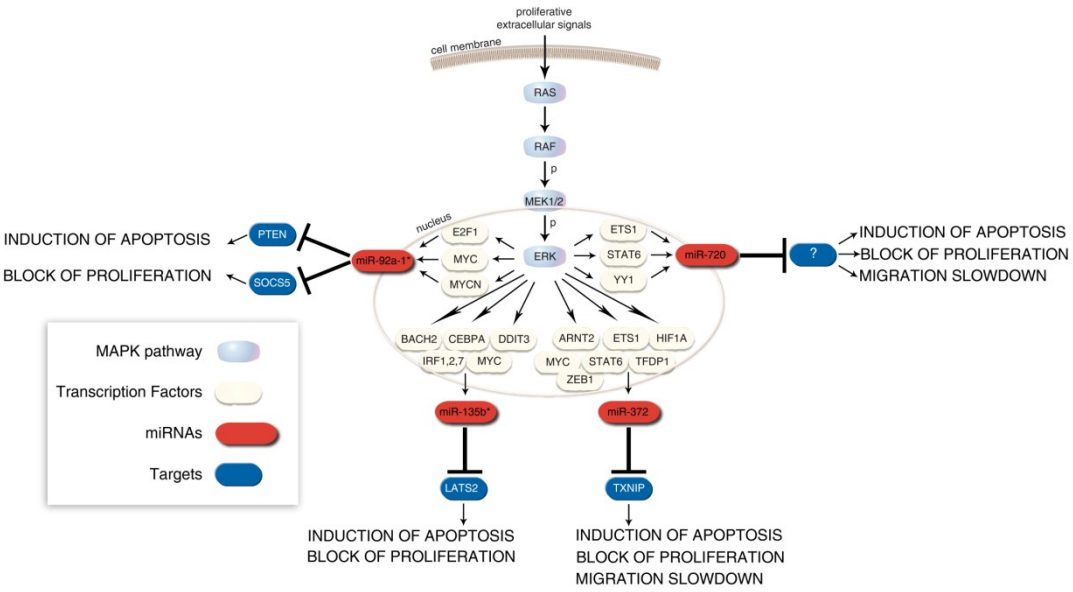

Figure 33. Hypothetical role of miR-92a-1*, miR-135b*, miR-372, miR-720 in CRC, based on experimental and computational data obtained in this study.

MiR-92a-1*, downregulated in Caco-2 after all treatments and in HCT-116 and SW-620 after treatment with U0126 and WAY265506, belongs to the oncogenic cluster 17-92 that is often amplified and upregulated in CRC. We found that this miRNA is overexpressed in CRC patients and also results more abundant in KRAS mutated samples; its knockdown caused upregulation of PTEN, SOCS5, TMEM52 in Caco-2 and HCT-116. Interestingly, PTEN was upregulated in Caco-2 after all treatments and in HCT-116 after U0126, while SOCS5 was upregulated in Caco-2 after exposure to FR180204 and in HCT-116 after U0126. It is known that inactivation of the tumor suppressor PTEN is one of the most important events in CRC progression, while the expression of SOCS5 leads to a marked reduction of

EGFR levels by promoting EGFR degradation [129, 130]. PTEN induces apoptosis and cell cycle arrest through phosphoinositol-3-kinase/Akt-dependent and independent pathways; there are literature evidences that ERK pathway inhibition could induce PTEN upregulation (via SMAD2). Knockdown of miR-92a-1* caused a decrease of Caco-2 and HCT-116 proliferation, possibly due to PTEN-induced cell cycle arrest. Notably, miR-92a-1* knockdown induced also an increase of apoptosis in HCT-116 and SW-620. MiR-135b* was downregulated in HCT-116 after treatment with U0126 and WAY265506, and in SW-620 after U0126. Interestingly, considerable upregulation of miR-135 family was detected in colorectal adenomas and carcinomas, which was significantly correlated with low APC mRNA levels [76]. Accordingly, our expression data on CRC patients showed miR-135b* higher expression in cancer tissues and KRAS mutated samples. MiR-135b* knockdown caused upregulation of LATS2 in Caco-2 and SW-620. LATS2 is a tumor suppressor downregulated in CRC samples, but its expression levels increased after U0126 treatment in all cell lines and after WAY265506 in Caco-2 and SW-620. This tumor suppressor increases p53-mediated apoptosis by promoting the proapoptotic function of ASPP1; it also prevents G1/S transition by negatively regulating CyclinE/CDK2 [131]. Interestingly, knockdown of miR-135b* induced apoptosis in all cell lines and decreased proliferation in Caco-2 and SW-620. MiR-372, negatively modulated after treatment with FR180204 in all cell lines, was already known to be upregulated in KRAS-mutated CRC cells [78]. Interestingly, our data on patients showed its higher expression in CRC tissues and in KRAS-mutated CRC patients. In our experiments, down modulation of miR-372 was associated in all three cell lines to upregulation of TXNIP which is involved in metabolism, induction of apoptosis, inhibition of cell proliferation, activation of PTEN by thioredoxin NADP(H)-dependent disulfide reduction [140]. Its expression is controlled by MAPKs and miR-17-5p [141]. Notably, TXNIP, significantly downregulated in

CRC samples, increased its expression levels in all cell lines after treatment with FR180204. We didn't find any information about miR-372 functions in literature, but it is a homolog of miR-373, which promotes breast cancer invasion and metastasis via inhibition of TXNIP, its direct target gene [142]. Knockdown of miR-372 affected proliferation and increased apoptosis in all cell lines: it is of note that its down modulation in HCT-116 resulted also in a decrease of cell migration. Taken together, these data suggest that through inhibition of TXNIP, miR-372 could have an active role in maintaining high proliferation rates and defective apoptosis in CRC, as well as regulating cell migration: in fact, it has been already demonstrated that TXNIP silencing strongly induces endothelial cell migration [143]. For miR-720 and miR-1226*, downregulated in SW-620 after all treatments and in all cell lines after U0126 treatment, respectively, we failed to find targets which expression was commonly modulated after knockdown experiments in the three cell lines. Interestingly, miR-720, but not miR1226*, was overexpressed in CRC patients and resulted statistically more abundant in KRAS mutated samples. Its knockdown induced decrease of proliferation, increase of apoptosis and decrease of cell migration in all cell lines analyzed. Our data obtained on cell lines and patients would suggest an oncogenetic role for miR-720 in CRC pathobiology; however, its molecular targets still remain to be unveiled. MiR-663b was upregulated in all three cell lines after treatment with WAY265506 and its forced over expression (by pre-miR transfection) induced downregulation of CCND2, GRB2, SRF. CCND2 activity is required for cell cycle G1/S transition; its overexpression was reported in ovarian granulose tumors, gastric cancer, and colon cancer [132]. Interestingly, CCND2 was downregulated in all cell lines after WAY265506 treatment. However, functional assays performed after its knock-in showed no noteworthy biological effect, but for delayed decrease of HCT-116 proliferation. Expression analysis of miR-663b in CRC patients showed no significant differences respect to controls.

6. CONCLUSIONS AND FUTURE PERSPECTIVES

The data reported in this thesis show for the first time a) the global involvement of miRNAs in the pharmacologic response to cetuximab in colorectal carcinoma (CRC), and b) a set of miRNAs able to globally affect the regulatory circuits governed by MAPK signaling, which is one of the major pathways involved in CRC. These results lead us to propose the miRNAs we have identified as putative predictive markers of drug response, setting up larger epidemiologic studies on CRC specimens for pharmacoresistance screenings in patients, to associate specific miRNA profiles to responsiveness classes for cetuximab. Finally, these studies could also identify chemoresistance related miRNAs as pharmacologic targets for combining therapy with antagomirs [144]. We have subsequently identified a set of miRNAs which are intimately associated to MAPK pathway: network-based studies coupled with functional analysis have demonstrated that miR-92a-1*, miR-135b*, miR-372, miR-720 affect cell proliferation, apoptosis, and migration in CRC. Most interesting, the main candidate miRNAs identified in these two studies were found to be more abundant in patients with mutated KRAS before treatment (i.e., miR-146b-3p, miR-486-5p, miR-92a-1*, miR-135b*, miR-372, miR-720). Our functional analysis, coupled to data from CRC patients, strongly suggest these miRNAs as new CRC oncomiRs regulated by MAPK/ERK signaling. Moreover, overexpression of miR-146b-3p and miR-486-5p in KRAS mutated patients could additionally improve KRAS based diagnosis to predict patients' sensitivity to cetuximab. These data are well inserted in the wider global goal of improving CRC patient classification, but most importantly, of identifying

new possible therapeutic strategies taking in account patients' genomic peculiarities, that can also overreach the problems related to drugs toxicity. It was widely discussed in the Introduction the importance of exosomal miRNAs as putative vectors for gene therapy. Exosomes secreted by a given cell type contain a population of RNA that is non-randomly packaged within these small vesicles: this suggests an important role for the miRNA secreted with this still un-characterized mechanism. We have recently identified for the first time a reliable set of RNA-binding proteins, many of them importantly involved in miRNA maturation and transport, which could be responsible of the specific miRNA shuttling within the exosomes based on the cellular context (Statello et al., submitted). Exosomal miRNA signatures have been reported to be potentially useful for cancer diagnosis, but so far, no data on miRNA transcriptome changes after specific treatments have been produced. We hypothesize that, since exosomal miRNAs are representative of a specific cell line signature, a specific sub-set of exosomal miRNAs could be subjected to modulation after drug treatment. To test this hypothesis, we are analyzing the molecular effects of cetuximab on exosomes molecular cargo and secretion in *in vitro* models. We want to understand if pharmacologically-treated cancer cells communicate with each other and how their molecular phenotype may be modified. Our specific aims are: (1) to identify and functionally characterize miRNAs selectively stored within exosomes following *in vitro* cetuximab treatment of sensitive and resistant CRC cell lines (Caco-2 and HCT-116); (2) to eventually validate these data in *ex vivo* studies from plasma exosomes of CRC patients cohorts responsive or resistant to cetuximab, before and after pharmacological treatment. By performing in vitro studies, we have identified a number of differentially expressed miRNAs in exosomes after cetuximab treatment; moreover, we observed that miRNAs are sorted asymmetrically within specific cell compartments, where they could be involved in different aspects of cancer etiopathogenesis. Subsequently, we will compare the amount of those

miRNAs involved in the response to cetuximab treatment in patients' cohorts, in order to identify the molecular profiles associated to the response to therapy. Our data should pave the way to the use of exosomes and their RNA content as innovative diagnostic, prognostic and therapeutic tools for neoplastic diseases.

7. BIBLIOGRAPHY

1. Siegel, R., D. Naishadham, and A. Jemal, *Cancer statistics, 2012.* CA Cancer J Clin, 2012. **62**(1): p. 10-29.
2. Rustgi, A.K., *The genetics of hereditary colon cancer.* Genes Dev, 2007. **21**(20): p. 2525-38.
3. Jass, J.R., *Classification of colorectal cancer based on correlation of clinical, morphological and molecular features.* Histopathology, 2007. **50**(1): p. 113-30.
4. Walther, A., et al., *Genetic prognostic and predictive markers in colorectal cancer.* Nat Rev Cancer, 2009. **9**(7): p. 489-99.
5. Pino, M.S. and D.C. Chung, *The chromosomal instability pathway in colon cancer.* Gastroenterology, 2010. **138**(6): p. 2059-72.
6. Fearnhead, N.S., J.L. Wilding, and W.F. Bodmer, *Genetics of colorectal cancer: hereditary aspects and overview of colorectal tumorigenesis.* Br Med Bull, 2002. **64**: p. 27-43.
7. Fearon, E.R., *Molecular genetics of colorectal cancer.* Annu Rev Pathol, 2011. **6**: p. 479-507.
8. Kanthan, R., J.L. Senger, and S.C. Kanthan, *Molecular events in primary and metastatic colorectal carcinoma: a review.* Patholog Res Int, 2012. **2012**: p. 597497.
9. Lievre, A., H. Blons, and P. Laurent-Puig, *Oncogenic mutations as predictive factors in colorectal cancer.* Oncogene, 2010. **29**(21): p. 3033-43.
10. Rampino, N., et al., *Somatic frameshift mutations in the BAX gene in colon cancers of the microsatellite mutator phenotype.* Science, 1997. **275**(5302): p. 967-9.
11. Brenner, D.E. and G. Rennert, *Fecal DNA biomarkers for the detection of colorectal neoplasia: attractive, but is it feasible?* J Natl Cancer Inst, 2005. **97**(15): p. 1107-9.
12. Dai, J., et al., *GWAS-identified colorectal cancer susceptibility loci associated with clinical outcomes.* Carcinogenesis, 2012. **33**(7): p. 1327-31.
13. Hackel, P.O., et al., *Epidermal growth factor receptors: critical mediators of multiple receptor pathways.* Curr Opin Cell Biol, 1999. **11**(2): p. 184-9.
14. Ponz-Sarvise, M., et al., *Epidermal growth factor receptor inhibitors in colorectal cancer treatment: what's new?* World J Gastroenterol, 2007. **13**(44): p. 5877-87.

15. Cohen, G., et al., *Epidermal growth factor receptor signaling is up-regulated in human colonic aberrant crypt foci.* Cancer Res, 2006. **66**(11): p. 5656-64.
16. Vecchione, L., et al., *EGFR-targeted therapy.* Exp Cell Res, 2011. **317**(19): p. 2765-71.
17. Vincenzi, B., et al., *The biological properties of cetuximab.* Crit Rev Oncol Hematol, 2008. **68**(2): p. 93-106.
18. Mendelsohn, J. and J. Baselga, *Status of epidermal growth factor receptor antagonists in the biology and treatment of cancer.* J Clin Oncol, 2003. **21**(14): p. 2787-99.
19. Montagut, C. and J. Settleman, *Targeting the RAF-MEK-ERK pathway in cancer therapy.* Cancer Lett, 2009. **283**(2): p. 125-34.
20. Wan, P.T., et al., *Mechanism of activation of the RAF-ERK signaling pathway by oncogenic mutations of B-RAF.* Cell, 2004. **116**(6): p. 855-67.
21. De Roock, W., et al., *Effects of KRAS, BRAF, NRAS, and PIK3CA mutations on the efficacy of cetuximab plus chemotherapy in chemotherapy-refractory metastatic colorectal cancer: a retrospective consortium analysis.* Lancet Oncol, 2010. **11**(8): p. 753-62.
22. Chang, T.C., et al., *Widespread microRNA repression by Myc contributes to tumorigenesis.* Nat Genet, 2008. **40**(1): p. 43-50.
23. Paroo, Z., et al., *Phosphorylation of the human microRNA-generating complex mediates MAPK/Erk signaling.* Cell, 2009. **139**(1): p. 112-22.
24. Fang, J.Y. and B.C. Richardson, *The MAPK signalling pathways and colorectal cancer.* Lancet Oncol, 2005. **6**(5): p. 322-7.
25. Lemmon, M.A. and J. Schlessinger, *Regulation of signal transduction and signal diversity by receptor oligomerization.* Trends Biochem Sci, 1994. **19**(11): p. 459-63.
26. Friday, B.B. and A.A. Adjei, *Advances in targeting the Ras/Raf/MEK/Erk mitogen-activated protein kinase cascade with MEK inhibitors for cancer therapy.* Clin Cancer Res, 2008. **14**(2): p. 342-6.
27. Watanabe, M., et al., *Overexpression of keratinocyte growth factor in cancer cells and enterochromaffin cells in human colorectal cancer.* Pathol Int, 2000. **50**(5): p. 363-72.
28. Wood, L.D., et al., *The genomic landscapes of human breast and colorectal cancers.* Science, 2007. **318**(5853): p. 1108-13.
29. Wilhelm, S., et al., *Discovery and development of sorafenib: a multikinase inhibitor for treating cancer.* Nat Rev Drug Discov, 2006. **5**(10): p. 835-44.
30. Chapman, P.B., et al., *Improved survival with vemurafenib in melanoma with BRAF V600E mutation.* N Engl J Med, 2011. **364**(26): p. 2507-16.
31. Sebolt-Leopold, J.S., *Advances in the development of cancer therapeutics directed against the RAS-mitogen-activated protein kinase pathway.* Clin Cancer Res, 2008. **14**(12): p. 3651-6.

32. Ahn, N.G., et al., *Pharmacologic inhibitors of MKK1 and MKK2.* Methods Enzymol, 2001. **332**: p. 417-31.
33. Ohori, M., et al., *Identification of a selective ERK inhibitor and structural determination of the inhibitor-ERK2 complex.* Biochem Biophys Res Commun, 2005. **336**(1): p. 357-63.
34. Bartel, D.P., *MicroRNAs: target recognition and regulatory functions.* Cell, 2009. **136**(2): p. 215-33.
35. Lee, R.C. and V. Ambros, *An extensive class of small RNAs in Caenorhabditis elegans.* Science, 2001. **294**(5543): p. 862-4.
36. Zhang, B., Q. Wang, and X. Pan, *MicroRNAs and their regulatory roles in animals and plants.* J Cell Physiol, 2007. **210**(2): p. 279-89.
37. Kim, V.N. and J.W. Nam, *Genomics of microRNA.* Trends Genet, 2006. **22**(3): p. 165-73.
38. Bentwich, I., et al., *Identification of hundreds of conserved and nonconserved human microRNAs.* Nat Genet, 2005. **37**(7): p. 766-70.
39. Rodriguez, A., et al., *Identification of mammalian microRNA host genes and transcription units.* Genome Res, 2004. **14**(10A): p. 1902-10.
40. Lee, Y., et al., *MicroRNA genes are transcribed by RNA polymerase II.* EMBO J, 2004. **23**(20): p. 4051-60.
41. Gregory, R.I., et al., *Human RISC couples microRNA biogenesis and posttranscriptional gene silencing.* Cell, 2005. **123**(4): p. 631-40.
42. Haase, A.D., et al., *TRBP, a regulator of cellular PKR and HIV-1 virus expression, interacts with Dicer and functions in RNA silencing.* EMBO Rep, 2005. **6**(10): p. 961-7.
43. Lee, Y., et al., *The role of PACT in the RNA silencing pathway.* EMBO J, 2006. **25**(3): p. 522-32.
44. Gregory, R.I. and R. Shiekhattar, *MicroRNA biogenesis and cancer.* Cancer Res, 2005. **65**(9): p. 3509-12.
45. Tolia, N.H. and L. Joshua-Tor, *Slicer and the argonautes.* Nat Chem Biol, 2007. **3**(1): p. 36-43.
46. Easow, G., A.A. Teleman, and S.M. Cohen, *Isolation of microRNA targets by miRNP immunopurification.* RNA, 2007. **13**(8): p. 1198-204.
47. Carthew, R.W. and E.J. Sontheimer, *Origins and Mechanisms of miRNAs and siRNAs.* Cell, 2009. **136**(4): p. 642-55.
48. Filipowicz, W., S.N. Bhattacharyya, and N. Sonenberg, *Mechanisms of post-transcriptional regulation by microRNAs: are the answers in sight?* Nat Rev Genet, 2008. **9**(2): p. 102-14.
49. Petersen, C.P., et al., *Short RNAs repress translation after initiation in mammalian cells.* Mol Cell, 2006. **21**(4): p. 533-42.
50. Guo, H., et al., *Mammalian microRNAs predominantly act to decrease target mRNA levels.* Nature, 2010. **466**(7308): p. 835-40.

51. Schratt, G.M., et al., *A brain-specific microRNA regulates dendritic spine development.* Nature, 2006. **439**(7074): p. 283-9.
52. Cimmino, A., et al., *miR-15 and miR-16 induce apoptosis by targeting BCL2.* Proc Natl Acad Sci U S A, 2005. **102**(39): p. 13944-9.
53. Johnson, S.M., et al., *RAS is regulated by the let-7 microRNA family.* Cell, 2005. **120**(5): p. 635-47.
54. Lee, Y.S. and A. Dutta, *The tumor suppressor microRNA let-7 represses the HMGA2 oncogene.* Genes Dev, 2007. **21**(9): p. 1025-30.
55. Garzon, R., G.A. Calin, and C.M. Croce, *MicroRNAs in Cancer.* Annu Rev Med, 2009. **60**: p. 167-79.
56. Voorhoeve, P.M., et al., *A genetic screen implicates miRNA-372 and miRNA-373 as oncogenes in testicular germ cell tumors.* Cell, 2006. **124**(6): p. 1169-81.
57. Mendell, J.T., *miRiad roles for the miR-17-92 cluster in development and disease.* Cell, 2008. **133**(2): p. 217-22.
58. Li, M., et al., *microRNA and cancer.* AAPS J, 2010. **12**(3): p. 309-17.
59. Volinia, S., et al., *A microRNA expression signature of human solid tumors defines cancer gene targets.* Proc Natl Acad Sci U S A, 2006. **103**(7): p. 2257-61.
60. Yan, L.X., et al., *MicroRNA miR-21 overexpression in human breast cancer is associated with advanced clinical stage, lymph node metastasis and patient poor prognosis.* RNA, 2008. **14**(11): p. 2348-60.
61. Lebanony, D., et al., *Diagnostic assay based on hsa-miR-205 expression distinguishes squamous from nonsquamous non-small-cell lung carcinoma.* J Clin Oncol, 2009. **27**(12): p. 2030-7.
62. Chen, X., et al., *Characterization of microRNAs in serum: a novel class of biomarkers for diagnosis of cancer and other diseases.* Cell Res, 2008. **18**(10): p. 997-1006.
63. Lawrie, C.H., et al., *Detection of elevated levels of tumour-associated microRNAs in serum of patients with diffuse large B-cell lymphoma.* Br J Haematol, 2008. **141**(5): p. 672-5.
64. Mitchell, P.S., et al., *Circulating microRNAs as stable blood-based markers for cancer detection.* Proc Natl Acad Sci U S A, 2008. **105**(30): p. 10513-8.
65. Hu, Z., et al., *Serum microRNA signatures identified in a genome-wide serum microRNA expression profiling predict survival of non-small-cell lung cancer.* J Clin Oncol, 2010. **28**(10): p. 1721-6.
66. Vickers, K.C., et al., *MicroRNAs are transported in plasma and delivered to recipient cells by high-density lipoproteins.* Nat Cell Biol, 2011. **13**(4): p. 423-33.
67. Xu, J., et al., *Circulating microRNAs: novel biomarkers for cardiovascular diseases.* J Mol Med (Berl), 2012. **90**(8): p. 865-75.

68. Kosaka, N., H. Iguchi, and T. Ochiya, *Circulating microRNA in body fluid: a new potential biomarker for cancer diagnosis and prognosis.* Cancer Sci, 2010. **101**(10): p. 2087-92.
69. Mathivanan, S., H. Ji, and R.J. Simpson, *Exosomes: extracellular organelles important in intercellular communication.* J Proteomics, 2010. **73**(10): p. 1907-20.
70. Denzer, K., et al., *Exosome: from internal vesicle of the multivesicular body to intercellular signaling device.* J Cell Sci, 2000. **113 Pt 19**: p. 3365-74.
71. Anand, P.K., *Exosomal membrane molecules are potent immune response modulators.* Commun Integr Biol, 2010. **3**(5): p. 405-8.
72. Zhang, H.G. and W.E. Grizzle, *Exosomes and cancer: a newly described pathway of immune suppression.* Clin Cancer Res, 2011. **17**(5): p. 959-64.
73. Valadi, H., et al., *Exosome-mediated transfer of mRNAs and microRNAs is a novel mechanism of genetic exchange between cells.* Nat Cell Biol, 2007. **9**(6): p. 654-9.
74. Taylor, D.D. and C. Gercel-Taylor, *MicroRNA signatures of tumor-derived exosomes as diagnostic biomarkers of ovarian cancer.* Gynecol Oncol, 2008. **110**(1): p. 13-21.
75. Rabinowits, G., et al., *Exosomal microRNA: a diagnostic marker for lung cancer.* Clin Lung Cancer, 2009. **10**(1): p. 42-6.
76. Nagel, R., et al., *Regulation of the adenomatous polyposis coli gene by the miR-135 family in colorectal cancer.* Cancer Res, 2008. **68**(14): p. 5795-802.
77. Slaby, O., et al., *MicroRNAs in colorectal cancer: translation of molecular biology into clinical application.* Mol Cancer, 2009. **8**: p. 102.
78. Bandres, E., et al., *Identification by Real-time PCR of 13 mature microRNAs differentially expressed in colorectal cancer and non-tumoral tissues.* Mol Cancer, 2006. **5**: p. 29.
79. Schetter, A.J., et al., *MicroRNA expression profiles associated with prognosis and therapeutic outcome in colon adenocarcinoma.* JAMA, 2008. **299**(4): p. 425-36.
80. Chang, T.C., et al., *Transactivation of miR-34a by p53 broadly influences gene expression and promotes apoptosis.* Mol Cell, 2007. **26**(5): p. 745-52.
81. Iorio, M.V., et al., *MicroRNA gene expression deregulation in human breast cancer.* Cancer Res, 2005. **65**(16): p. 7065-70.
82. Hayashi, H. and T. Kume, *Foxc transcription factors directly regulate Dll4 and Hey2 expression by interacting with the VEGF-Notch signaling pathways in endothelial cells.* PLoS One, 2008. **3**(6): p. e2401.
83. Lanza, G., et al., *mRNA/microRNA gene expression profile in microsatellite unstable colorectal cancer.* Mol Cancer, 2007. **6**: p. 54.

84. Schepeler, T., et al., *Diagnostic and prognostic microRNAs in stage II colon cancer.* Cancer Res, 2008. **68**(15): p. 6416-24.
85. Asangani, I.A., et al., *MicroRNA-21 (miR-21) post-transcriptionally downregulates tumor suppressor Pdcd4 and stimulates invasion, intravasation and metastasis in colorectal cancer.* Oncogene, 2008. **27**(15): p. 2128-36.
86. Ng, E.K., et al., *Differential expression of microRNAs in plasma of patients with colorectal cancer: a potential marker for colorectal cancer screening.* Gut, 2009. **58**(10): p. 1375-81.
87. Monzo, M., et al., *Overlapping expression of microRNAs in human embryonic colon and colorectal cancer.* Cell Res, 2008. **18**(8): p. 823-33.
88. Huang, Z., et al., *Plasma microRNAs are promising novel biomarkers for early detection of colorectal cancer.* Int J Cancer, 2010. **127**(1): p. 118-26.
89. Rossi, L., E. Bonmassar, and I. Faraoni, *Modification of miR gene expression pattern in human colon cancer cells following exposure to 5-fluorouracil in vitro.* Pharmacol Res, 2007. **56**(3): p. 248-53.
90. Svoboda, M., et al., *Micro-RNAs miR125b and miR137 are frequently upregulated in response to capecitabine chemoradiotherapy of rectal cancer.* Int J Oncol, 2008. **33**(3): p. 541-7.
91. Alvarez-Erviti, L., et al., *Delivery of siRNA to the mouse brain by systemic injection of targeted exosomes.* Nat Biotechnol, 2011. **29**(4): p. 341-5.
92. Wahlgren, J., et al., *Plasma exosomes can deliver exogenous short interfering RNA to monocytes and lymphocytes.* Nucleic Acids Res, 2012.
93. Chang, K.H., et al., *MicroRNA expression profiling to identify and validate reference genes for relative quantification in colorectal cancer.* BMC Cancer, 2010. **10**: p. 173.
94. Vandesompele, J., et al., *Accurate normalization of real-time quantitative RT-PCR data by geometric averaging of multiple internal control genes.* Genome Biol, 2002. **3**(7): p. RESEARCH0034.
95. Lievre, A., et al., *KRAS mutations as an independent prognostic factor in patients with advanced colorectal cancer treated with cetuximab.* J Clin Oncol, 2008. **26**(3): p. 374-9.
96. Ruike, Y., et al., *Global correlation analysis for micro-RNA and mRNA expression profiles in human cell lines.* J Hum Genet, 2008. **53**(6): p. 515-23.
97. Liang, Y., et al., *Characterization of microRNA expression profiles in normal human tissues.* BMC Genomics, 2007. **8**: p. 166.
98. Daleke, D.L., *Regulation of transbilayer plasma membrane phospholipid asymmetry.* J Lipid Res, 2003. **44**(2): p. 233-42.
99. Bardelli, A. and S. Siena, *Molecular mechanisms of resistance to cetuximab and panitumumab in colorectal cancer.* J Clin Oncol, 2010. **28**(7): p. 1254-61.

100. Bertram, J., et al., *Overexpression of ribosomal proteins L4 and L5 and the putative alternative elongation factor PTI-1 in the doxorubicin resistant human colon cancer cell line LoVoDxR.* Eur J Cancer, 1998. **34**(5): p. 731-6.
101. Zhong, D., et al., *The SAM domain of the RhoGAP DLC1 binds EF1A1 to regulate cell migration.* J Cell Sci, 2009. **122**(Pt 3): p. 414-24.
102. Voutsadakis, I.A., *The ubiquitin-proteasome system in colorectal cancer.* Biochim Biophys Acta, 2008. **1782**(12): p. 800-8.
103. Yeh, J.J., et al., *KRAS/BRAF mutation status and ERK1/2 activation as biomarkers for MEK1/2 inhibitor therapy in colorectal cancer.* Mol Cancer Ther, 2009. **8**(4): p. 834-43.
104. Mhaidat, N.M., et al., *Inhibition of MEK sensitizes paclitaxel-induced apoptosis of human colorectal cancer cells by downregulation of GRP78.* Anticancer Drugs, 2009. **20**(7): p. 601-6.
105. Diosdado, B., et al., *MiR-17-92 cluster is associated with 13q gain and c-myc expression during colorectal adenoma to adenocarcinoma progression.* Br J Cancer, 2009. **101**(4): p. 707-14.
106. Arvey, A., et al., *Target mRNA abundance dilutes microRNA and siRNA activity.* Mol Syst Biol, 2010. **6**: p. 363.
107. Hansen, T.B., et al., *miRNA-dependent gene silencing involving Ago2-mediated cleavage of a circular antisense RNA.* EMBO J, 2011. **30**(21): p. 4414-22.
108. Khan, A.A., et al., *Transfection of small RNAs globally perturbs gene regulation by endogenous microRNAs.* Nat Biotechnol, 2009. **27**(6): p. 549-55.
109. Clancy, J.L., et al., *mRNA isoform diversity can obscure detection of miRNA-mediated control of translation.* RNA, 2011. **17**(6): p. 1025-31.
110. Chen, C.Y., et al., *Coregulation of transcription factors and microRNAs in human transcriptional regulatory network.* BMC Bioinformatics, 2011. **12 Suppl 1**: p. S41.
111. Ritchie, W., et al., *Conserved expression patterns predict microRNA targets.* PLoS Comput Biol, 2009. **5**(9): p. e1000513.
112. Zhou, Y., et al., *Inter- and intra-combinatorial regulation by transcription factors and microRNAs.* BMC Genomics, 2007. **8**: p. 396.
113. Alenzi, F.Q., *Links between apoptosis, proliferation and the cell cycle.* Br J Biomed Sci, 2004. **61**(2): p. 99-102.
114. Guo, M. and B.A. Hay, *Cell proliferation and apoptosis.* Curr Opin Cell Biol, 1999. **11**(6): p. 745-52.
115. Marhaba, R. and M. Zoller, *CD44 in cancer progression: adhesion, migration and growth regulation.* J Mol Histol, 2004. **35**(3): p. 211-31.

116. Wong, K., U. Rubenthiran, and S. Jothy, *Motility of colon cancer cells: modulation by CD44 isoform expression.* Exp Mol Pathol, 2003. **75**(2): p. 124-30.
117. Han, J.D., *Understanding biological functions through molecular networks.* Cell Res, 2008. **18**(2): p. 224-37.
118. Nilsen, T.W., *Mechanisms of microRNA-mediated gene regulation in animal cells.* Trends Genet, 2007. **23**(5): p. 243-9.
119. Wilusz, J.E., H. Sunwoo, and D.L. Spector, *Long noncoding RNAs: functional surprises from the RNA world.* Genes Dev, 2009. **23**(13): p. 1494-504.
120. Valeri, N., C.M. Croce, and M. Fabbri, *Pathogenetic and clinical relevance of microRNAs in colorectal cancer.* Cancer Genomics Proteomics, 2009. **6**(4): p. 195-204.
121. Fulda, S., *Tumor resistance to apoptosis.* Int J Cancer, 2009. **124**(3): p. 511-5.
122. Damia, G. and M. D'Incalci, *Targeting DNA repair as a promising approach in cancer therapy.* Eur J Cancer, 2007. **43**(12): p. 1791-801.
123. Zheng, T., et al., *Role of microRNA in anticancer drug resistance.* Int J Cancer, 2010. **126**(1): p. 2-10.
124. Zhang, W., et al., *A let-7 microRNA-binding site polymorphism in 3'-untranslated region of KRAS gene predicts response in wild-type KRAS patients with metastatic colorectal cancer treated with cetuximab monotherapy.* Ann Oncol, 2011. **22**(1): p. 104-9.
125. Santarius, T., et al., *A census of amplified and overexpressed human cancer genes.* Nat Rev Cancer, 2010. **10**(1): p. 59-64.
126. Hovanes, K., et al., *Beta-catenin-sensitive isoforms of lymphoid enhancer factor-1 are selectively expressed in colon cancer.* Nat Genet, 2001. **28**(1): p. 53-7.
127. Kohno, K., et al., *Transcription factors and drug resistance.* Eur J Cancer, 2005. **41**(16): p. 2577-86.
128. Wang, Y.P. and K.B. Li, *Correlation of expression profiles between microRNAs and mRNA targets using NCI-60 data.* BMC Genomics, 2009. **10**: p. 218.
129. Siena, S., et al., *Biomarkers predicting clinical outcome of epidermal growth factor receptor-targeted therapy in metastatic colorectal cancer.* J Natl Cancer Inst, 2009. **101**(19): p. 1308-24.
130. Kario, E., et al., *Suppressors of cytokine signaling 4 and 5 regulate epidermal growth factor receptor signaling.* J Biol Chem, 2005. **280**(8): p. 7038-48.
131. Li, Y., et al., *Lats2, a putative tumor suppressor, inhibits G1/S transition.* Oncogene, 2003. **22**(28): p. 4398-405.

132. Sarkar, R., et al., *Expression of cyclin D2 is an independent predictor of the development of hepatic metastasis in colorectal cancer.* Colorectal Dis, 2010. **12**(4): p. 316-23.
133. Debucquoy, A., et al., *Molecular response to cetuximab and efficacy of preoperative cetuximab-based chemoradiation in rectal cancer.* J Clin Oncol, 2009. **27**(17): p. 2751-7.
134. Patnaik, S.K., et al., *Evaluation of microRNA expression profiles that may predict recurrence of localized stage I non-small cell lung cancer after surgical resection.* Cancer Res, 2010. **70**(1): p. 36-45.
135. Chou, C.K., et al., *miR-146b is highly expressed in adult papillary thyroid carcinomas with high risk features including extrathyroidal invasion and the BRAF(V600E) mutation.* Thyroid, 2010. **20**(5): p. 489-94.
136. Hurst, D.R., et al., *Breast cancer metastasis suppressor 1 up-regulates miR-146, which suppresses breast cancer metastasis.* Cancer Res, 2009. **69**(4): p. 1279-83.
137. Giubellino, A., T.R. Burke, Jr., and D.P. Bottaro, *Grb2 signaling in cell motility and cancer.* Expert Opin Ther Targets, 2008. **12**(8): p. 1021-33.
138. MacDonald, B.T., K. Tamai, and X. He, *Wnt/beta-catenin signaling: components, mechanisms, and diseases.* Dev Cell, 2009. **17**(1): p. 9-26.
139. Scartozzi, M., et al., *Nuclear factor-kB tumor expression predicts response and survival in irinotecan-refractory metastatic colorectal cancer treated with cetuximab-irinotecan therapy.* J Clin Oncol, 2007. **25**(25): p. 3930-5.
140. Sheth, S.S., et al., *Hepatocellular carcinoma in Txnip-deficient mice.* Oncogene, 2006. **25**(25): p. 3528-36.
141. Zhuo de, X., et al., *Vitamin D3 up-regulated protein 1(VDUP1) is regulated by FOXO3A and miR-17-5p at the transcriptional and post-transcriptional levels, respectively, in senescent fibroblasts.* J Biol Chem, 2010. **285**(41): p. 31491-501.
142. Yan, G.R., et al., *Global identification of miR-373-regulated genes in breast cancer by quantitative proteomics.* Proteomics, 2011. **11**(5): p. 912-20.
143. Ng, M.K., et al., *A central role for nicotinic cholinergic regulation of growth factor-induced endothelial cell migration.* Arterioscler Thromb Vasc Biol, 2007. **27**(1): p. 106-12.
144. Krutzfeldt, J., et al., *Silencing of microRNAs in vivo with 'antagomirs'.* Nature, 2005. **438**(7068): p. 685-9.